

625713
2001
C.2

SPATIAL VARIATION IN SOILS DEVELOPED ON FLUVIAL TERRACES,
SOCORRO BASIN, RIO GRANDE RIFT, CENTRAL NEW MEXICO

by
Harland L. Goldstein

Submitted in Partial Fulfillment of the Requirements of the Degree of
Masters of Science in Geology
December 2001

Department of Earth and Environmental Science
New Mexico Institute of Mining and Technology
Socorro, New Mexico, USA

UNIVERSITY
LIBRARY
SOCORRO, NM

To my parents, Ronald and Sybil Goldstein, whose continual support and confidence has made my academic career a possibility. Thank You!

ABSTRACT

Soils are commonly used for correlation and age estimation in geomorphology. However, many of these studies do not consider the variable nature of soils in a way to validate the use of soil development as an estimator of time and a tool for correlation.

Tributary terraces in the Socorro Basin were correlated based on the height of the terrace tread above the modern stream channel. Five terrace levels are present throughout the Socorro Basin in at least four tributaries to the Rio Grande. In addition, these terraces can also be correlated to tributary and Rio Grande terraces outside of the Socorro Basin. Hypsometric analysis for each tributary drainage basin suggests that the response times, and thus the timing of terrace formation, are similar even though total drainage basin areas are different among tributaries. Therefore, because terraces are correlated independent of soil development and because the timing of terrace formation is similar, soil variability on same-aged surfaces could be determined.

To validate correlations and age estimates made in this study, soil variability was determined for 1) a single Pleistocene terrace surface in Walnut Creek, and 2) correlated terraces throughout the Socorro Basin. Statistical analysis of the Walnut Creek terrace suggests that swale soils are less variable than bar soils. In addition, only two soil parameters from correlated terraces in Socorro Canyon and Tiffany Canyon fall within the range of the Walnut Creek soils; CaCO_3 mass and silt + clay mass.

CaCO₃ accumulation rates for the Socorro Basin range from 0.067 g/cm³/kyr to 0.073 g/cm³/kyr. These rates are based on Pleistocene soils and vary from previous rates in New Mexico that are often used as guides for correlations and age estimates throughout the southwest United States.

The five correlated tributary terrace surfaces in the Socorro Basin represent regional geomorphic surfaces related to the Rio Grande. Two major fill terraces are associated with an underlying erosional surface and are Late Pleistocene (oxygen isotope stage 6) and Early Holocene (oxygen isotope stage 2) in age, based on calibrated soil ages. Three minor strath terraces are less widespread and preserved than the major fill terraces, and except for the highest terrace preserved (early middle Pleistocene), these terraces are estimated to be Holocene in age based on calibrated soil ages.

ACKNOWLEDGEMENTS

I would like to acknowledge and thank my thesis committee, Bruce Harrison, Peter Mozley, and Dave Love for guidance and constructive criticism regarding this project. In particular, I would like to extend further gratitude to Bruce Harrison, whose friendship, support and knowledge greatly improved my graduate career.

As with any project, many people deserve recognition for their help. Bruce's soil classes are thanked tremendously for digging a number of my soil pits. Nedra Alexander, Melissa Bordeaux, Layla Hall, Anna Jaramillo, and Amy Gibson are also thanked for helping analyze my soil samples in the laboratory. Also, Eric Fisher of the U.S.G.S. was instrumental in re-analyzing samples after my computer death. Finally, Ben Wear is thanked for sharing his knowledge and providing critical assistance while surveying.

TABLE OF CONTENTS

	<u>Page</u>
Acknowledgements	ii
Table of Contents	iii
List of Figures	vi
List of Tables	viii
List of Appendices	viii
1. Introduction	1
1.1 Approach	2
2. Background	5
2.1. Geologic Setting	5
2.1.1. Development of Rio Grande Rift	5
2.1.2. Development of Rio Grande	7
2.1.3. Rio Grande Basin Sediments	10
2.1.4. Socorro Basin Sediments	10
2.1.5. Physiographic Setting of the Socorro Basin	12
2.2. Fluvial System Theory	13
2.3. Development of Stream Terraces	15
2.4. Soils	16
2.4.1. Factors Influencing CaCO ₃ Accumulation in Soils	16
2.4.2. Calcic Soil Formation	17

2.4.3. Climate and Depth to Calcic Horizon	19
3. Methods	22
3.1. Selection and Topographic Analyses for Terrace Studies	22
3.2. Field Methods	23
3.3. Laboratory Methods	25
4. Results	29
4.1. Geomorphic and Soil Characteristics of Socorro Basin Tributaries	29
4.1.1. Little Nogal Arroyo	29
4.1.2. Socorro Canyon	33
4.1.3. Walnut Creek	43
4.1.4. Tiffany Canyon	45
5. Discussion	52
5.1. Socorro Basin Tributary Terrace Correlation	52
5.2. Comparison of Other Rio Grande Tributaries to Socorro Basin Tributaries	52
5.2.1. Arroyo de la Parida	54
5.2.2. Palo Duro Wash	56
5.2.3. Cuchillo Negro Creek	56
5.2.4. Albuquerque Rio Grande Terrace Sequence	56
5.3. Response Time for Terrace Formation	57
5.3.1. Response Time Indicated by Drainage Basin Area	57
5.3.2. Response Time Indicated by Longitudinal Profiles	61
5.3.3. Response Time Summary	65

5.4. Soil Variability	65
5.4.1. Soil Variability on a Single Surface	65
5.4.1.1. Bar Soils vs. Swale Soils	66
5.4.1.2. Statistical Analysis of Soil Development on Bar and Swale Sites	67
5.4.1.3. Variability of Soils Developed in Bar and Swale Sites	72
5.4.2. Variability of Soils on Correlated Pleistocene Terraces	75
5.4.3. Variability of Soils on Different Aged Terrace Surfaces	76
5.4.3.1. CaCO ₃ Profile Mass	76
5.4.3.2. Soil Development Index	78
5.4.3.3. Depth to Calcic Horizon	80
5.5. Spatial Variation in Calcium Carbonate Accumulation Rates	83
5.6. Formation of Correlated Tributary Terraces in the Socorro Basin	86
5.6.1. Fill Terraces	87
5.6.2. Strath Terraces	89
6. Summary	92
6.1. Soil Variability	92
6.2. CaCO ₃ Accumulation Rates	93
6.3. Terrace Ages and Controls on Terrace Formation	93
7. References Cited	95

LIST OF FIGURES

	<u>Page</u>
Figure 1. Location map of the Socorro Basin.	3
Figure 2. Map of Rio Grande Rift sub-basins.	6
Figure 3. Generalized geologic map of the Rio Grande basin.	8
Figure 4. Average monthly precipitation for Socorro and surrounding areas.	14
Figure 5. Graph showing the relationship between the depth of soluble salts and mean annual precipitation.	21
Figure 6. Shaded relief map of the Socorro Basin showing tributary drainage basin areas.	30
Figure 7. Geomorphic map of Little Nogal Arroyo.	31
Figure 8. LNA-T1 soil profile.	34
Figure 9. LNA-T2 soil profile.	35
Figure 10. LNA-T3 soil profile.	36
Figure 11. Geomorphic map of Socorro Canyon.	38
Figure 12. SC-T2 soil profile.	40
Figure 13. SC-T3 soil profile.	41
Figure 14. SC-T4 soil profile.	42
Figure 15. Geomorphic map of Walnut Creek.	44
Figure 16. WC-T1 soil profile.	46
Figure 17. WC-T4 soil profile.	47

Figure 18. Geomorphic map of Tiffany Canyon.	49
Figure 19. Arroyo cut exposures in Tiffany Canyon.	50
Figure 20. TC-T1 soil profile.	51
Figure 21. Graph of hypothetical hypsometric curves.	62
Figure 22. Hypsometric curves of tributary drainage basins.	63
Figure 23. Longitudinal profiles of correlated terraces.	64
Figure 24. Map of WC-T1 showing the location of soil pits.	69
Figure 25. Quartile comparison of Walnut Creek bar and swale soil parameters.	70
Figure 26. Box plot comparison between soil parameters from correlated terraces and Walnut Creek bar and swale soils.	77
Figure 27. Trench exposure along SC-T2 terrace riser.	79
Figure 28. Depth to calcic horizon and carbonate mass comparison between correlated terraces and Walnut Creek bar and swale soils.	82

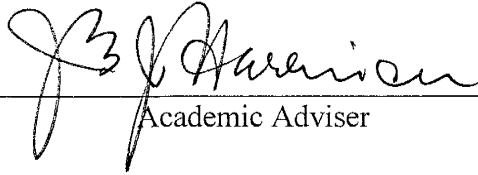
LIST OF TABLES

	<u>Page</u>
Table 1. Characteristics of Socorro Basin tributaries.	32
Table 2. Correlation chart of Socorro Basin tributary terraces.	53
Table 3. Correlation chart Socorro Basin tributary terraces and other Rio Grande tributary terraces.	55
Table 4. Bedrock vs. alluvium percents for each Socorro Basin tributary.	59
Table 5. Walnut Creek soil parameter data.	68
Table 6. Results from Mann-Whitney test on soil parameters.	73
Table 7. Soil Development Index of tributary terrace soils.	81
Table 8. Range of calcium carbonate accumulation rates in the Socorro Basin.	85

LIST OF APPENDICES

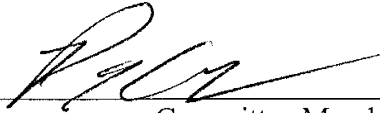
Appendix 1. Soil Descriptions	101
Appendix 2. Soil Development Index Values	107

This Thesis is accepted on behalf of the faculty
of the Institute by the following committee:

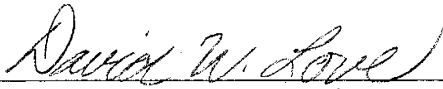


Academic Adviser

Research Advisor

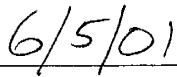


Committee Member



Committee Member

Committee Member



Date

CHAPTER 1. INTRODUCTION

Landscape development is the result of various processes and occurs over a range of time scales. Many types of landforms make up the landscape some of which include alluvial fans, fluvial terraces and aeolian sand sheets. One particular component of the landscape is the geomorphic surface (Ruhe, 1956), which can occupy a significant portion of the landscape as well as include many landforms (Tonkin et al., 1981; Ruhe, 1956). A geomorphic surface is defined as a mappable element of the landscape (both depositional and erosional) that has formed over a discrete period of time, the latter of which is represented through soil development (Ruhe, 1956). For example, as used in this study, soils that are developed on a tributary terrace landform constitute a geomorphic surface. Thus, A geomorphic surface is a time – stratigraphic unit.

Correlation and relative dating of geomorphic surfaces is commonly based on the degree of soil development. (Gile et al.,1981; Harden and Taylor, 1983; Machette, 1985; Mc Grath and Hawley, 1987; Harrison et al., 1990; Eppes, 1998; Treadwell, 1996; Narwold, 1999). For example, in the desert southwest United States, arid soils, which accumulate calcium carbonate over time, are commonly used in correlations and age estimations (Gile et al., 1981; Machette, 1985; McGrath and Hawley, 1987; Narwold, 1999).

However, all factors (except time) that influence soil development (Jenny, 1994) vary across a geomorphic surface thereby influencing rates of soil development. Some

workers have shown variations in soil development on the same aged surface (Eppes, 1998), particularly in bar and swale sites on fluvial terraces (Harrison et al., 1990). Unfortunately, in most soil geomorphic studies, correlations and age estimates are based on a limited number of soil pits per surface. Therefore, if soils are to be used to correlate and estimate ages of geomorphic surfaces, variations in soil development on a single geomorphic surface must be determined.

1.1. Approach

The present study addresses soil variability on tributary terraces of the Rio Grande within the Socorro Basin in central New Mexico (Fig. 1). Because the tributaries develop in response to incision of the Rio Grande, and incision along the Rio Grande is assumed consistent over the entire reach of the Socorro Basin, each tributary will respond by incising approximately the same amount in order to attain equilibrium with the new base level. Tributary terraces are correlated based on elevation above the respective modern arroyo, a method independent of soil development. Furthermore, because terraces represent the tributary paleo-stream channel that was graded to the Rio Grande, terrace heights represent the approximate paleo-elevations of the Rio Grande. Therefore, because the modern stream channels are graded to the modern Rio Grande, terrace heights above their respective stream channel can be used as a tool for correlating tributary terraces.

As the terraces are correlated by elevation rather than soil development, soils on correlated terraces in different tributaries can be compared to evaluate soil variability on the same-aged surface. To evaluate soil variability, this study considers 1) the variability

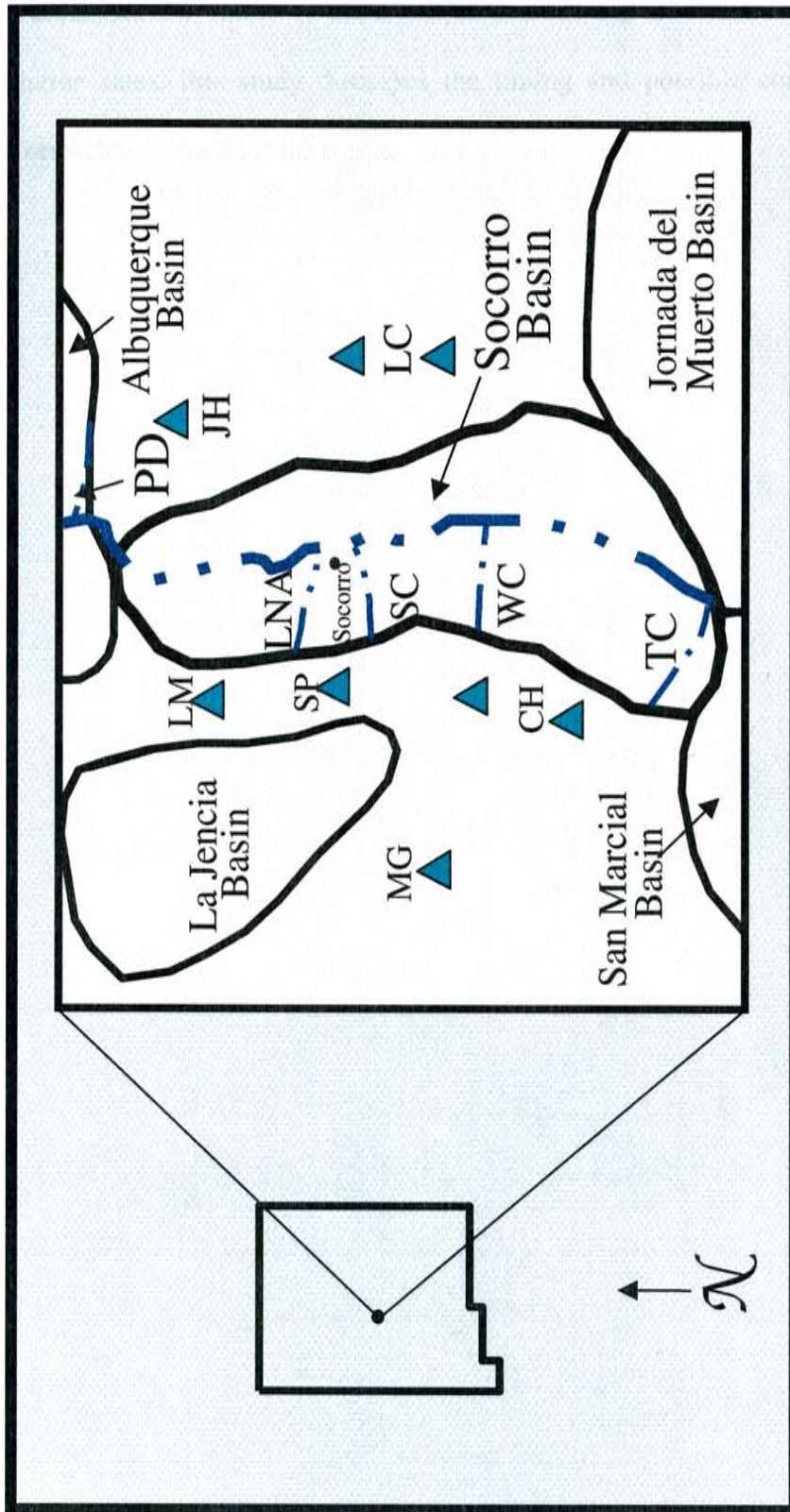


Figure 1. Location map of the Socorro Basin showing tributaries used in this study: (PD; Palo Duro Wash, LNA; Little Nogal Arroyo, SC; Socorro Canyon, WC; Walnut Creek, TC; Tiffany Canyon) and physiographic features: LM; Lemitar Mountains, SP; Socorro Peak, MG; Magdalena Mountains, CH; Chupadera Mountains JH; Joyita Hills, LC; Loma de las Canas.

on a single surface, 2) the variability between correlated terraces, and 3) variable CaCO_3 accumulation rates. Finally, after considering soil variability and variable accumulation rates, this study discusses the timing and possible controls on tributary terrace formation in the Socorro Basin.

CHAPTER 2. BACKGROUND

2.1. Geologic Setting

The Rio Grande Rift, located in the southwestern United States, is a north trending break in the continental lithosphere and is composed of many structurally controlled sub-basins (Fig. 2). These sub-basins are typically asymmetrical half grabens, which range from 55 to 240 km in length and from 5 to 95 km in width (Chapin and Cather, 1994). North of Socorro, the sub-basins form a right-stepping en-echelon pattern, whereas south of Socorro, the rift widens into a series of parallel sub-basins.

The modern Rio Grande flows from southern Colorado, through New Mexico and Texas, and ends in Tamaulipas, Mexico, where it flows into the Gulf of Mexico. The Rio Grande runs through the approximate center of the Socorro Basin and receives water and sediment from numerous tributaries.

2.1.1. Development of Rio Grande Rift

Rifting began approximately 30 Ma, after the Laramide orogenic event, and was synchronous with widespread volcanism. Rifting occurred along a general north-south structural grain imposed by the Laramide orogeny, where crustal inhomogeneities provided zones of weakness (Morgan and Golombek, 1984). At least two phases of extension have occurred within the Rio Grande Rift.

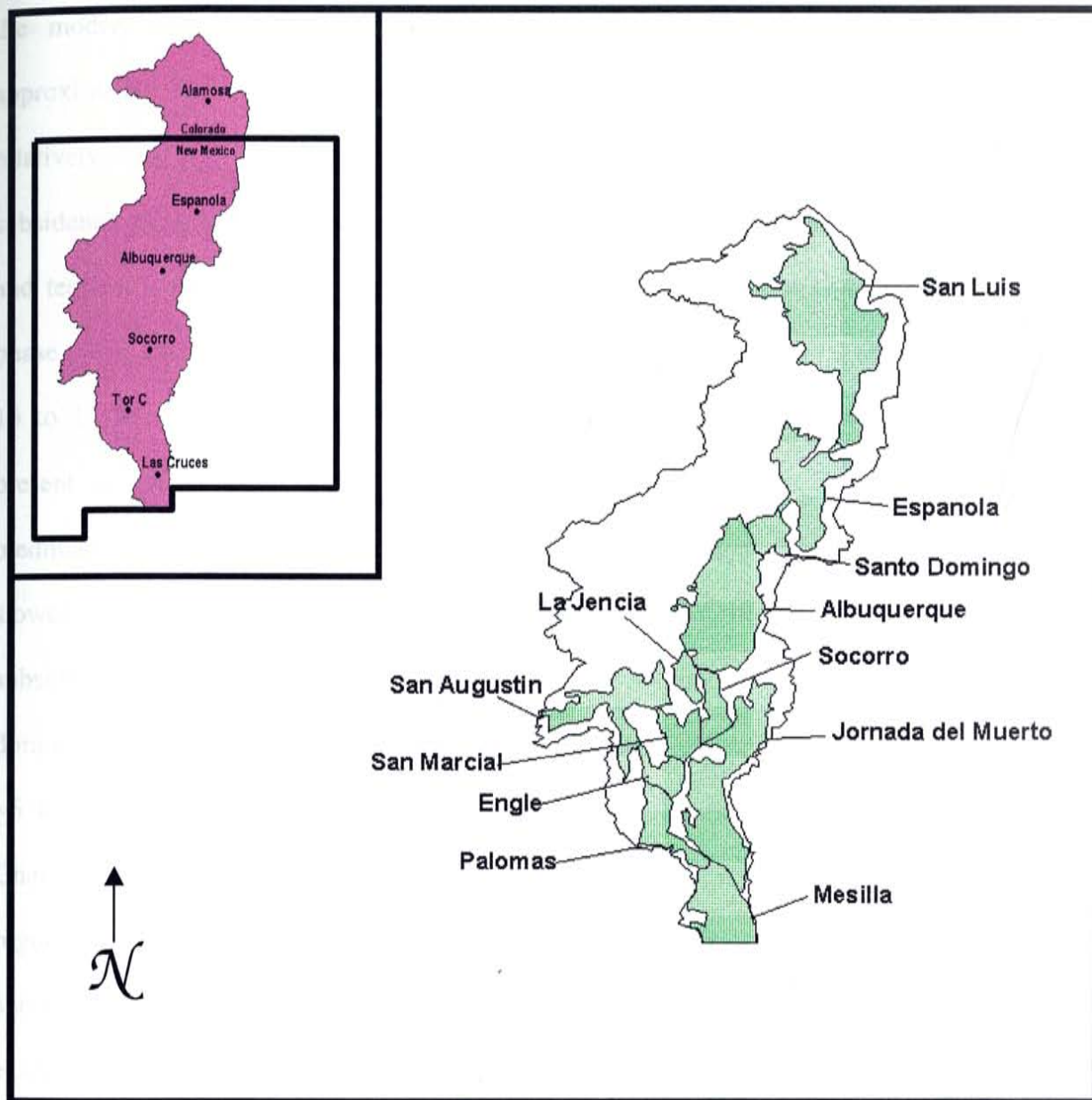


Figure 2. Map of Rio Grande basins. The sub-basins form a right-stepping en-echelon pattern north of Socorro, and widen into a series of parallel sub-basin south of Socorro. Inset map shows location and major towns. (Modified from Wilkins, 1986)

In the Socorro Basin, the first phase had a northeast axis of extension (oblique to the modern extensional axis), was contemporaneous with volcanism, and began approximately 28.6 Ma (Eaton, 1979; Cather et al., 1994). This phase of extension was relatively rapid and produced shallow, broad sub-basins through crustal thinning and subsidence along low-angle normal faults. After a few million years of relative volcanic and tectonic quiescence, the second phase of extension began to overprint the earlier phase. This later phase had an east-west axis of extension and lasted from approximately 16 to 10 Ma (Morgan and Golombek, 1984). Extension has continued through the present as evidenced by a number of Quaternary fault scarps located within many piedmont slopes of the basin margins. This second phase is generally characterized by slower extension than the first phase and produced narrow, deep sub-basins through subsidence along high angle normal faults. Block faulting during this phase had a dominant vertical component as evidenced by kilometers of vertical displacement (e.g. ~6 km in the Sandia Mountains, Albuquerque, NM). In the Socorro area however, Chamberlin (1983) has characterized Cenozoic extension as having a domino-style regime whereby older high angle faults have rotated to a flatter orientation and have subsequently been cut by the younger high angle normal faults of the second phase of extension. Volcanism was also contemporaneous with this phase of extension, producing primarily rhyolitic and basaltic lithologies.

2.1.2. Development of the Rio Grande

Although the major mountains and sub-basins (Fig. 3) of the Rio Grande Rift were developing during the Oligocene (~26 Ma), an axial river system did not develop

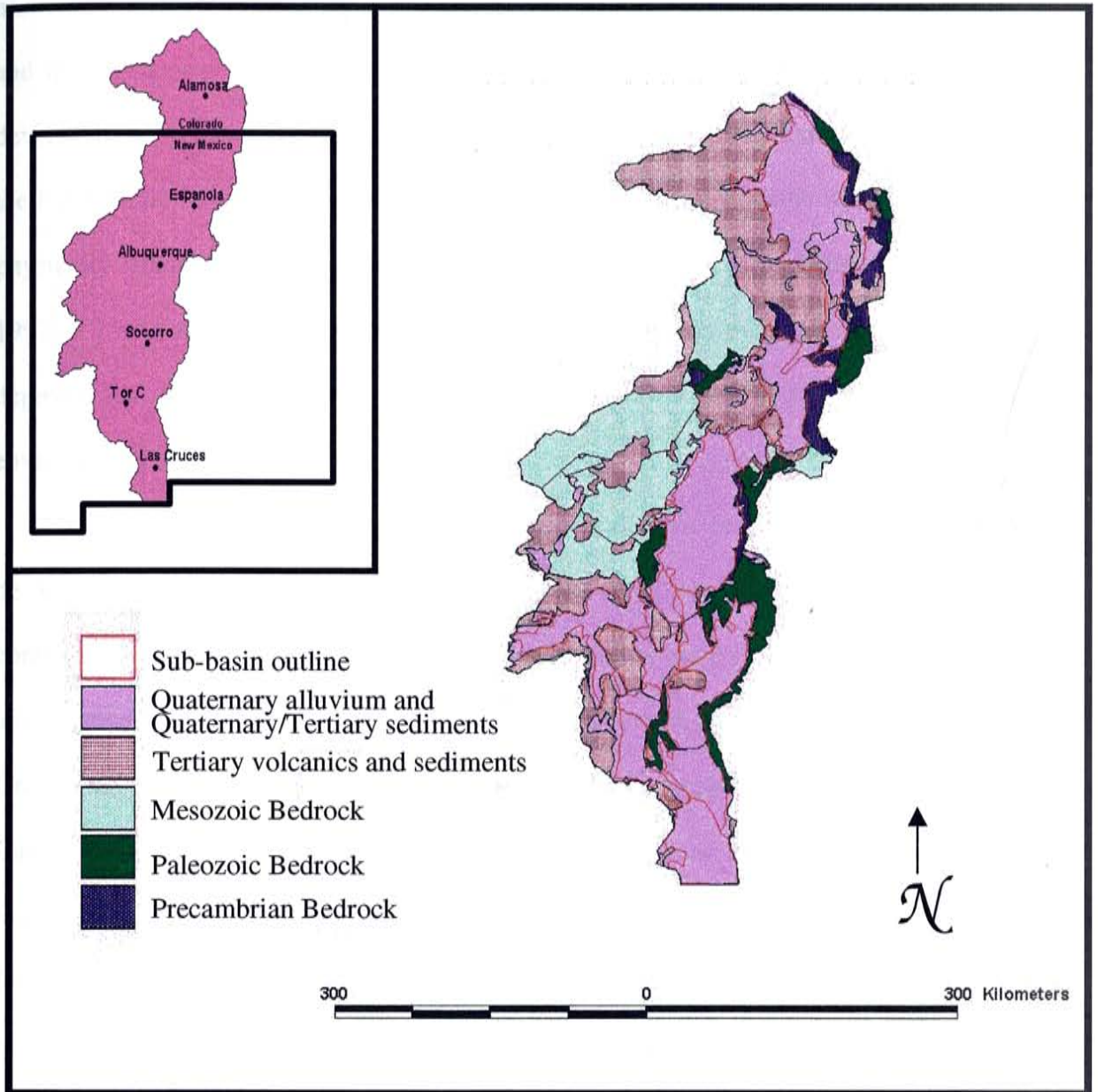


Figure 3. Generalized geologic map of the Rio Grande basin. Inset map shows location and major towns. (Modified from Wilkins, 1986)

until approximately the Pliocene (Mc Grath and Hawley, 1987). For example, in the northern Albuquerque Basin an axial Rio Grande had developed by approximately 7 Ma, and in the Socorro Basin (at the mouth of Socorro Canyon), an axial Rio Grande had developed by approximately 3.73 Ma (Love, in press). The earlier river system occupied the Rio Grande Rift; however, the ancestral Rio Grande was discontinuous, as it was not physically connected to the lower Rio Grande and the Gulf of Mexico (Mack et al., 1997). The discontinuous nature of the early Rio Grande is evident from basin floor deposits in southern New Mexico that represent fluviolacustrine depositional environments (Mack et al., 1997).

The upper and lower reaches of the Rio Grande were separated by Lake Cabeza de Vaca in southern New Mexico. The base level of the Rio Grande was largely controlled by Lake Cabeza de Vaca located in the Mesilla basin in southern New Mexico and northern Mexico (Gile et al., 1996). As the lake filled, base level rose and the Rio Grande aggraded until the lake overflowed (~750,000 years ago). The draining of Lake Cabeza de Vaca ultimately caused a drop in the base level and thus the onset of incision into the previously aggraded deposits. The present Rio Grande valley is an erosional feature of the river, which is incising into the ancient basin-fill deposits. At least four major episodes of river incision separated by long intervals of valley back filling or base level equilibrium have occurred since the onset of river incision during the mid-Pleistocene (Mc Grath and Hawley, 1987; Connell and Love, 2000).

2.1.3. Rio Grande Basin Sediments

The Santa Fe Group is the Rio Grande basin fill unit. The maximum thickness of the Santa Fe Group ranges from approximately 2,500 meters in the southern basins to 9,000 meters in the northern-most San Luis Basin (Wilkins, 1986). It consists of unconsolidated to moderately consolidated sediments, and volcanic rocks. These sediments are composed of layers of gravel, sand, silt, and clay, interbedded with local volcanic flows and tuffs (Wilkins, 1986). Deposition of Santa Fe Group sediments began during the Late Oligocene and continued until mid- to late- Pleistocene (~1.2 Ma in the Socorro area), a time that spans both phases of extension (McGrath and Hawley, 1987; Cather et al., 1994).

2.1.4. Socorro Basin Sediments

The Santa Fe Group in the Socorro Basin is subdivided into the Sierra Ladrones Formation (Pliocene to mid Pleistocene) and the Popotosa Formation (Oligocene-Miocene) (Machette, 1978). Both formations are comprised of piedmont facies, as well as volcanic deposits. However, in addition to the piedmont facies and volcanic deposits, the Sierra Ladrones and Popotosa Formations are also comprised of axial river and playa facies, respectively. Interfingering of piedmont and axial or playa deposits are common in areas of transition along the basin margin (Bruning, 1973).

The piedmont facies is characterized by interbedded conglomerate and sandstone. Conglomerates are typically clast supported and poorly sorted. The sandstone is typically a lenticular unit that is medium to coarse grained, pebbly, and contains either cross beds or horizontal bedding. The main difference in this facies between the Sierra Ladrones and

the Popotosa Formations is that the Popotosa Formation represents an internally drained basin, which lacks an axial river, whereas the Sierra Ladrones represents the development of an axial river system. For example, the Sierra Ladrones Formation is dominated by extra-basinal clasts of Mesozoic, Paleozoic and Precambrian siliciclastics, with minor volcanoclastic detritus. Conversely, the Popotosa Formation is dominated by volcanoclastic sediment (Bruning, 1973).

The axial river facies are characterized by channel and floodplain deposits of the ancestral Rio Grande. Interbeds of conglomerates, sandstones, siltstones, and claystones are present within this facies. The conglomerate is well - to sub - rounded fluvial pebbles (quartzite, chert, granite, gneiss, schist, obsidian) of a non-local source. The sandstone in this facies is typically cross-bedded and poorly indurated.

Playa and lake facies are dominated by mudstone with lesser amounts of sandstone. The mudstone is typically a laminated unit that is red/brown in color with a few green/gray zones that are parallel to bedding. The sandstone in this facies is typically thin tabular beds (<.3 meters) that are very fine to medium grained.

Volcanic deposits consist of flows, cinders, ash, and pumice of mafic and silicic compositions, all of which are incorporated within both the Sierra Ladrones and Popotosa Formations. Ash and pumice deposits have typically been reworked by water and deposited within the sedimentary formations.

In addition to these facies, transitional facies are also present in both formations, representing overlap in depositional environments. The axial-piedmont facies of the Sierra Ladrones Formation consists of the interfingered piedmont and axial river facies mentioned above. The playa margin facies of the Popotosa Formation consists of

interbedded sandstone and mudstone that in turn is interfingered with distal piedmont facies deposits (Bruning, 1973).

Hawley (1998), identified four stratigraphic components of the basin-fill material: 1) coarse grained, basin margin piedmont and related alluvial slope deposits, 2) fine-grained closed basin lake, playa, and alluvial flat sediments, 3) basin floor deposits of an axial stream, and 4) local aeolian sand deposits. The coarse grained, basin-margin piedmont and related alluvial slope deposits are associated with both the early phase of extension as well as with the response to block faulting during the later phase of extension. The fine-grained closed basin lake, playa, and alluvial flat sediments represent deposits associated with the time prior to a through flowing axial river system (>5 Ma). The basin floor deposits of the axial Rio Grande in the Socorro Basin are typically channel and floodplain deposits of the through flowing Rio Grande. After deposition of the Santa Fe Group sediments, widespread geomorphic surfaces (Ruhe, 1956, 1974) developed along the piedmont slopes of the basin margins.

2.1.5. Physiographic Setting of the Socorro Basin

The Socorro Basin, located in Central New Mexico, is a relatively narrow sub-basin within the Rio Grande Rift. It is approximately 55 km long and 16 km wide and is estimated to be at least 1.2 km deep (Sanford, 1968) (Fig. 1). The eastern boundary of the Socorro Basin consists of the hills and mesas of Loma de las Canas and the Joyita Hills. The Lemitar, Socorro and Chupadera Mountains comprise the western basin margin, which is the boundary between the Socorro and La Jencia Basins.

The climate in the study area typically consists of hot summers and cool winters, where maximum summer temperatures average 94° F and minimum winter temperatures average 23° F. Although the annual total precipitation is 9.5 inches, the majority of precipitation falls during intense summer monsoons (Western Regional Climate Center, 2000; Fig. 4).

2.2. Fluvial System Theory

When considering rivers or streams, the fluvial landscape is an open geomorphic system where interaction occurs between mass and energy within the landscape over time (Bull, 1991a). In a general sense, base level (the lowest altitude to which erosion can lower the landscape) largely controls the interactions that occur within fluvial systems over large timescales. However, on shorter timescales, base-level-independent processes such as stream gradient adjustments and local aggradation within the drainage area, largely control the interactions that occur within the fluvial system (Bull, 1991a).

Open geomorphic systems are characterized by reversible processes (Bull, 1991a). In a fluvial setting, an example of reversible processes is aggradation and degradation of the valley floor. These processes are controlled by changes in both the internal (dependent variable) and external (independent variable) components of the fluvial system. However, most fluvial systems respond primarily, over longer time periods, to independent variables such as climate and relief, which are external to the fluvial system (Bull, 1991a).

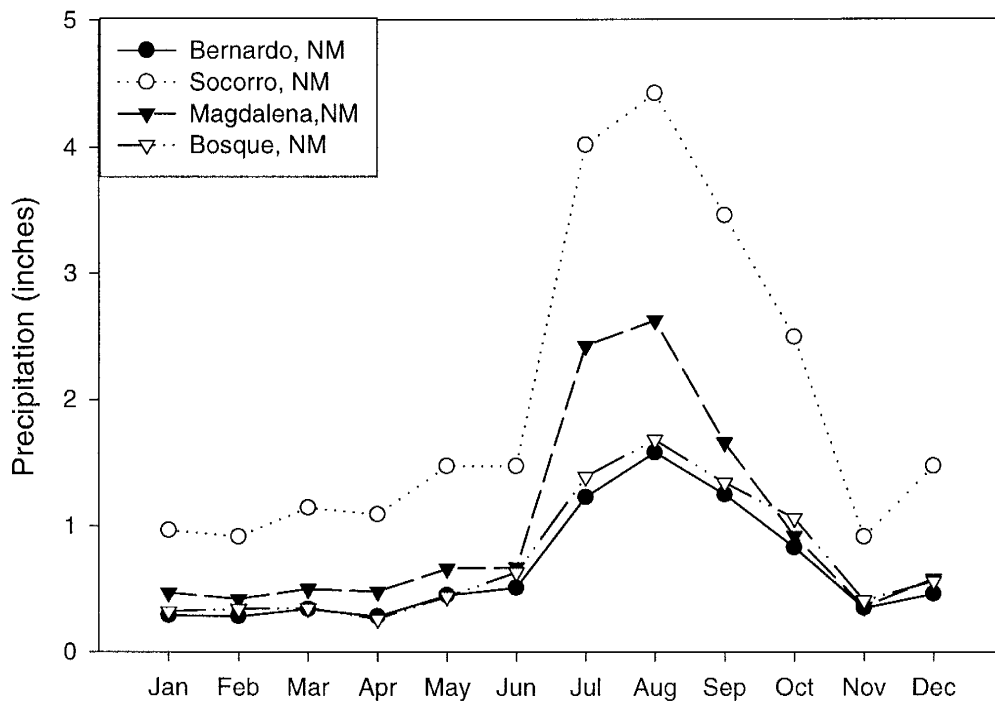


Figure 4. Average monthly total precipitation for Socorro, New Mexico and surrounding areas. (source: Western Regional Climate Center, 2000)

2.3. Development of Stream Terraces

Aggradation and degradation of the valley floor can be described as the balance between two major components of fluvial processes; stream power and resisting power.

Stream power is the power *available* to transport sediment and resisting power is the power *needed* to transport sediment (Bull, 1991a). Stream power can be considered as a function of discharge. That is, high stream power is coincident with high discharge. Resisting power on the other hand can be considered as a function of potential sediment yield. That is, changes in the amount and size of bedload from hillslope subsystems, and variables related to bedload sources (i.e. vegetation abundance) affect the resisting power. For example, during an interglacial when the climate is relatively dry and hot, more erodable hillslopes may be exposed due to sparse vegetation distributions. In this case, the increase in sediment availability from the hillslopes increases the resisting power.

The threshold of critical power is the ratio of stream power to resisting power and 'the variables that affect the numerator and the denominator interact to determine the capacity and competence of a stream to transport bedload' (Bull, 1991a). When stream power exceeds resisting power, the ratio is greater than 1 and degradation occurs. Conversely, when stream power is less than resisting power, the ratio is less than 1 and aggradation occurs given the availability of mobile sediment. Aggradation and degradation cycles dictate the formation of stream channels as well as the subsequent abandonment by the stream channel to form terrace treads. For example, if conditions favor aggradation, the stream channel and floodplain will continue to accumulate material until a time when conditions change. The change in conditions may then favor degradation and ultimately, incision will leave a terrace tread as a remnant of the former

stream channel. Thus, terrace treads represent a remnant of the former valley floor that has been abandoned by the stream as a result of channel incision (Bull, 1991a). Two main types of fluvial terraces exist, fill and strath/cut, and each one forms from different changes in variables.

Fill terraces are depositional terraces that are typically greater than 2 meters in thickness (Bull, 1990). They form by aggradation of the valley floor followed by subsequent incision, which abandons the former stream channel as a terrace tread. Strath/cut terraces are erosional terraces that typically form by lateral erosion while the fluvial system is in or close to relative equilibrium with base level. Strath terraces are eroded into bedrock, while cut terraces are eroded into alluvium. Because strath and cut terraces are erosional, they are generally associated with thin (<2 meters) gravel caps, which are considered the cutting tools of the erosional surface, or a lag deposit (Bull, 1991b).

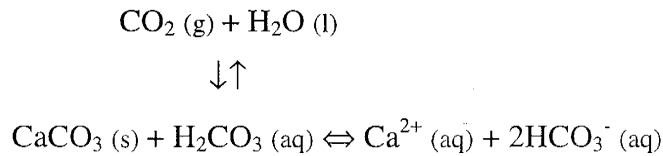
2.4. Soils

2.4.1. Factors Influencing CaCO₃ Accumulation in Soils

Soils forming in semi-arid environments are characterized by accumulation of CaCO₃ to form calcic horizons. Variability between calcic soils can be seen in both the depth to and morphology of the calcic horizons as well as the total profile mass of calcium carbonate (Machette et al., 1997). Parameters that influence the distribution of CaCO₃ in soils include: the solubility of CaCO₃, the accumulation of aeolian material, the available moisture, the presence and type of vegetation, and the textures of deposits.

2.4.2. Calcic Soil Formation

The incorporation of CaCO_3 into a soil profile is described through the reactions:



(Birkeland, 1999). An increase in either CO_2 pressure or H^+ concentrations increases the solubility of CaCO_3 and drives the reaction to the right. Conversely, as the reaction is driven to the left, precipitation of CaCO_3 results from 1) a decrease in CO_2 pressure or H^+ concentrations, 2) the occurrence of calcium saturated soil water, or 3) evapotranspiration of the soil water (Birkeland, 1999). In addition, temperature also affects the solubility of CaCO_3 and H_2CO_3 . An increase in temperature will decrease the solubility of CaCO_3 , as $\text{CO}_2 (\text{g})$ is less soluble in warm water than in cold water (Arkley, 1963).

The Ca^{2+} ion can be derived from mineral weathering, and CaCO_3 is limestone. However, CaCO_3 derived from atmospheric additions, either dissolved in rainwater or as particulate matter in dust, is the dominant constituent in the formation of calcic soils in the desert southwest United States (Gile et al., 1981). The development of calcic soils where CaCO_3 is of atmospheric origin is a function of dust composition and accumulation rates, and rainfall (Birkeland, 1999).

A dissolved source for secondary calcium carbonate is primarily the presence of Ca^{2+} in precipitation. The solid source of secondary calcium carbonate is mainly through dust deposition. Dust trap data in Las Cruces, New Mexico indicate that modern dust consists of almost 5% carbonate (Gile et al., 1981; Birkeland, 1999). In addition, dust trap data from southern Nevada and California indicate that modern dust measured between 1985-1989 contains 8% to 32% carbonate (Reheis and Kihl, 1995).

Once dust accumulates on the surface, the Ca^{2+} and CaCO_3 are translocated into the soil profile by water. Because of plant growth and biologic activity, the CO_2 partial pressure ($p\text{CO}_2$), which is a major control on CaCO_3 dissolution, (Drever, 1997) is high in the upper portion of the soil profile where roots are most abundant. In addition, upon contact with water, CO_2 forms HCO_3^- . Once enough water is added, the Ca^{2+} and HCO_3^- are leached downward to a depth, dependent on the amount of water available. Precipitation of CaCO_3 and thus the formation of calcic horizons occur as a result of 1) decreasing CO_2 partial pressure below the root zone and biologic activity and 2) a progressive increase in Ca^{2+} and HCO_3^- with depth as water moves downward and/or as water is lost by evapotranspiration.

Continual accumulation of CaCO_3 in a soil results in changes in the soil profile morphology. Gile et al., (1981) recognized four progressive stages of carbonate development in arid soils in southern New Mexico. The four stages of carbonate development have been defined for both fine- and coarse-grained material. Because the deposits in this study are coarse grained, only the carbonate stages for coarse alluvium will be discussed here. The stages of carbonate development begin with stage I, where the undersides of clasts begin to show signs of carbonate coatings. Stage II and III are represented by 1) progressively more carbonate coatings surrounding clasts (stage II), and 2) complete induration of carbonate around clasts and within voids (stage III). Stage III eventually becomes so indurated with carbonate that all voids become plugged, preventing vertical movement of water. Stage IV is characterized by thin laminar layers that form from the collection of water over the plugged (Stage III) material. Machette (1985) recognized two additional stages to the initial carbonate stage classification of

Gile et al., (1981). Stage V is characterized by a thicker laminar layer (>1 cm), thin to thick pisolites (accretionary masses of carbonate) and vertical faces and fractures that are coated with carbonate. Stage VI morphology is characterized by multiple episodes of brecciation and pisolite formation that has subsequently been recemented and relaminated.

2.4.3. *Climate and Depth to the Calcic Horizon*

The depth to the calcic horizon is largely dependent on climate, specifically, precipitation (Arkley, 1963; Dan and Yaalon, 1982; Mc Donald, 1994). Some Pleistocene soils exhibit bimodal calcium carbonate distributions with depth (Mc Donald, 1994). In other words, two areas of calcium carbonate accumulation are present throughout the soil profile, one near the surface and one at some depth. Model simulations of Pleistocene soils containing bimodal calcium carbonate distributions suggest that this distribution reflects a shift into a relatively drier climate in the Holocene (Mc Donald, 1994). In addition, Mc Donald (1994) suggests that deep movement of soil water, and thus translocation of calcium carbonate in Pleistocene soils is due to precipitation patterns analogous to modern slow moving frontal storms during the spring and winter, rather than large high intensity convective summer storms.

Dan and Yaalon (1982), present a climate-soil transect from southern Israel, which relates the depths to carbonate, and gypsum with mean annual precipitation (Fig. 5). Their findings show greater depths to carbonate with increasing mean annual precipitation. Furthermore, Figure 5 also shows an absence of carbonate where mean annual precipitation is less than about 9 cm. In a hyper-arid environment with low

precipitation, there is very little vegetation. Thus, the $p\text{CO}_2$ is so low that precipitation of carbonate yields to precipitation of gypsum (Birkeland, 1999).

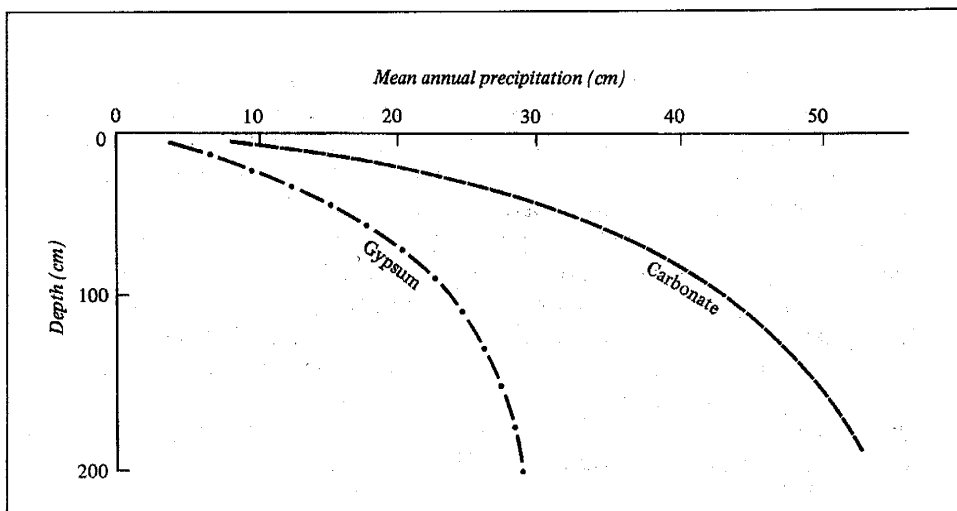


Figure 5. Depth to calcium carbonate and gypsum versus mean annual precipitation. (Dan and Yaalon, 1982)

CHAPTER 3. METHODS

3.1. Selection and Topographic Analyses for Terrace Studies

Tributaries were selected based on reconnaissance field investigation of Rio Grande tributaries throughout the Socorro Basin. Tributaries were selected for this study based on good spatial coverage throughout the basin (from the northern to the southern portion of the Socorro Basin) and the number of terraces within the tributary terrace sequence. Good spatial coverage of field sites throughout the Socorro Basin was necessary to determine the regional extent of correlated surfaces. To attain the most complete record of tributary terraces, selected tributaries contain at least two terrace surfaces.

The main tributaries used in this study are, from north to south, Little Nogal Arroyo, Socorro Canyon, Walnut Creek and Tiffany Canyon (Fig. 1). These tributaries occupy the western piedmont slopes of the Socorro Basin. Tributaries on the western margin of the basin were chosen for this study in part because the terraces are typically better preserved than those occurring on the eastern margin. In addition, because calcic soils were a fundamental component of this study, it was necessary to avoid CaCO_3 inputs to the soil from sources other than aeolian additions. Therefore, tributaries on the western margin were selected because, unlike the eastern margin, only minor amounts of limestone bedrock occur in the western margin drainage basins. The tributaries used in this study provide adequate spatial coverage throughout the Socorro Basin, from Little

Nogal Arroyo near the northern boundary of the basin, to Tiffany Canyon near the southern boundary thereby permitting the evaluation of variability along the length of the Socorro Basin.

Drainage basin area was determined for all tributaries by using geo-referenced USGS 7.5' topographic maps. The area of the drainage basins and hypsometric analysis was completed using USGS 7.5' Digital Elevation Models (DEM's) and Arc View 3.2a.

After locating the tributaries, selection of the terrace sequence within the drainage was constrained to 1) areas where the terraces were well preserved, and 2) areas within the drainage where major bedrock outcrops do not occur. The lack of major bedrock outcrops is important because, since fluvial activity in the tributaries are considered regional processes, the resistance of the material being incised into must be consistent throughout all drainages. Therefore, sites within the drainage where incision into unconsolidated alluvial fans or moderately consolidated Santa Fe Group sediments were used. Terrace surfaces were identified and mapped at a scale of approximately 1:6000.

3.2 . Field Methods

One soil pit, approximately 1m³ in size was dug on each terrace surface in each tributary to compare the degree of soil development among tributaries. One soil pit per surface was adequate to assess soil development because they were located in areas shown to have the least soil variability (Harrison, 1990; and this study). Soil pits were located near the center of the terrace treads, in an area that lacked deposition from the adjacent terrace riser, or erosion from the terrace edge. Three backhoe trenches were dug on two terrace surfaces in Socorro Canyon. Four trenches, located on small terrace

remnants near the Walnut Creek and Hwy 25 intersection were discovered late in the project. The Walnut Creek trenches were excavated by an unknown source likely related to gravel exploration.

Soil profiles were described according to the Soil Survey Staff (1951, 1975) and Machette (1985), and then sampled for laboratory analyses. Sampling of the soil profile was on a per horizon basis, although when soil horizons exceeded 40cm in thickness, the soil horizon was sampled at 20cm intervals.

The elevations of terrace treads above the modern arroyo bottom were measured using a digital theodolite and EDM (Electronic Distance Measuring Instrument) provided by the New Mexico Bureau of Mines and Mineral Resources. Because terraces are not preserved throughout the length of each arroyo, elevation measurements were made at different distances from the Rio Grande within the tributaries. Survey transects were determined prior to surveying and were perpendicular to the terrace trends and the stream channels.

The terraces were classified as either strath or fill terraces based on the thickness of the gravel terrace deposit, the type of underlying material (i.e. tributary valley fill or bedrock), and the elevation and type of contact (i.e. depositional or erosional) between the terrace gravels and underlying stratigraphy.

The elevation of terraces above their respective streambed was used to correlate terraces between the tributaries. Because complete terrace stratigraphy is not exposed in every tributary, the elevation of the top of the fluvial gravel deposit was used to correlate terrace surfaces. However, few exposures of the cut or strath surface do occur, and the elevation of these surfaces above their respective stream channels appear to be consistent

between tributaries. Heights of major fill terraces do not vary significantly along the reach of the stream where they are preserved, and comparable terrace heights between tributaries occur. Therefore, the fact that the terraces are located at different distances within each tributary does not appear to hinder the use of terrace height as a correlative tool in this study.

3.3. Laboratory Methods

Laboratory analysis was conducted on soil samples collected from soil pits, trench excavations and stream cuts, and followed the standard methods described by Singer and Janitzky (1986). Analyses of the soil samples included particle size distribution (PSD), calcium carbonate (CaCO_3) percent, and bulk density of the soils fine ($<2\text{mm}$) fraction. To ensure internal consistency between runs of samples, randomly chosen samples were reanalyzed during each new run. In addition, the CaCO_3 and bulk density analyses were combined with field descriptions to calculate total CaCO_3 profile mass.

Samples were collected on a per horizon basis. Samples were sieved to separate the fine fraction ($<2\text{mm}$) from the coarse fraction, and then the fine fraction was split into the appropriate amounts for each laboratory procedure.

Particle size distribution (PSD) is a textural classification, and yields percentages of sand, silt, and clay, and was determined using the pipette method as described by Singer and Janitzky (1986). Because CaCO_3 tends to bind the clay particles together, CaCO_3 digestion using a 0.5 N Sodium Acetate solution was the initial step in this procedure. In addition, clays were deflocculated using a 10% Sodium Pyrophosphate dispersant.

Soil development in arid environments is characterized by the accumulation of CaCO_3 in the soil matrix and/or as clast coatings (Gile, et al., 1981). Therefore, the CaCO_3 in the fine fraction of the soil as well as the CaCO_3 coatings on clasts were considered when quantifying the accumulation of CaCO_3 (McDonald, 1994, Eppes, 1996). The contribution of CaCO_3 rinds to the total CaCO_3 profile mass was determined in both the field and the laboratory. Rind thickness was measured using a caliper and/or a comparator, average clast size was determined by measuring a number of clasts per horizon, and percent of rind coverage per clast was visually estimated, as was gravel percent per horizon. These field observations were then combined with laboratory analyses (discussed later) to determine the total CaCO_3 content per horizon. Total CaCO_3 profile mass is calculated by summing the CaCO_3 mass per horizon as denoted in the following equation:

$$[(\text{BD}_F * \%C_F * (1-\%G)) + (\%R * \text{BD}_R * \%C_R)] * T$$

BD_F = bulk density of the <2mm fraction of sample

$\%C_F$ = weight percent of CaCO_3 in the <2mm fraction of sample excluding the contribution from the parent material

$\%G$ = volume percent of gravels in each soil horizon

$\%R$ = volume percent of CaCO_3 rind in each horizon

BD_R = average bulk density of CaCO_3 rinds

$\%C_R$ = weight percent of CaCO_3 in rinds

T = horizon thickness

CaCO₃ percent was determined using a Chittick apparatus as described by Singer and Janitzky (1986). In addition, the CaCO₃ contribution from the fluvial parent materials fine fraction was subtracted from each sample. However, the A horizons in most soil profiles are formed in accumulated aeolian material and the parent material CaCO₃ contribution was not subtracted from these horizons. The bulk density of soil fine fractions and CaCO₃ rinds were measured using the Paraffin clod method described by Singer and Janitzky (1986).

The Soil Development Index (SDI) of Harden (1982) and Harden and Taylor (1983) is a semi-quantitative measure of soil development and can be used to compare soils on different-aged surfaces as well as to correlate similar-aged surfaces. Any soil parameter(s) can be used to calculate the SDI, some of which are color, structure, texture, clay films, and carbonate morphology. The SDI was calculated for all tributary terraces used in this study. The SDI values represent soil development based on actual total profile depth, whereas the nSDI values represent soil development based on a common depth of 135 cm for all soil profiles. Because most soil profiles are described to variable depths based on the age of the soil, the SDI values of younger soils may vary significantly depending on the total soil depth described. Therefore, the SDI of each soil was calculated to the depth of maximum soil development in that soil pit.

Soil parameters that appear to best characterize semi-arid soils were used in SDI calculations and include structure, texture, and carbonate morphology. The carbonate morphology calculation uses the laboratory values of CaCO₃ percent of each horizon minus the CaCO₃ percent of the parent material. In addition, laboratory textures determined through particle-size analysis were used in the SDI calculations.

Means, standard deviations, and 95% confidence intervals for soil parameters were determined using the computer program Minitab. In addition, Minitab was used to perform the non-parametric Mann-Whitney test.

CHAPTER 4. RESULTS

4.1. Geomorphic and Soil Characteristics of Socorro Basin Tributaries

4.1.1. Little Nogal Arroyo

Little Nogal arroyo is approximately 3.5 km north of the town of Socorro (Fig 1). Its headwaters are approximately 20 km west of Socorro, in Water Canyon in the Magdalena Mountains. The Little Nogal Arroyo drainage basin is the largest of all tributaries used in this study and is approximately 315 km² (Fig. 6). The arroyo trends toward the east where it cuts between Socorro Peak to the south and Strawberry Peak to the north. It continues to trend eastward where it runs through the community of Escondida before reaching the Rio Grande. Little Nogal Arroyo terraces used in this study are located on the eastern side of Strawberry and Socorro Peaks, where the arroyo has incised into Rio Grande valley-fill deposits. The lithologies of terrace gravels in this arroyo are locally derived rhyolite and andesite, although minor amounts of limestone and other sedimentary rocks are also present locally.

Three terrace surfaces are preserved on the southern side of this arroyo (LNA-T1, LNA-T2 and LNA-T3; Fig. 7). LNA-T1 is the topographically highest terrace at approximately 7 meters above the current arroyo bottom, LNA-T2 is the intermediate terrace at approximately 4 meters, and LNA-T3 is the lowest at approximately 1 meter (Table 1).

Drainage Basin Area

Little Nogal Arroyo	315 km ²
Socorro Canyon	123 km ²
Walnut Creek	87 km ²
Tiffany Canyon	140 km ²

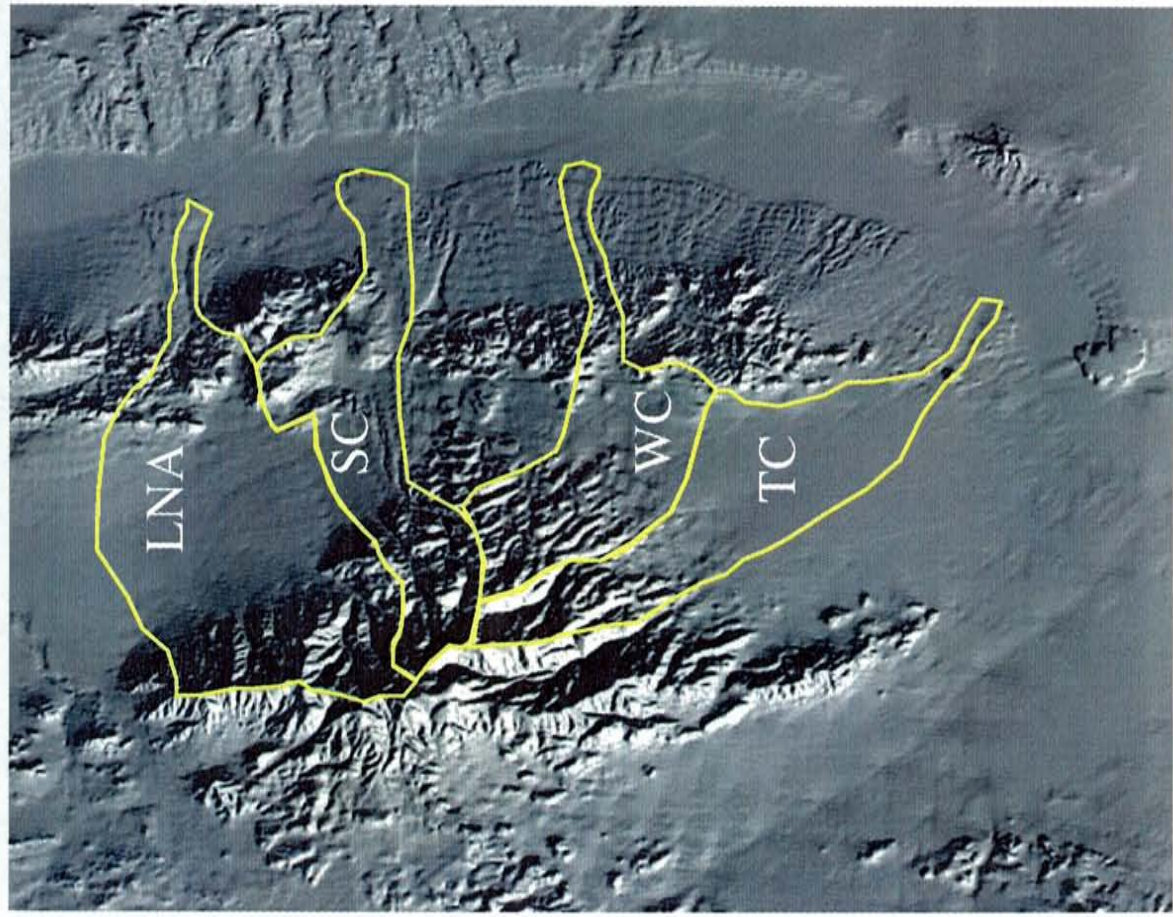


Figure 6. Shaded relief map showing tributary drainage basins.

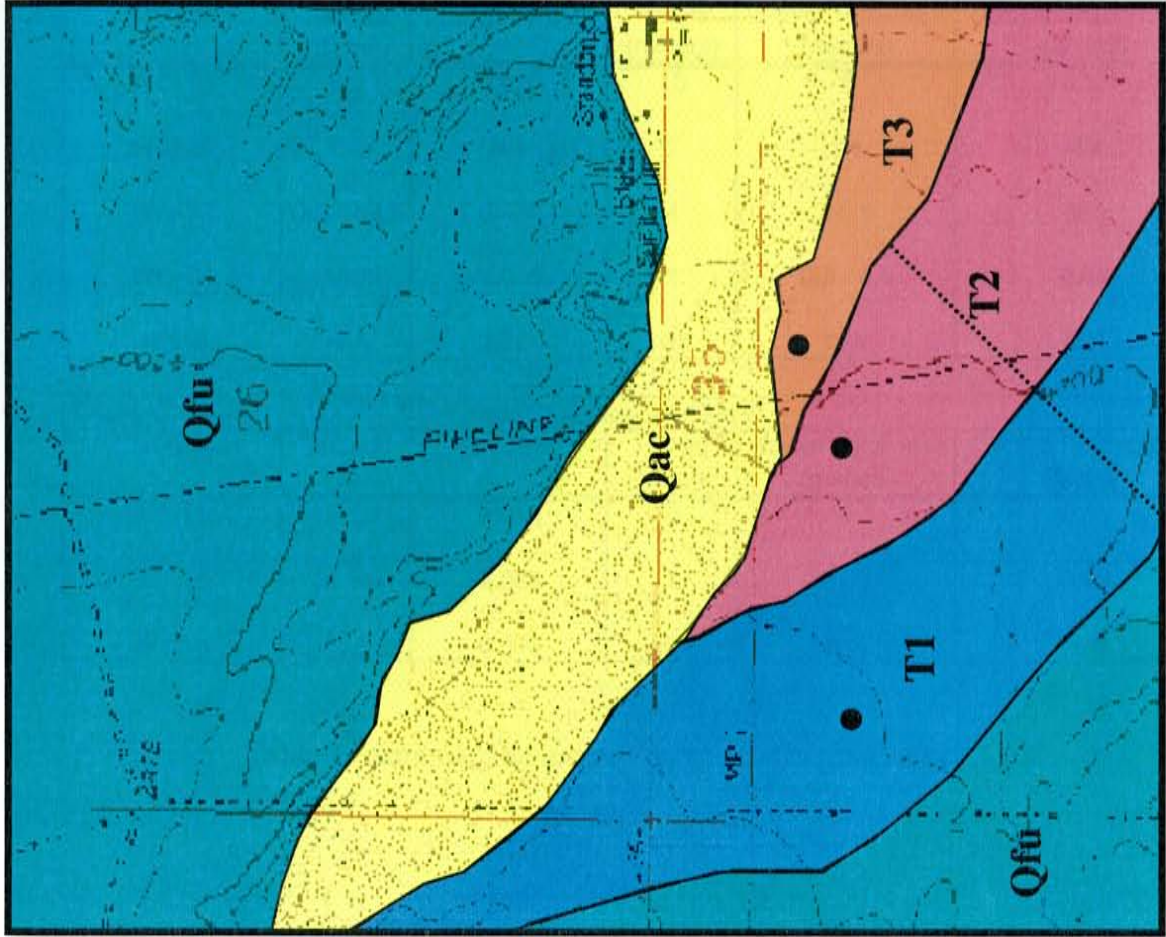
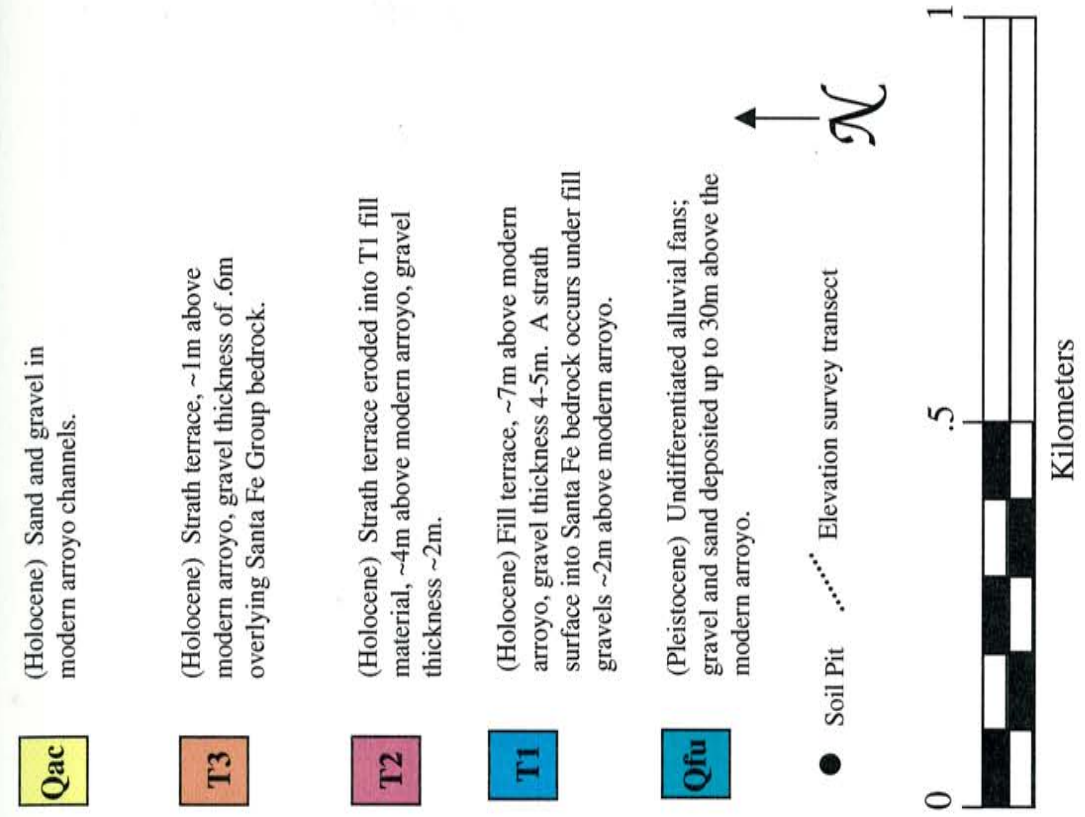


Figure 7. Geomorphologic Map of Little Nogal Arroyo

Map Source: Socorro quadrangle, NM-Socorro County, USGS 7.5' series (topographic), 1979

Lillite Nogal Arroyo		Drainage Basin Area: 315 km ²			
Terrace	Terrace Type	Gradient	Height (meters)	Gravel Thickness (meters)	CaCO ₃ Profile Mass (g/cm ²)
LNA-T1	Fill	0.014	7	<4-5	1.81
LNA-T2	Cut/Strath	0.013	4	<2	1.81
LNA-T3	Strath	0.015	1	0.6	1.15
Arroyo	N/A	0.025	N/A	N/A	N/A

Socorro Canyon		Drainage Basin Area: 123 km ²			
Terrace	Terrace Type	Gradient	Height (meters)	Gravel Thickness (meters)	CaCO ₃ Profile Mass (g/cm ²)
SC-T1	Strath	0.029	29	<2	55.82
SC-T2	Fill	0.022	9	>3	8.93
SC-T3	Fill	0.021	6	~3	1.01
SC-T4	Cut/Strath	0.018	5	0.6	1.11
SC-T5	Strath	0.022	1	<0.6	N/A
Arroyo	N/A	0.029	N/A	N/A	N/A

Walnut Creek		Drainage Basin Area: 87 km ²			
Terrace	Terrace Type	Gradient	Height (meters)	Gravel Thickness (meters)	CaCO ₃ Profile Mass (g/cm ²)
WC-T1	Fill	0.023	10	8	8.17
WC-T2	Fill	N/A	7	>4	N/A
WC-T3	Cut/Strath	0.023	4	>1.3	N/A
WC-T4	Strath	0.016	1	0.3 - 0.6	0.68
Arroyo	N/A	0.021	N/A	N/A	N/A

Tiffany Canyon		Drainage Basin Area: 140 km ²			
Terrace	Terrace Type	Gradient	Height (meters)	Gravel Thickness (meters)	CaCO ₃ Profile Mass (g/cm ²)
TC-T1	Fill	0.018	9	6	8.60
TC-T2	Strath	0.023	1	0.65	0.83
Arroyo	N/A	0.016	N/A	N/A	N/A

Table 1. Summary tables for Socorro Basin tributaries

LNA-T1 is a fill terrace that is no more than 4 to 5 meters thick (Table 1). The erosional contact between the fill material and the underlying Rio Grande valley-fill bedrock is approximately 2 meters above the modern arroyo bottom. LNA-T2 is an erosional terrace that has cut into the fill material of LNA-T1, and has possibly eroded into Rio Grande valley-fill. LNA-T3 is a strath terrace because it has eroded into Rio Grande valley-fill bedrock. The gravel thickness of LNA-T2 is unknown due to lack of exposure. However, based on the heights of the erosional surfaces under the LNA-T1 fill and the LNA-T3 strath, LNA-T2 gravel thickness may be as much as 2 m (Table 1). Stream cuts of the LNA-T3 surface reveal an average gravel thickness of 0.60 m (Table 1).

LNA-T1 and LNA-T2 surfaces have very similar degrees of soil development, with identical carbonate profile masses of 1.81 g/cm^2 (Table 1). In addition, soil horization is similar between the LNA-T1 and LNA-T2 surfaces (Fig. 8 and 9). Both profiles are capped by a thin A horizon and contain Bt, Btk, Bkt and Ck horizons with a maximum carbonate morphology of stage I (Appendix 1). The carbonate profile mass of LNA-T3 is less than that of the upper two terraces at 1.15 g/cm^2 (Table 1). In addition, the juvenile horization of the soil profile also shows that the soil is less developed than LNA-T1 and LNA-T2 (Fig. 10). The LNA-T3 profile consists of a thin A horizon overlying a juvenile Btk and a Ck horizon (Appendix 1).

4.1.2. Socorro Canyon

Socorro Canyon is approximately 7 km southwest of Socorro (Fig. 1) and contains the most complete terrace sequence of all tributaries. Socorro Canyon's

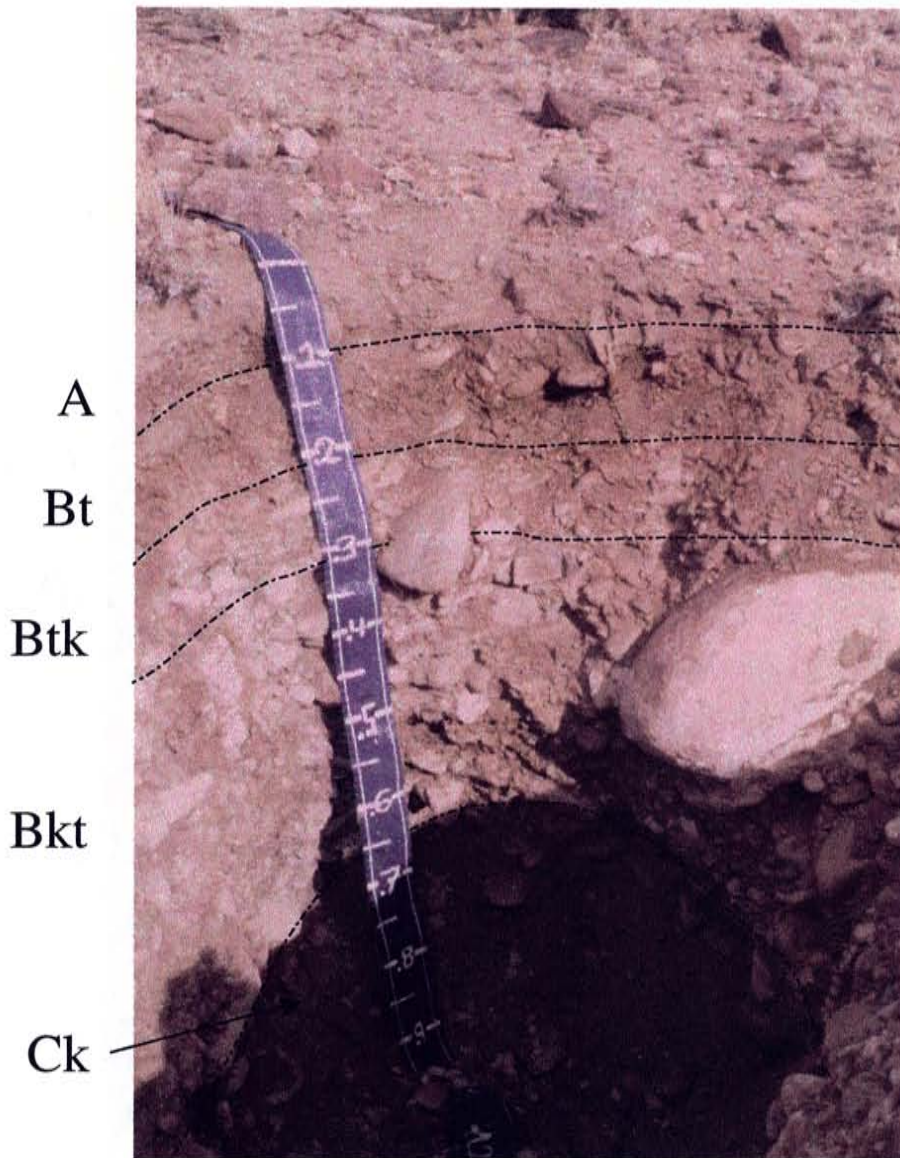


Figure 8. LNA-T1 soil profile. Scale in centimeters.

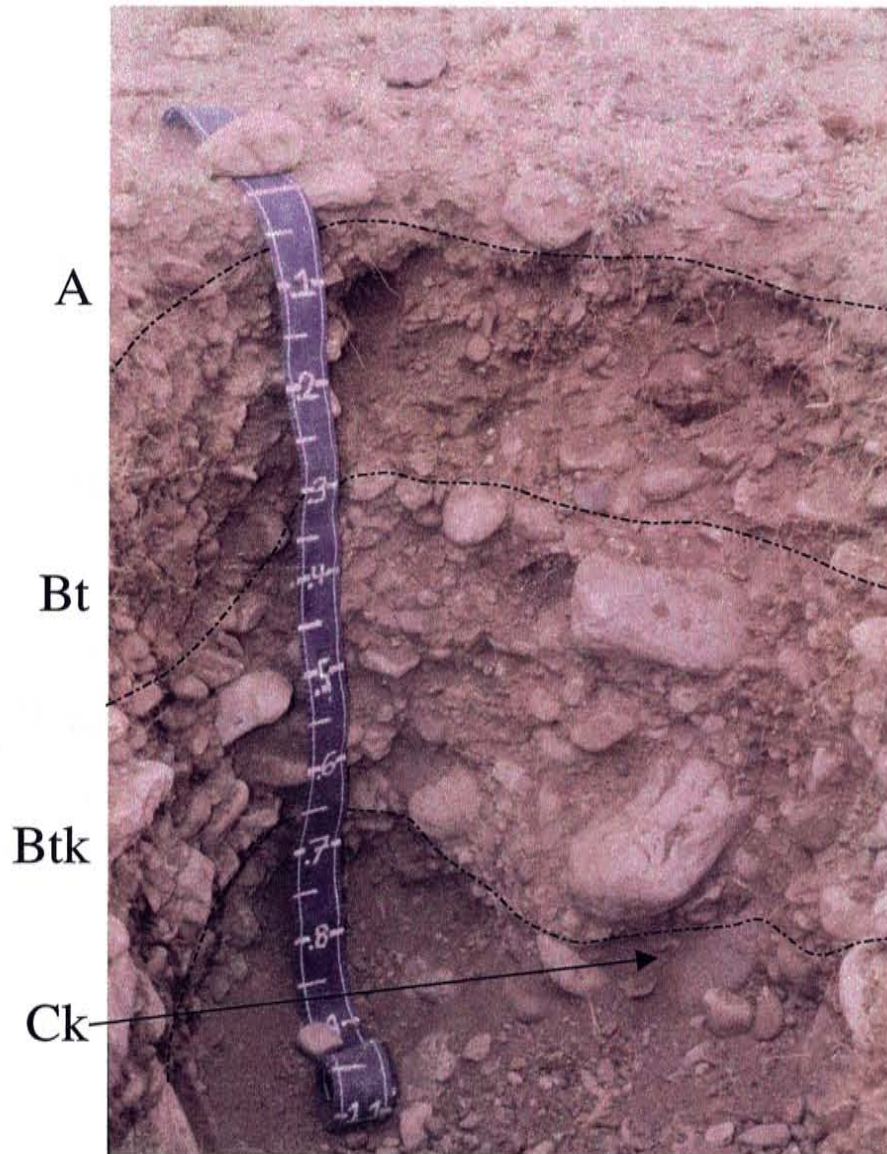


Figure 9. LNA-T2 soil profile. Scale in centimeters.

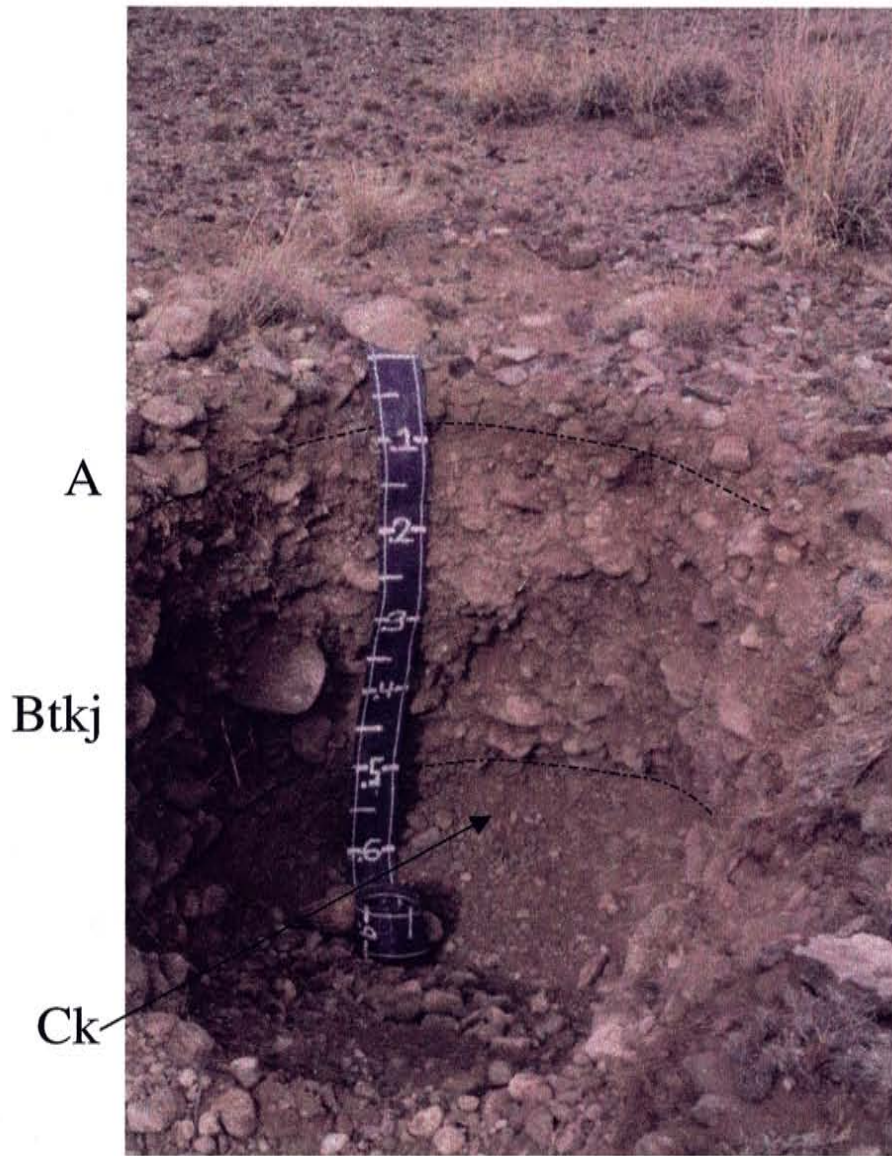
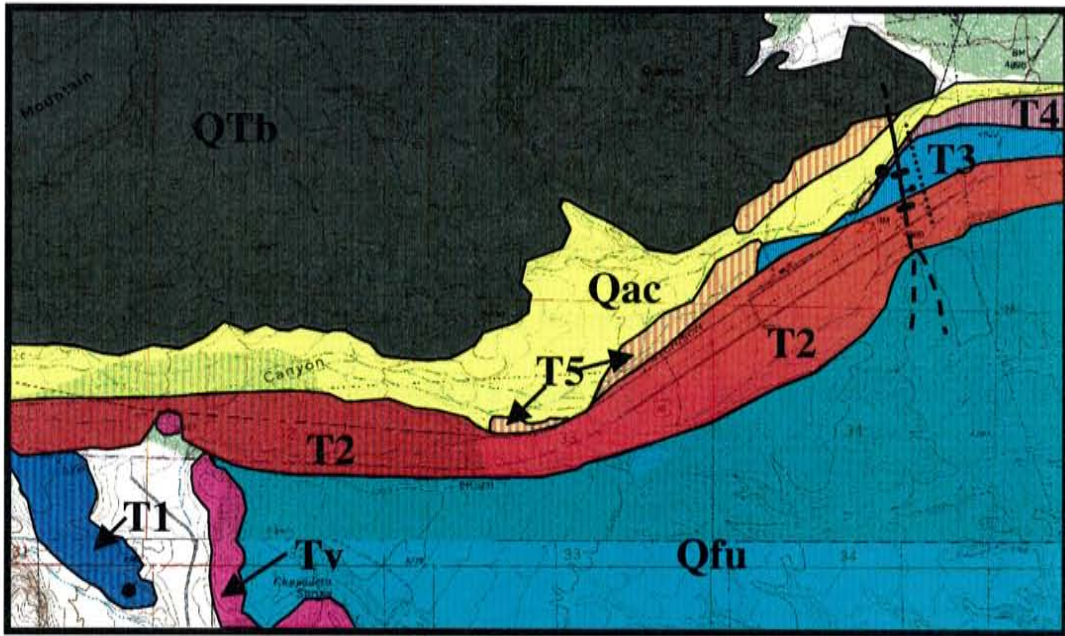


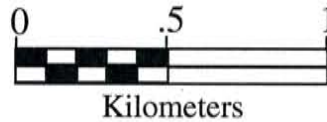
Figure 10. LNA-T3 soil profile. Scale in centimeters.

drainage basin area is approximately 123 km² (Fig. 6). The headwaters of Socorro Canyon are located in the Magdalena Mountains. Six Mile Canyon flows out of the Magdalena Mountains and joins Socorro Canyon up valley, approximately 9 km from the valley mouth. Socorro Canyon is situated between the Socorro Mountains to the north and the Chupadera Mountains to the south and flows east-northeast towards the town of Socorro. Terrace gravels consist of local lithologies that are dominantly rhyolite, although minor amounts of andesite and sedimentary rocks are also present in terrace gravels. The Socorro Canyon terraces used in this study are located on the eastern edge of the Socorro Mountains, where a fault scarp of the Socorro Canyon Fault offsets two terrace surfaces. However, the highest terrace surface is only preserved approximately 5 km up valley.

All terraces in Socorro Canyon are preserved on the southern side of the arroyo (Fig. 11). Located up valley, SC-T1 is the topographically highest terrace at approximately 29 meters above the current stream channel (Table 1). Because lake/playa sediments of the older Rio Grande Rift-fill are exposed a few meters below the SC-T1 surface, this terrace is probably a strath, with a thin (<2 meters) veneer of gravel at the surface. SC-T2 is the most extensive and preserved terrace in the Socorro Canyon sequence and is approximately 9 meters above the current stream channel (Table 1). SC-T2 is the only terrace in this study that has been dated with a Cl-36 age of 122 kyr (Ayarbe, 2000). A trench exposure on this surface shows a gravel thickness of at least 3 meters, and is therefore interpreted as a fill terrace. This terrace surface is offset approximately 5 meters by at least three movements on the Socorro Canyon fault (Ayarbe, 2000). The latest movement on the fault also offsets the younger SC-T3 terrace



Map Source: Socorro quadrangle, NM-Socorro County. USGS 7.5' series (topographic), 1979
 Luis Lopez quadrangle, NM-Socorro County. USGS 7.5' series (topographic), 1982



- | | | |
|---|--|---|
| <div style="background-color: yellow; border: 1px solid black; padding: 2px; display: inline-block; margin-bottom: 10px;">Qac</div> <div style="background-color: #f4b084; border: 1px solid black; padding: 2px; display: inline-block; margin-bottom: 10px;">T5</div> <div style="background-color: #c44e52; border: 1px solid black; padding: 2px; display: inline-block; margin-bottom: 10px;">T4</div> <div style="background-color: #0070c0; border: 1px solid black; padding: 2px; display: inline-block; margin-bottom: 10px;">T3</div> <div style="background-color: #c00000; border: 1px solid black; padding: 2px; display: inline-block; margin-bottom: 10px;">T2</div> <div style="background-color: #0056b3; border: 1px solid black; padding: 2px; display: inline-block; margin-bottom: 10px;">T1</div> <div style="background-color: #0070c0; border: 1px solid black; padding: 2px; display: inline-block; margin-bottom: 10px;">Qfu</div> <div style="background-color: #333333; border: 1px solid black; padding: 2px; display: inline-block; margin-bottom: 10px;">Qtb</div> <div style="background-color: #c00040; border: 1px solid black; padding: 2px; display: inline-block;">Tv</div> | <p>(Holocene) Sand and gravel in modern arroyo channels.</p> <p>(Holocene) Strath terrace, .95m above modern arroyo, gravel thickness of <.6m overlying Santa Fe Group bedrock.</p> <p>(Holocene) Strath terrace eroded into Santa Fe Group bedrock, 4m above modern arroyo, gravel thickness ~.6 m.</p> <p>(Holocene) Fill terrace, ~6m above modern arroyo, gravel thickness at least 2.5m.</p> <p>(Late Pleistocene) Fill terrace, ~9m above modern arroyo, gravel thickness is >3m.</p> <p>(Early-Middle Pleistocene) Strath terrace eroded into Santa Fe Group bedrock, ~29m above modern arroyo, gravel thickness <2m.</p> <p>(Pleistocene) Undifferentiated alluvial fans; gravel and sand deposited up to 30m above the modern arroyo.</p> <p>Basalt; flows capping mesas (~4 m.y.), and recent blocky colluvial slopes.</p> <p>Rhyolitic tuff and volcanoclastic conglomerates</p> | <p> Normal fault; ball on downthrown side</p> <p> Elevation survey transect</p> <p> Trench</p> <p> Soil Pit</p> |
|---|--|---|

Figure 11. Geomorphic map of Socorro Canyon. Color change on Qfu is due to color differences between adjoining topographic maps.

(80 cm offset), which is approximately 6 meters above the stream bottom. A 3-meter deep trench on this surface exposed fluvial gravels over the entire depth. In addition, based on the height of this terrace and the height of the strath surface exposed in an arroyo cut on the SC-T4 surface, the gravel thickness of the SC-T3 surface is at least 2.5 m (Table 1). Therefore, this terrace surface is interpreted as a fill terrace. SC-T4 is about 4 meters above the stream channel and is a strath terrace. An arroyo cut exposure shows approximately 60 cm of terrace gravels overlying fine-grained sand and silt of Rio Grande Rift-fill. Therefore, the SC-T4 surface is a strath terrace (Table 1). SC-T5 is approximately 95 cm above the current arroyo bottom. Because the erosional contact between the terrace gravels of SC-T4 and the Rio Grande valley fill is almost 4 meters above the arroyo, the SC-T5 surface is clearly a strath terrace as well (Table 1).

The carbonate profile mass of SC-T1 is about 55 g/cm^2 (Table 1). In addition, the soil on this terrace exhibits a stage IV- carbonate morphology with a 1 to 2 cm thick laminar layer. A thin Ak horizon, and Bkt, Bk, K, and Ck horizons (Appendix 1) characterize this profile. This is by far the most developed soil in this study. The SC-T2 carbonate profile mass is 8.93 g/cm^2 (Table 1). The soil profile on this surface has Bt, Bkt, Bk, and Ck horizons, and contains pockets and tubes of carbonate (Fig. 12). The maximum carbonate morphology on the SC-T2 surface is stage III which is limited to areas of the carbonate pockets and tubes (Appendix 1). SC-T3 and SC-T4 show similar amounts of carbonate profile mass at 1.01 g/cm^2 and 1.11 g/cm^2 , respectively (Table 1). Both profiles lack significant amounts of soil development as seen in their A, Bt, Ck horizons (Fig. 13 and 14). SC-T5 was not analyzed in the laboratory, therefore carbonate profile mass was not determined. However, visual inspection and minimal

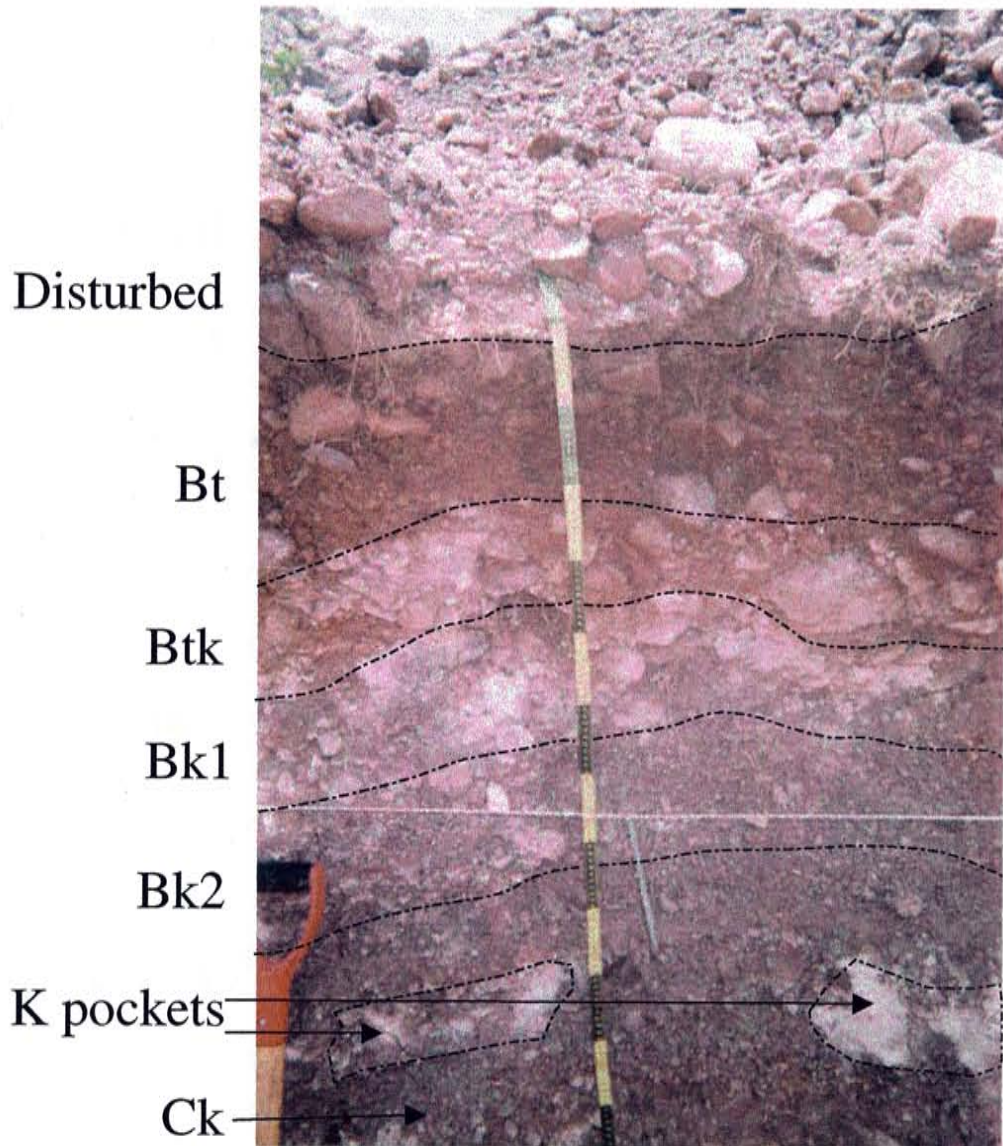


Figure 12. SC-T2 soil profile. Scale in centimeters.

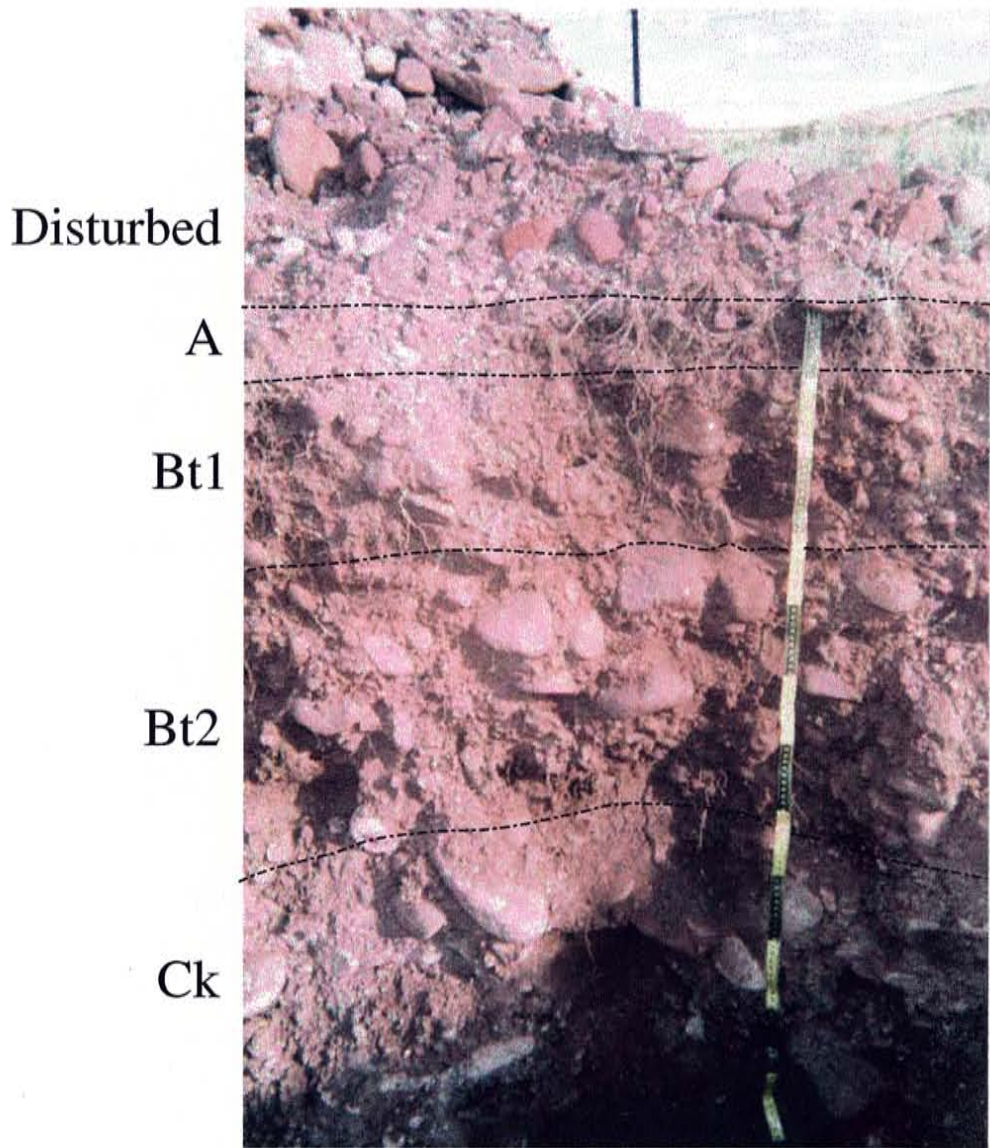


Figure 13. SC-T3 soil profile. Scale in 10 centimeters increments.

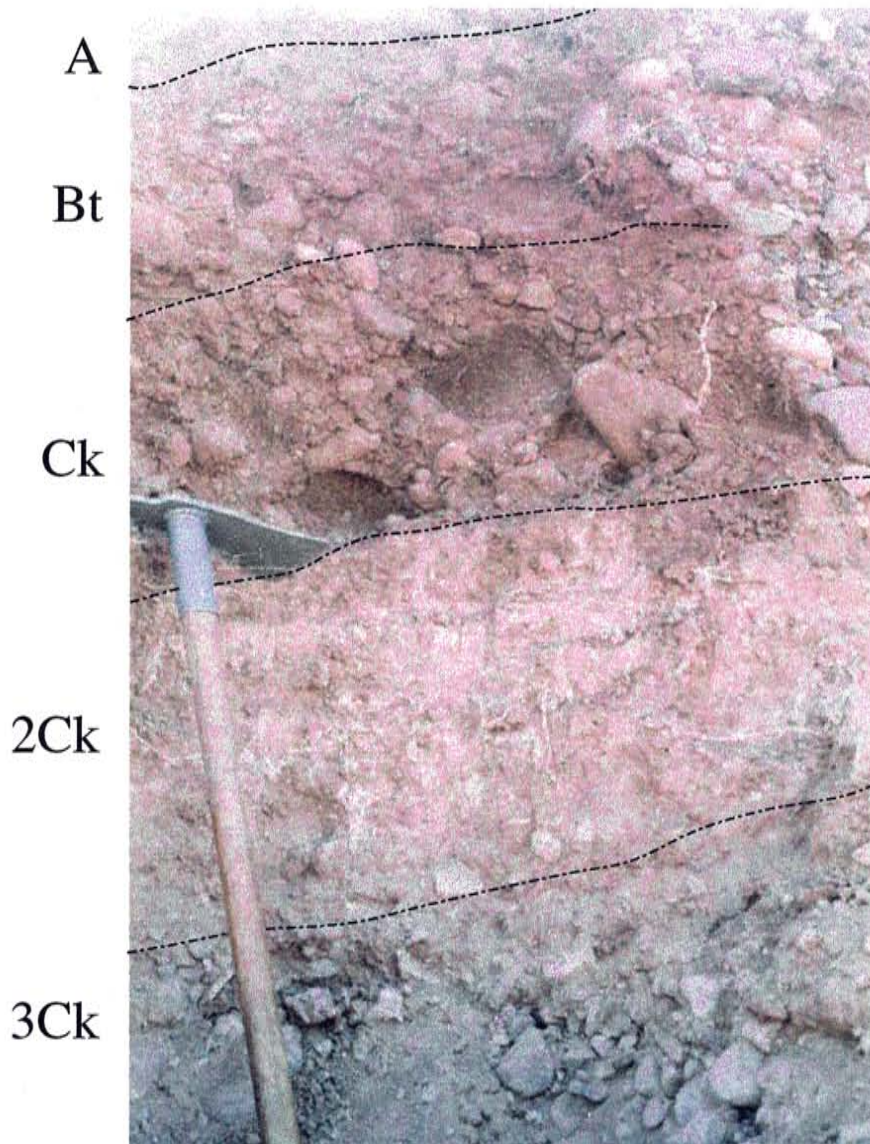


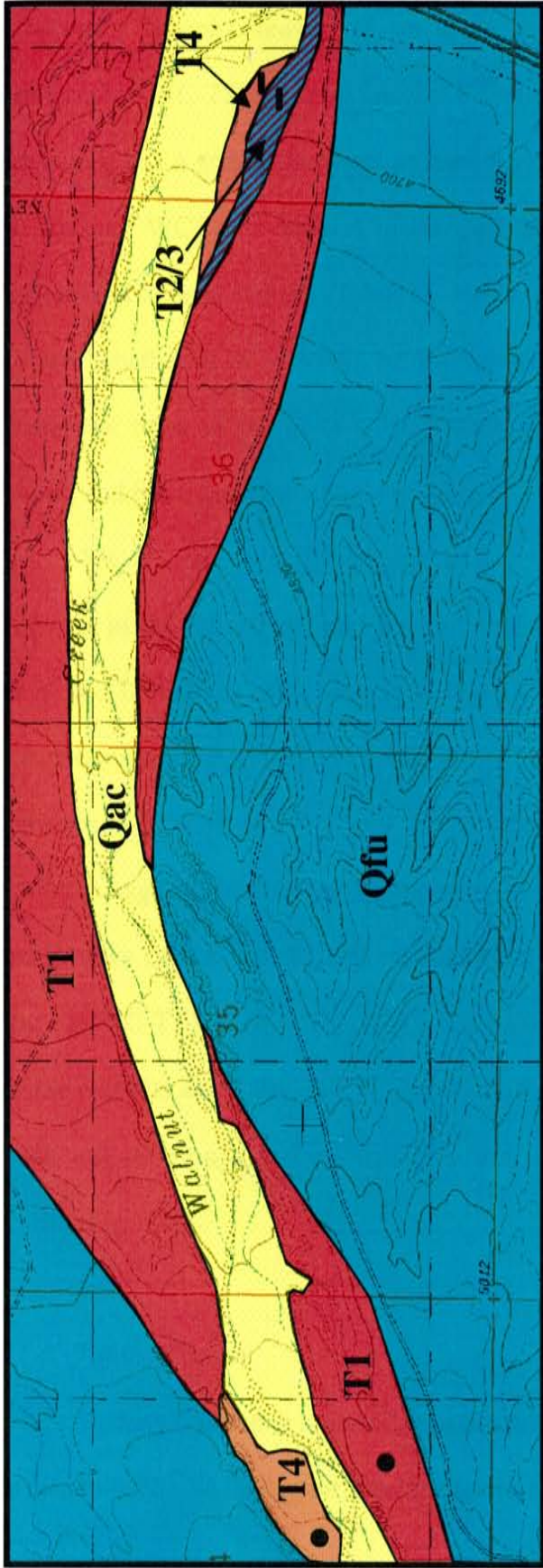
Figure 14. SC-T4 soil profile. (60 cm long grubber for scale)

reaction to contact with hydrochloric acid, indicates the lack of any significant amounts of CaCO_3 accumulation.

4.1.3. Walnut Creek

Walnut Creek is approximately 15 km south of Socorro near the town of San Antonio (Fig. 1). The drainage basin area for Walnut Creek is the smallest of all tributaries used in this study and is approximately 87 km^2 (Fig. 6). The headwaters for the Walnut Creek tributary are located in the southeastern slopes of the Magdalena Mountains. Walnut Creek flows out of Nogal Canyon in the Chupadera Mountains and reaches the Rio Grande near the town of San Antonio. The Walnut Creek terraces are located on both sides of the arroyo east of the Chupadera Mountains. The Chupadera Mountains are the major source of terrace gravels, which are dominated by rhyolitic compositions but also include other Tertiary volcanic and clastic sedimentary rocks.

Four terraces are preserved in this tributary (Fig. 15). WC-T1 is the highest and most extensive terrace in this sequence and is approximately 10 meters above the modern arroyo. It is preserved on both sides of the arroyo as a paired terrace. Arroyo-cut exposures of this surface show approximately 8 meters of fill, suggesting that this surface is a fill terrace (Table 1). WC-T2 and WC-T3 are only preserved as small remnant terraces on the south side of the arroyo within the lower limits of the tributary. As previously mentioned, trenches on each of these surfaces were discovered late in the project and show that the terraces have been covered with 30-65 cm of colluvial material from the adjacent terrace riser. Therefore, soil development on these terraces was not utilized. The colluvial cover was excluded from terrace height and gravel thickness



Map Source: Luis Lopez quadrangle, NM-Socorro County. USGS 7.5' series (topographic), 1982








- | | | | |
|---|--|---|--|
|  | (Holocene) Sand and gravel in modern arroyo channels. |  | (Late Pleistocene) Fill terrace, ~10m above modern arroyo, gravel thickness is ~8m. A strath surface eroded into Santa Fe Group bedrock occurs under fill gravels ~2m above modern arroyo. |
|  | (Holocene) Strath terrace, ~1m above modern arroyo, gravel thickness of .3 to .6m overlying Santa Fe Group bedrock. |  | (Pleistocene) Undifferentiated alluvial fans; gravel and sand deposited up to 30m above the modern arroyo. |
|  | (Holocene) Two terraces undistinguishable at map scale. T3: strath (?) terrace, ~4m above modern arroyo, gravel thickness >1.3m. T2: fill terrace, ~6.5m above modern arroyo, gravel thickness is ~4m. |  | ● Soil Pit |
| | |  | — Trench |

Figure 15. Geomorphic Map of Walnut Creek

estimates. Trench excavations on these terraces are the only exposures of terrace stratigraphy. WC-T2 is approximately 6.5 meters high and, based on trench and arroyo exposures, has a gravel thickness at least 4 meters (Table 1), therefore, it is considered a fill terrace. WCT-3 is about 4 meters high and based on trench exposure has a gravel thickness of at least 130 cm (Table 1). However, it is not apparent from exposures of this surface whether it is a strath or fill terrace. WC-T4 is a strath terrace preserved throughout most of the arroyo. It is approximately 1 meter above the modern arroyo bottom and has a gravel thickness of 30 to 60 cm (Table 1).

WC-T1 and WC-T4 are the only terraces in the Walnut sequence that were analyzed in the laboratory, and the carbonate profile masses of these surfaces are 8.17 g/cm^2 and 0.68 g/cm^2 , respectively (Table 1). Due to the hazardous nature of the trench excavations, soil observations on the WC-T2 and WC-T3 surfaces were limited to visual comparison to each other as well as the other soils in the sequence. The WC-T2 soil exhibits stage II- carbonate morphology and is similar to the stage I+ carbonate morphology of the WC-T3 soil. In addition, the WC-T2 soil is clearly less developed than the WC-T1 soil (Fig. 16), which has a stage III carbonate morphology. The WC-T1 profile exhibits an A, Btk, Bk, K, and Ck horization (Appendix 1). The WC-T4 soil is much less developed and consists of a thin A/C horizon that overlies an Akj, Bk, Ck profile (Fig. 17).

4.1.4. Tiffany Canyon

Tiffany Canyon is located approximately 32 km south of Socorro within the Pedro Armendaris No. 34 land grant, near the towns of San Marcial and Tiffany (Fig. 1). Its

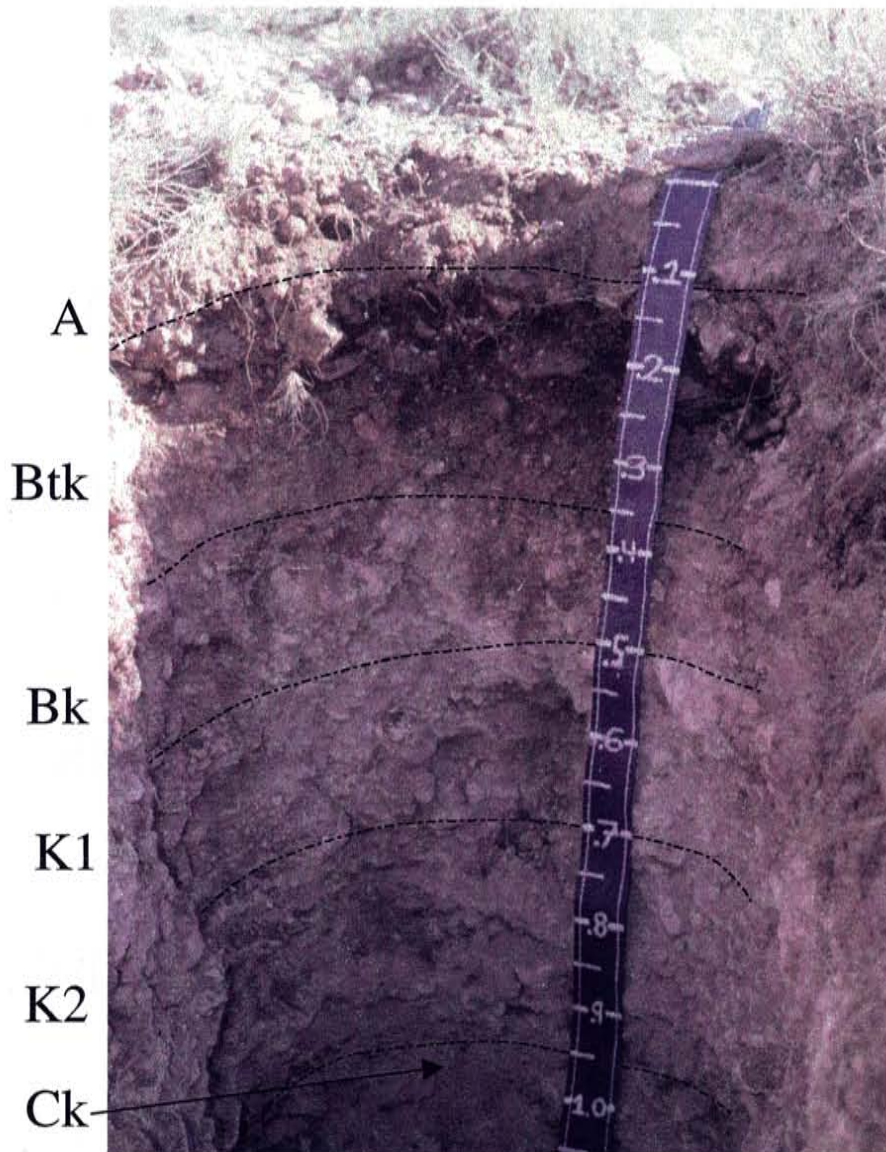


Figure 16. WC-T1 soil profile. Scale in centimeters.

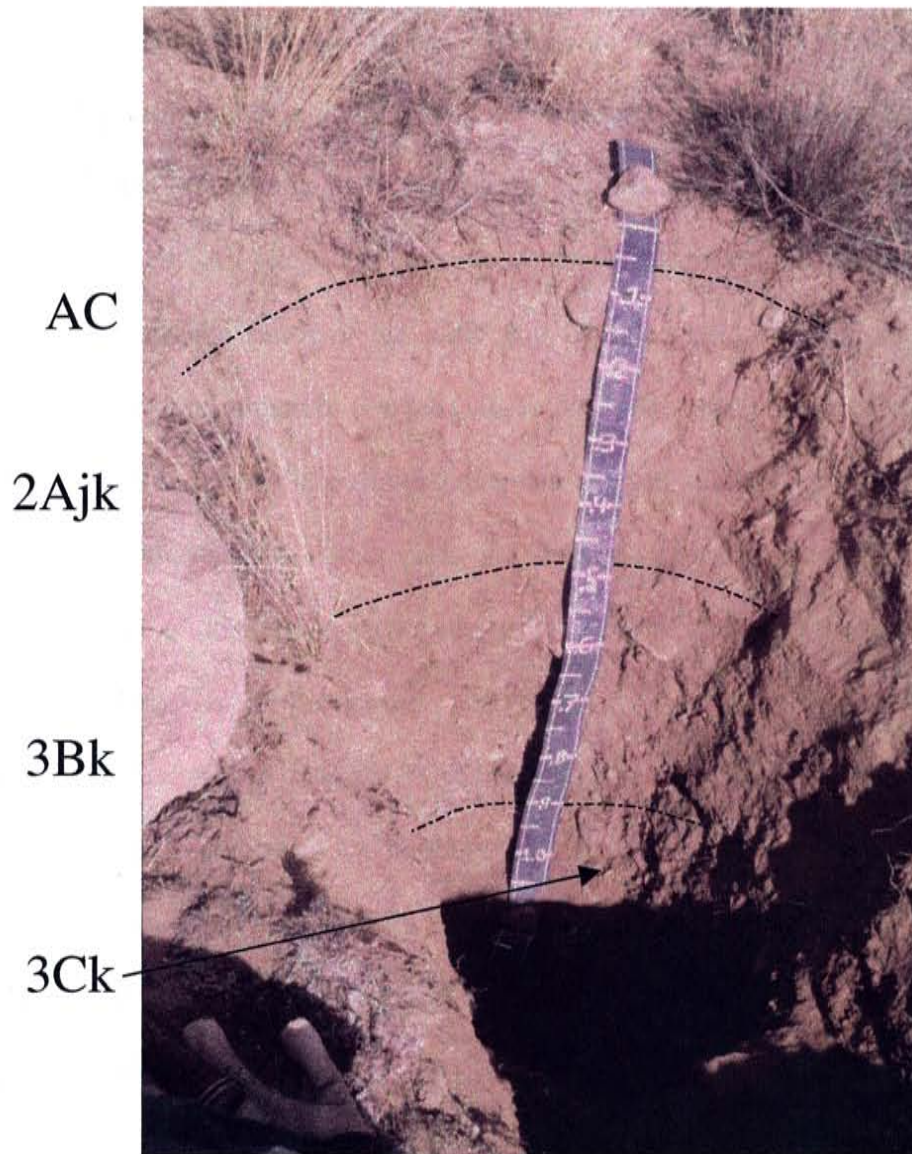


Figure 17. WC-T4 soil profile. Scale in centimeters.

headwaters are located on the southeastern slopes of the Magdalena Mountains and it flows through the southernmost the Chupadera Mountains before reaching the Rio Grande near the town of Tiffany. Tiffany Canyon's drainage basin area is approximately 140 km² (Fig. 6). The terraces used in this tributary are located on the eastern side of the Chupadera Mountains where only two terrace surfaces have been preserved (Fig. 18).

TC-T1 is the topographically highest terrace and is approximately 9 meters above the current streambed. An arroyo cut exposure of this terrace shows an erosional contact between gravels and fine sands of the older Rio Grande valley-fill bedrock (Fig. 19). Gravel thickness is approximately 6 meters; therefore, this surface is interpreted as a fill terrace (Table 1). TC-T2 is 95 cm above the stream channel and has a gravel thickness of approximately 65 cm; therefore, this terrace is considered a strath terrace (Table 1). The arroyo cut exposure of this terrace shows an erosional contact between the terrace gravels and an earlier Tiffany Canyon fill deposit.

The carbonate profile mass for TC-T1 is 8.60 g/cm² (Table 1) and the soil on this surface has a stage II+ carbonate morphology (Fig. 20). The TC-T1 profile has an Avk, Btk, Bk, Ck horizonation (Appendix 1). The TC-T2 soil has a carbonate profile mass of 0.83 g/cm² (Table 1). Soils on this surface are weakly developed, and characterized by a simple Akj, Ck profile (Appendix 1).

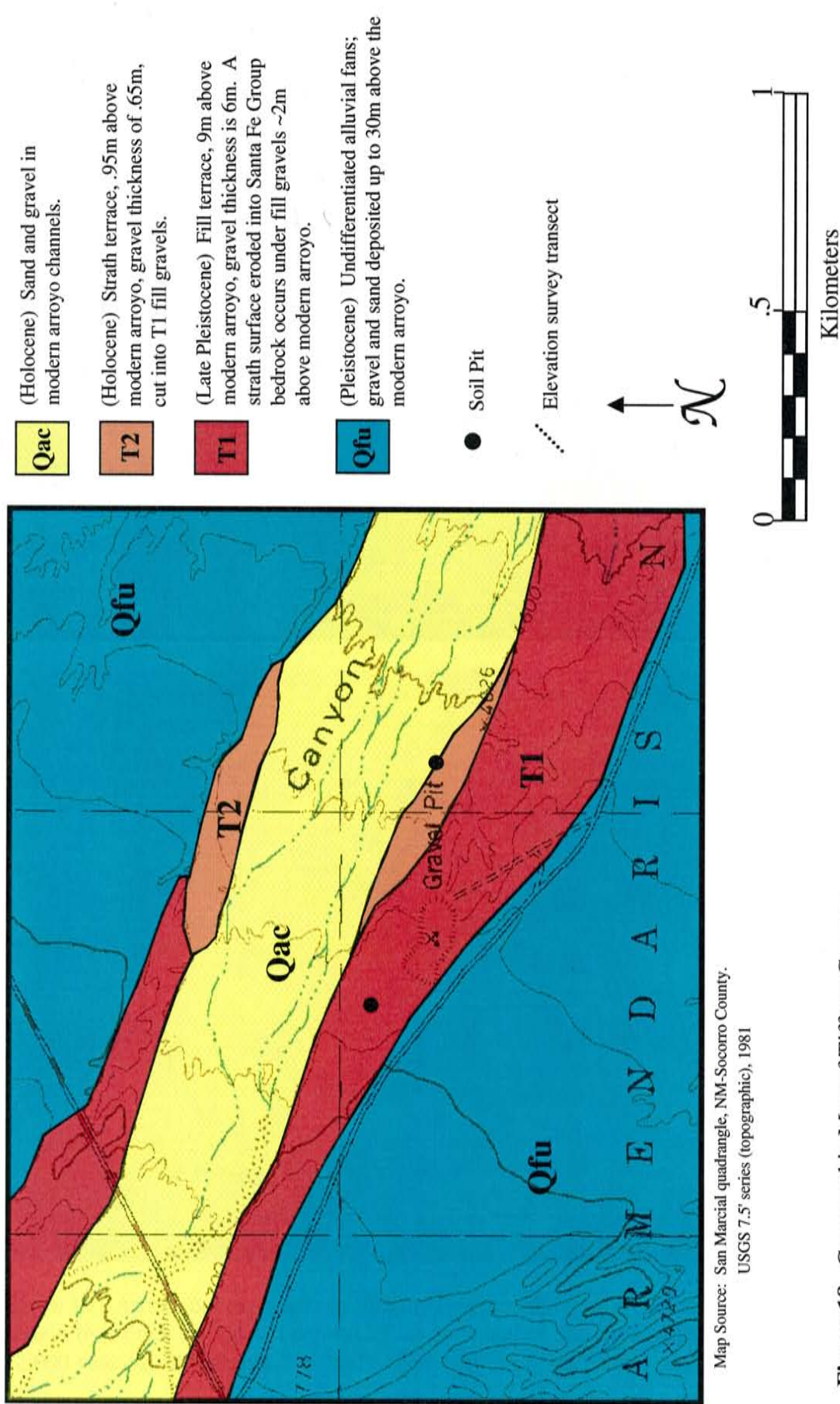


Figure 18. Geomorphic Map of Tiffany Canyon.



Figure 19. Arroyo cut exposures in Tiffany Canyon, showing erosional strath contact overlain by a thick fluvial fill deposit. This is typical of the stratigraphy on all 122,000 year old fill terraces.

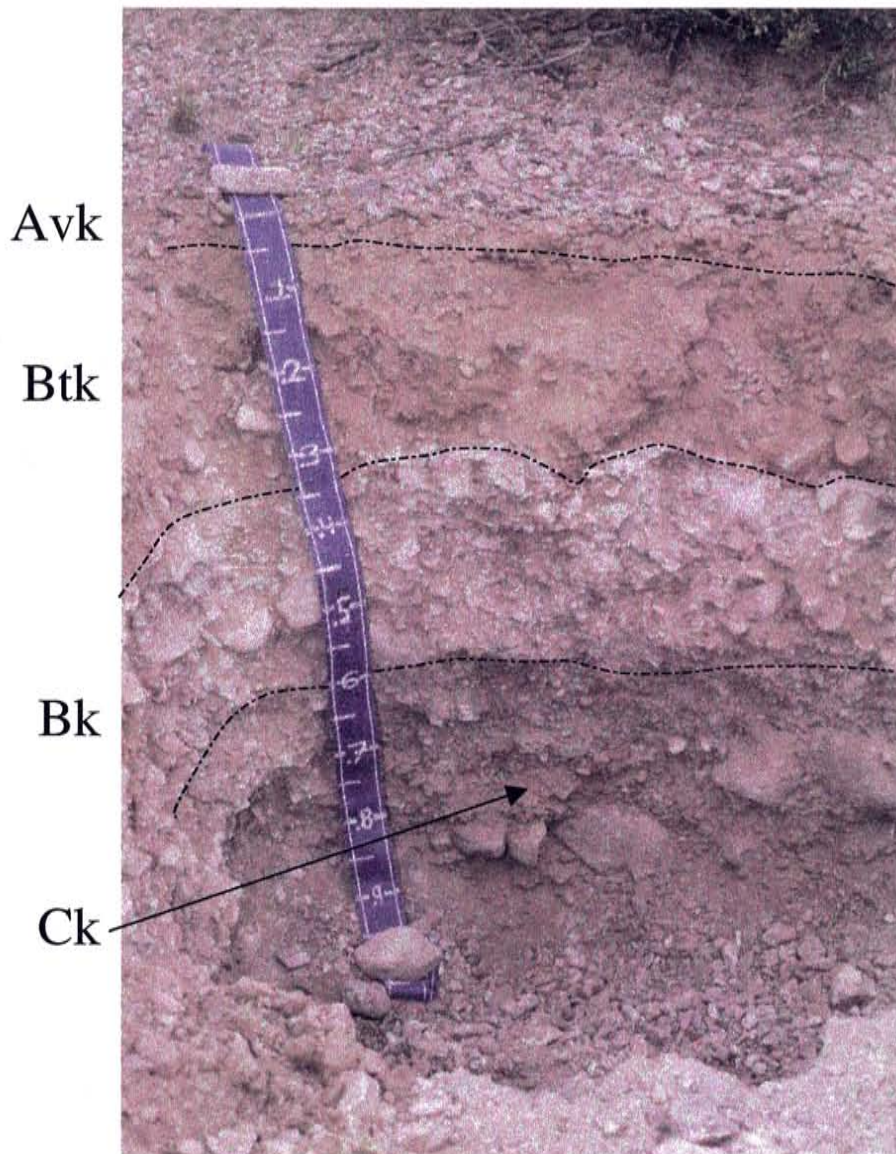


Figure 20. TC-T1 soil profile. Scale in centimeters.

CHAPTER 5. DISCUSSION

5.1 Socorro Basin Tributary Terrace Correlation

Tributary terraces were correlated based on the heights of the terrace treads above the stream channel. Five terrace heights are represented in the Socorro Basin tributaries (Table 2). T1 is 29 meters high, T2 is 9-10 meters high, T3 is 6-7 meters high, T4 is 4-5 meters high and T5 is 1 meter high. Although T1 is only preserved in Socorro Canyon, T2 through T5 are preserved within at least three of the four tributaries, suggesting that the terraces are regional in extent.

5.2 Comparison of Other Rio Grande Tributaries to Socorro Basin Tributaries

Tributary and Rio Grande terrace sequences within and outside the Socorro Basin were compared to the record preserved in the Socorro Basin. Comparison to surfaces outside of the Socorro Basin helps to further determine the regional extent of these surfaces. Terrace elevations for one tributary in the Socorro Basin (Arroyo de la Parida) were compared to the elevations correlated using the tributaries mentioned above. In the Albuquerque Basin to the north, one tributary (Palo Duro Wash), and one Rio Grande terrace sequence were also used for comparison (Treadwell, 1996; Connell and Love, 2000). In addition, south of the Socorro Basin near Elephant Butte Reservoir, one tributary (Cuchillo Negro Creek) terrace sequence was used for comparison (Lozinsky, 1985).

Little Nogal Arroyo			Socorro Canyon			Walnut Creek			Tiffany Canyon			
Terrace	Height	CaCO3 profile mass (g/cm2)	Terrace	Height	CaCO3 profile mass (g/cm2)	Terrace	Height	CaCO3 profile mass (g/cm2)	Terrace	Height	CaCO3 profile mass (g/cm2)	Correlated Terrace
			SC-T1	29m	55.82							T1
			SC-T2	9m	8.93	WC-T1	10m	8.17	TC-T1	9m	8.60	T2
LNA-T1	7m	1.81	SC-T3	6m	1.01	WC-T2	7m	N/A				T3
LNA-T2	4m	1.81	SC-T4	5m	1.11	WC-T3	4m	N/A				T4
LNA-T3	1m	1.15	SC-T5	1m	N/A	WC-T4	1m	0.68	TC-T2	1m	0.83	T5

Table 2. Correlated tributary terraces in the Socorro Basin record five elevations related to the Rio Grande. T1 and T3 are fill terraces and T2, T4, and T5 are strath terraces.

5.2..1. *Arroyo de la Parida*

Arroyo de la Parida is located in the northern portion of the Socorro Basin. It flows out of Quebradas uplands on the east side of the basin, and gravel lithologies include sedimentary rocks of the Santa Fe Group as well as older Pennsylvanian-Permian sedimentary rocks, which include significant amounts of limestone. Arroyo de la Parida was initially intended to be included with the other tributaries used within the Socorro Basin. However, because of the large amounts of limestone in the terrace gravels, CaCO_3 profile mass as a measure of soil development could not be utilized. In addition, many of the preserved terraces in this arroyo are covered with small alluvial fan deposits and/or sand sheets. Exploratory soil pits revealed similar degrees of soil development on different-aged terraces indicating additions of aeolian sand across all surfaces. Therefore, elevations were correlated cautiously and soil development was not quantified on these terraces. In addition to the tributary terraces, four Rio Grande terraces are preserved near the mouth of Arroyo de la Parida. Elevations of these terraces were also compared to the other tributary terraces in the Socorro Basin. The three highest terrace elevations recorded in the Socorro Basin (29m, 9-11m, and 6-7m) have correlative surfaces (both tributary and Rio Grande terraces) in Arroyo de la Parida (Table 3). The highest surface in Arroyo de la Parida (51m) does not have a correlative surface preserved in the other Socorro Basin tributaries. However, it can be correlated to Rio Grande terraces in the Albuquerque Basin (Connell and Love, 2000) as well as to terrace surfaces in the Elephant Butte area (Table 3).

		Tributary Terraces				Rio Grande Terraces				Both	
Socorro Basin (this study)		Treadwell, 1996		Diether et al., 1988		Arroyo de La Parida (this study)		Connell and Love, 2000		Lozinsky, 1985	
Terrace	Height	Terrace	Height	Terrace	Height	Terrace	Height	Terrace	Height	Terrace	Height
								T1	65-75m		
T1	29m	QT3 QT4	29m 21-23m	C3 C4	25-50m 10-20m	T0	51m	T2 T3	12-24m (base) 42-48m	T1 T2	36-42m 30-36m
T2	9-11 m	QT5	9m	"Holocene"	10m	T1 T2&T3	30 17-24	T4 T5	23-41m 15-21m	T3 T4	24-30m 18-24m
T3	6-7m					T4	12m			T5	6-12m
T4	4-5m	QT6	4.6m	"Holocene"	3m	T5	6m				
T5	1m										
										T6	2m

Table 3. Correlative terraces outside Socorro Basin. Treadwell, 1996; Palo Duro Wash, Diether et al., 1988; Rio Chama, Connell and Love, 2000; Albuquerque Basin, Lozinsky, 1985; Cuchillo Negro Creek.

5.2.2. *Palo Duro Wash*

Palo Duro Wash is located near the Sevilleta National Wildlife Refuge, in the southern Albuquerque Basin near its boundary with the Socorro Basin. It flows out of the Los Pinos Mountains on the east side of the Albuquerque Basin and gravel lithologies are dominantly limestone, with minor amounts of Precambrian and sedimentary rocks (Treadwell, 1996). Terrace elevations as calculated by Treadwell (1996), were compared to the terraces in the Socorro Basin. Terraces in Palo Duro Wash correlate to three surface elevations in the Socorro Basin (29m, 9-11m, and 4-5m) (Table 3).

5.2.3. *Cuchillo Negro Creek*

Cuchillo Negro Creek lies on the eastern margin of the Rio Grande Rift at the boundary between the Engle and Palomas Basins (Fig. 2). Five terraces are preserved in this tributary and gravel lithologies are dominantly rhyolite and other porphyritic volcanic rocks, with minor amounts of sandstone and other sedimentary rocks (Lozinsky, 1985). Terrace types and elevations as presented by Lozinsky (1985), were compared to the terraces in the Socorro Basin. Three Cuchillo Negro Creek terraces are correlative to the two highest surfaces (29 meters and 9-11 meters) as well as the youngest, lowest surface in the Socorro Basin (Table 3).

5.2.4. *Albuquerque Rio Grande Terrace Sequence*

Rio Grande terraces in the Albuquerque Basin were differentiated based on elevation and soil morphology by Connell and Love (2000). The terraces are preserved between the San Felipe Pueblo and the city of Los Lunas. The terrace gravel lithology is

dominated by quartzite clasts. Elevations of these Rio Grande terraces were compared to the elevations of the terraces in the Socorro Basin. The only correlative terrace in this sequence that, based on elevation appears correlative to the 29m high Socorro Canyon terrace has an elevation of approximately 23 – 41 meters. This terrace is the second lowest in the Albuquerque Rio Grande terrace sequence and is correlative to the highest terrace surface in the Socorro Basin (Table 3).

5.3 Response Time for Terrace Formation

5.3.1. Response Time Indicated by Drainage Basin Area

Tributary terraces in the Socorro Basin are correlative by elevation to other tributary terraces outside the basin. Therefore, they are considered regional surfaces that have responded to Rio Grande base level changes. However, understanding the timing of surface formation is crucial in confidently assessing soil variability on correlated surfaces. Therefore, the factors that influence response to base level change are discussed.

The response time of the tributaries to fluctuations in base level is largely dependent on drainage basin areas (Bull, 1991a). For example, the balance between stream power and critical power dictates how fluvial systems respond to base level change. Leopold et al., (1964), note the strong dependence of stream power on discharge whereby suspended sediment transport rates (G) may increase by an exponential factor of approximately 2.5 with an increase in discharge (Q) (p is a constant).

$$G = pQ^{2.5}$$

In addition, discharge is dependent on the slope of the stream channel. However, if all tributaries have experienced climatic perturbations of the same magnitude, discharge is then strongly dependent on drainage basin area. That is, large drainage basins have higher discharge than smaller drainage basins, and thus may have a quicker response time (geology being constant).

Figure 6 shows approximate drainage basin boundaries for all tributaries as well as total drainage basin areas. Little Nogal arroyo has the largest drainage basin area (~315 km²) and Walnut Creek has the smallest (~87 km²). In addition, the drainage basin area for Socorro Canyon and Tiffany Canyon are ~123km² and ~140km², respectively. Based on these values of total drainage basin area, it would appear that Little Nogal arroyo would respond quickest, followed by Socorro Canyon and Tiffany Canyon, with Walnut Creek the last to respond.

However, the Socorro Basin tributary drainage basins are complex in that the tributaries head in bedrock contributing areas, flow across alluvial plains and through more bedrock before they reach the Rio Grande. Little Nogal Arroyo for example, begins in the Magdalena Mountains, flows across the alluvial plains of the La Jencia Basin, and continues across the northern portion of the Socorro Mountains before reaching the Rio Grande. Socorro Canyon has a similar course as Little Nogal Arroyo, except that its extent over the alluvial plains of the La Jencia Basin is less. Tiffany Canyon also crosses broad alluvial plains. Although these tributaries originate in the Magdalena Mountains, more than 60% of the drainage basin areas are located at lower elevation most of which encompass the alluvial plains (Table 4). There are similarities in the area of the drainage

	LNA	SC	WC	TC
Total Area (km ²)	315	123	87	140
Total Contributing Area (km ²)	125	35	34	29
Total Contributing Area %	40	28	39	21
% Over Alluvial Plains	60	72	61	79

Table 4. Alluvial plains comprise at least 60% of the total drainage basin area for each tributary.

basins that occur over bedrock, but differences in the percent of the drainage basin within these higher elevations where the bulk of precipitation falls ($> 2400\text{m}$). For example, 4.5% of the Walnut Creek drainage basin occurs higher than 2400 m, whereas 11% of the Little Nogal Arroyo drainage basin occurs at this altitude. Although there are differences in the percentage of the drainage basins at high elevations ($>2400\text{ m}$), it is unlikely that this difference has a large effect on tributary development at lower elevations, given the complex form of these drainage basins.

Because of the differences between the lithologic regimes (i.e. bedrock and alluvium) within the drainage areas, the absolute area of the drainage basins may not be an accurate measure of response time to base level change. That is, smaller drainages comprising mostly bedrock may respond as quickly as larger drainage areas comprised of a larger portion of alluvium. Therefore, a better measure of response time with respect to drainage basin area is through hypsometry, where area is related to altitude (Strahler, 1952).

The main use for hypsometry in this study is to evaluate the different drainage basin areas based on relative area versus relative altitude. The hypsometric curve established for each drainage basin represents the total area above a particular elevation. Comparison of the shapes of the curves for each drainage basin suggests any similarities or differences between the basins with respect to development over time. That is, drainage basins in equilibrium (mature) have distinctly different shapes than drainage basin that are not in equilibrium (youthful; Strahler, 1952). For example, Figure 21 shows the differences between hypothetical 'mature' and 'youthful' drainage basins. The mature drainage basin curve shows, in contrast to the youthful drainage, removal of

upland surface material, suggesting that the entire drainage basin has had enough time to respond to base level changes. Conversely, the youthful drainage basin curve shows a significant amount of upland surface that still exists, thereby suggesting that the drainage basin adjustments have not been occurring for a very long time.

The hypsometric curves for the Socorro Basin tributaries that are presented in Figure 22 show similarities between the different drainage basins. That is, the areas above each elevation, independent of total drainage basin area, are similar for larger (Little Nogal Arroyo) and smaller (Walnut Creek) drainage basin sizes. This similarity suggests that the time for the drainage basins to respond to base level changes is not sufficient to cause large differences in the timing of terrace formation. Furthermore, the similarity in curves also suggests that any lithologic differences between drainages are not dramatic enough to hinder the time necessary for basin development towards a mature (equilibrium) state.

5.3.2. Response Time Indicated by Longitudinal Profiles

Although the terraces that were measured are representative of only a short distance of the paleo stream channel, the overall shape of longitudinal terrace profiles suggests the condition of stream equilibrium prior to abandonment (Bull, 1991a). The correlated 9-11 meter high fill terraces in the Socorro Basin all have a linear form (Fig. 23), suggesting equilibrium conditions with base level had been met prior to abandonment of these terrace surfaces.

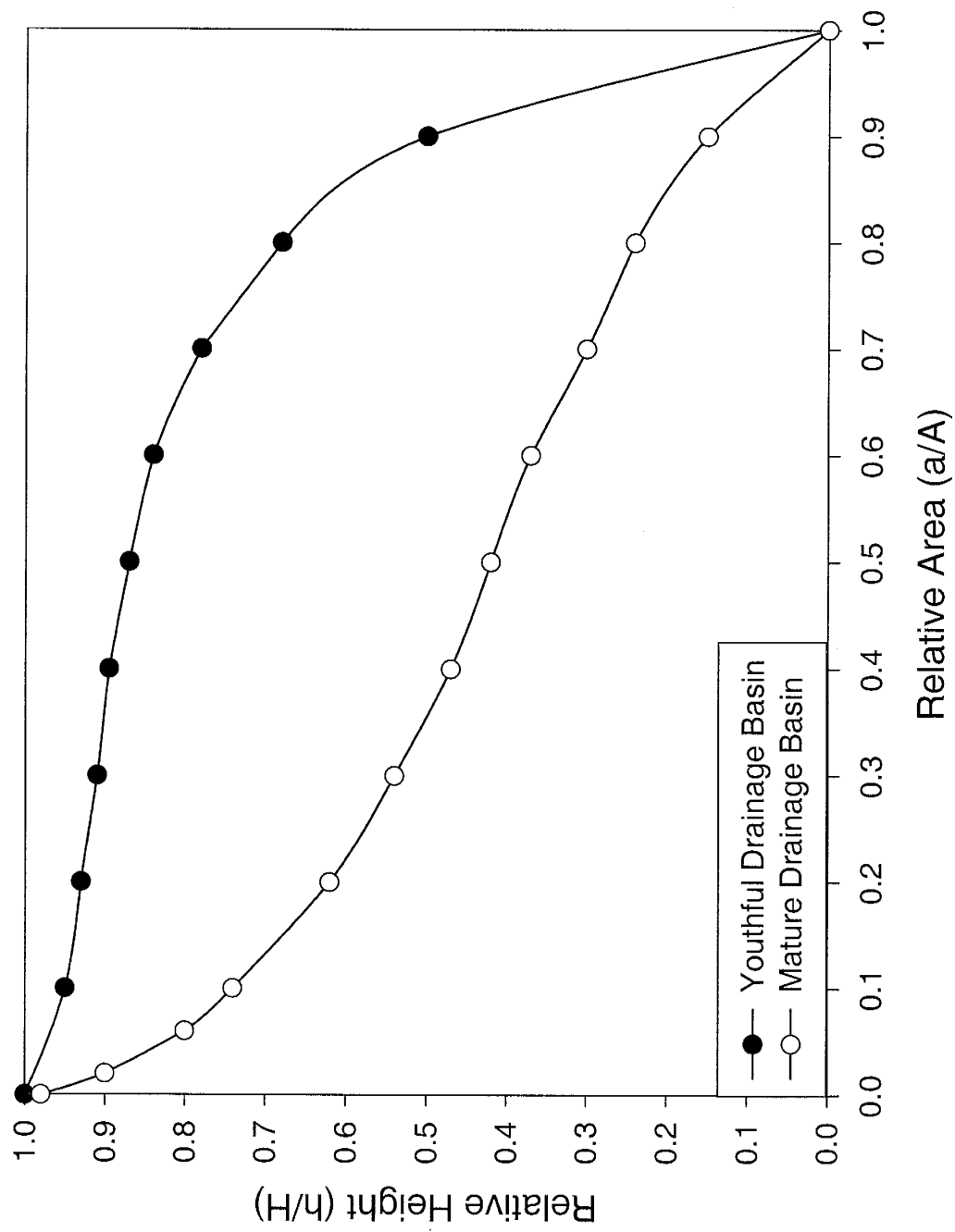


Figure 21. Hypothetical hypsometric curves reflected developed (mature) and undeveloped (youthful) drainage basins. (modified from Strahler, 1952)

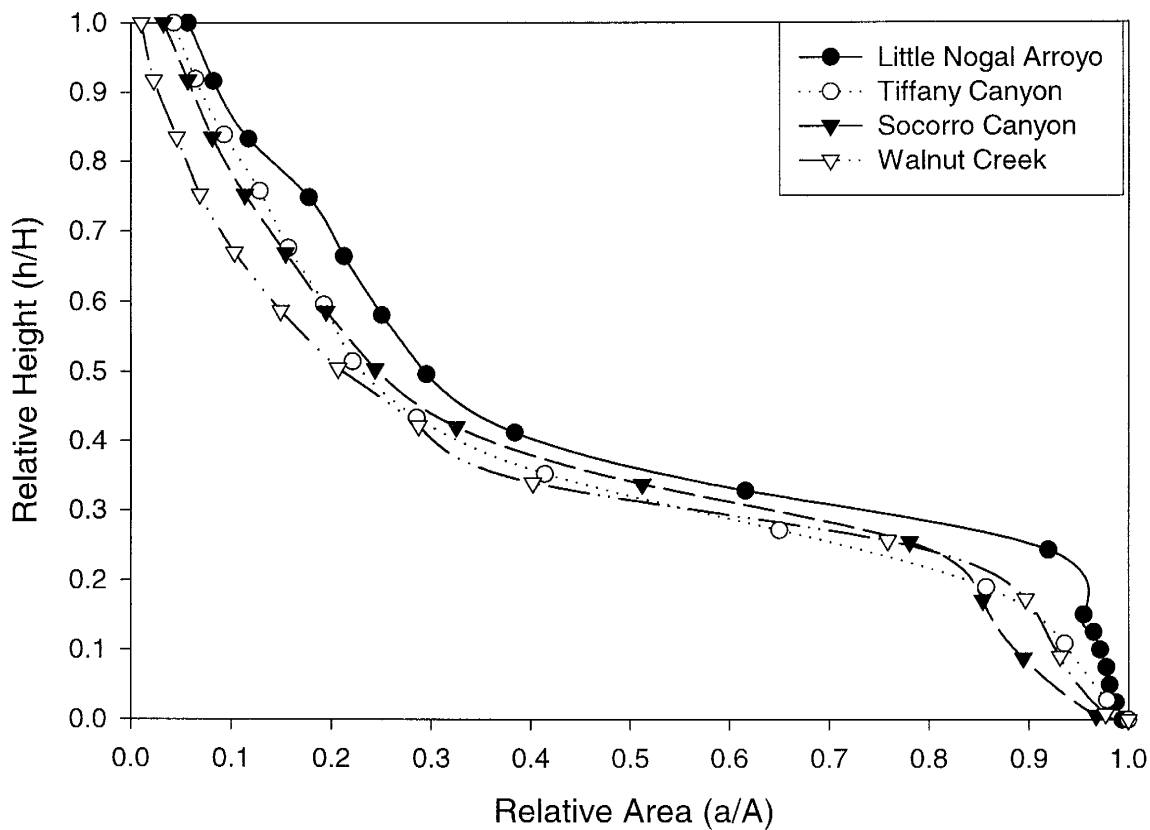


Figure. 22. Hypsometric curves for each drainage basin. Relative area is the ratio between the area above a particular elevation to the total drainage basin area, and relative height is the ratio between a particular height and the total elevation change in the drainage basin. Terraces used in this study are located at extreme bottom right of each curve. (Note: The hump in Little Nogal Arroyo is a consequence of the graphing program and should appear smoother between the two points)

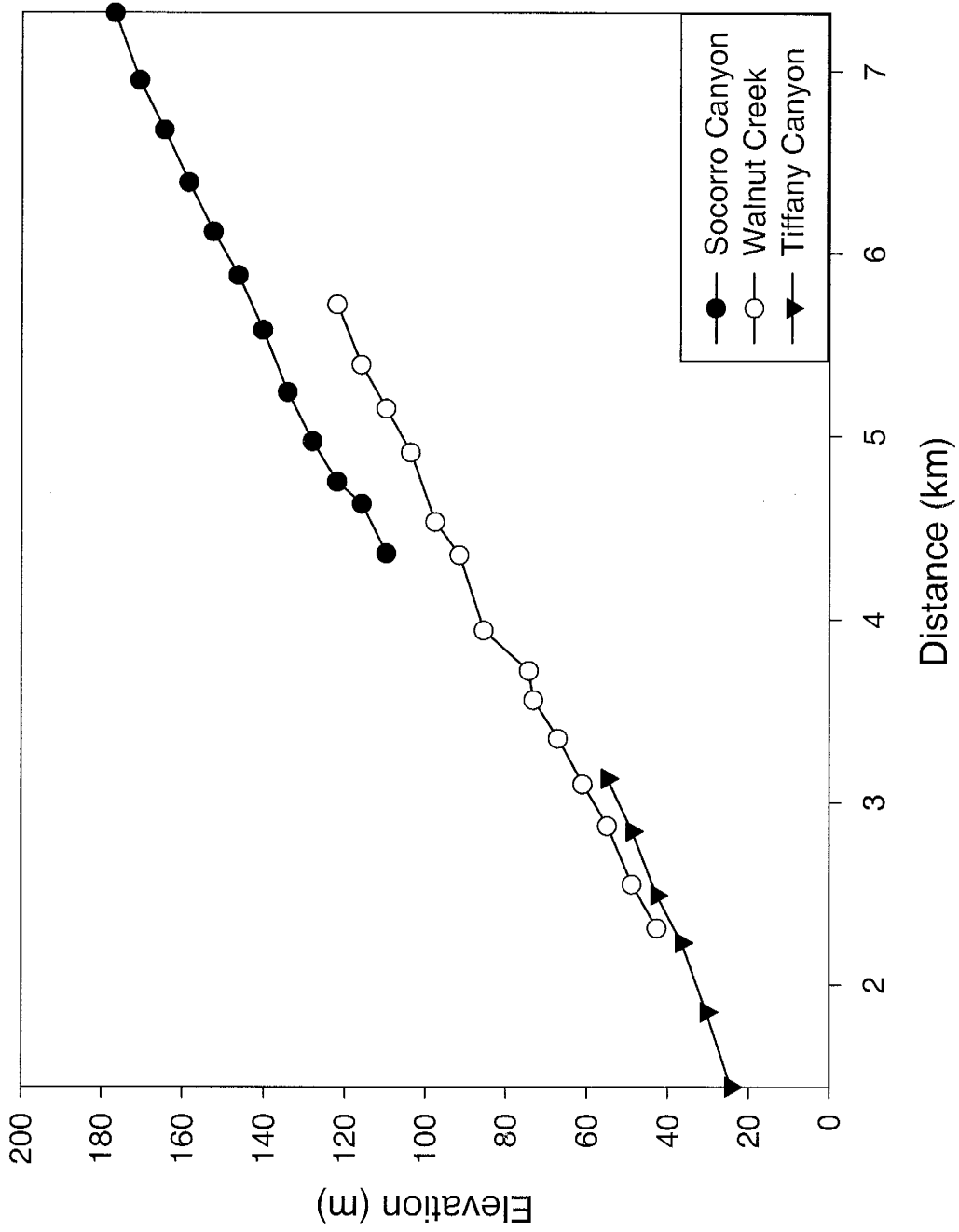


Figure 23. Longitudinal profiles of the correlated 122,000 year old terraces. Tiffany Canyon terrace gradient is 0.020, Walnut Creek and Socorro Canyon terrace gradients are both 0.023.

5.3.3. Response Time Summary

The drainage basin analysis in conjunction with the terrace profiling suggest that despite variable drainage basin areas, there is not a significant variance in drainage basin development or response time to base level change. It appears that lithologic (unconsolidated alluvium vs. crystalline and sedimentary bedrock) differences within each drainage basin area offset the total area/stream power relationship (response time). That is, the response of smaller drainage basins that occur mostly over bedrock is similar to larger drainage basins that consist of significant portions of unconsolidated alluvial material. Therefore, by using hypsometric analysis, the response times do not appear to be significantly different between tributaries, thus the correlated terraces are similar in age and represent regional geomorphic surfaces.

5.4. Soil Variability

The assumption that correlated terraces have formed contemporaneously permits the evaluation of soil variability on same aged terraces in different tributaries. However, in order to evaluate soil variability between tributaries, the variability in soil development on a single terrace must be considered first.

5.4.1. Soil Variability on a Single Terrace

Soil development on a surface begins once the rate of pedogenesis exceeds the rate of deposition or erosion (Birkeland, 1999; Jenny, 1994, Vreeken, 1975). Thus, soil development on a fluvial terrace surface begins after abandonment (incision) by the stream channel and the degree of soil development reflects the time since abandonment.

However, factors such as the texture of the deposit and climate contribute to variations in the degree of soil development. For example, micro-topographic and textural differences across a single fluvial terrace tread influence the degree and morphology of soil development (Harrison et al., 1990).

Close investigation of fluvial terraces reveals the persistence of the original stream channel topography: in particular topographically high, coarse-grained gravel bars, and topographically low, finer-grained swales. Due to these textural and topographical differences, soil development on terrace treads vary between gravel bars and finer grained swales (Harrison et al., 1990). However, over time, the topographic relief between these two features typically lessens as the swales collect aeolian material and the gravel bars erode.

A terrace tread in Walnut Creek (WCT-1) that was correlated to a dated terrace in Socorro Canyon, was used to assess the variability of soils on a single Pleistocene-aged terrace tread. To determine the variation in the degree of soil development on the Walnut Creek terrace tread, 11 soils were described in both bar and swale positions.

5.4.1.1. Bar Soils vs. Swale Soils

Harrison et al. (1990) documented distinct differences between soils developed on bar and swale sites on Late Pleistocene and Holocene-aged fluvial terraces in Cajon Pass, California. In addition, they concluded that bar soils are less variable and thus are better for developing soil chronosequences for Late Pleistocene and Holocene terraces.

To determine if differences exist between bar and swale soils on Pleistocene surfaces in the Socorro Basin, 11 soils were described on a single surface. Parameters

used in assessing significant differences between these soil locations (bar soils and swale soils) include: silt mass, clay mass, silt + clay mass, CaCO₃ mass, depth to calcic horizon, and the Soil Development Index (SDI) (Table 5). Because soil development in semi-arid areas involves the accumulation of CaCO₃, the parameters associated with CaCO₃ accumulation are most likely to indicate differences between bar and swale soils. However, aeolian additions that contribute to the accumulation of CaCO₃ in semi-arid soils also contribute to the total profile mass of silt and clay in the soil profile. Therefore, differences in silt and clay mass may also suggest differences between the bar and swale soils.

Soil pit locations were based on field observations of the original stream channel topography (Fig. 24). Although topographic relief between bars and swales is very subtle on this terrace surface, they were delineated based on surface clast size and abundance. Eleven soil pits (6 bars and 5 swales) were excavated, described and sampled for laboratory analysis.

5.4.1.2. Statistical Analysis of Soil Development on Bar and Swale Sites

5.4.1.2.a. Box Plot Overlap

The first approach used to test whether any significant differences occur in the degree of soil development on bar and swale locations was to graphically compare the overlap of the 25th and 75th quartiles for bar and swale soil parameters (Fig. 25). For example, if overlap does not occur between the 25th and 75th quartiles of each soil parameter, then it can be confidently concluded that the two soil locations are different.

Swales	Clay Mass (g/cm ²)	Silt Mass (g/cm ²)	Clay + Silt Mass (g/cm ²)
WCT1-2	9.87	46.61	56.48
WCT1-5	7.25	36.35	43.6
WCT1-6	9.1	43.54	52.64
WCT1-8	5.57	28.55	34.12
WCT1-11	5.11	24.31	29.42
mean	7.38	35.87	43.25
sd	2.1	9.51	11.6

Bars	Clay Mass (g/cm ²)	Silt Mass (g/cm ²)	Clay + Silt Mass (g/cm ²)
WCT1-1	5.55	26.62	32.17
WCT1-3	3.29	14.82	18.11
WCT1-4	4.12	20.57	24.69
WCT1-7	4.24	16.73	20.97
WCT1-9	7.55	37.9	45.45
WCT1-10	5.9	33.6	39.51
mean	5.11	25.04	30.15
sd	1.54	9.32	10.82

Bars and Swales	Clay Mass (g/cm ²)	Silt Mass (g/cm ²)	Clay + Silt Mass (g/cm ²)
WCT1-1	5.55	26.62	32.17
WCT1-2	9.87	46.61	56.48
WCT1-3	3.29	14.82	18.11
WCT1-4	4.12	20.57	24.69
WCT1-5	7.25	36.35	43.6
WCT1-6	9.1	43.54	52.64
WCT1-7	4.24	16.73	20.97
WCT1-8	5.57	28.55	34.12
WCT1-9	7.55	37.9	45.45
WCT1-10	5.9	33.6	39.51
WCT1-11	5.11	24.31	29.42
mean	5.14	24.7	29.84
s.d	2.3	11.57	13.84

Table 5a. Walnut Creek soil parameter data, including means and standard deviations.

Swales	SDI	CO3 Prof.Mass (g/cm2)	Depth to CO3 (cm)
WCT1-2	36.42	8.16	19
WCT1-5	18.37	9.40	22
WCT1-6	34.08	9.72	25
WCT1-8	30.67	7.36	21
WCT1-11	35.12	6.60	25
mean	30.93	8.25	22.40
sd	7.34	1.32	2.61
mean without WCT1-5	34.07		
sd without WCT1-5	2.46		

Bars	SDI	CO3 Prof.Mass (g/cm2)	Depth to CO3 (cm)
WCT1-1	33.78	5.36	21
WCT1-3	28.07	4.83	24
WCT1-4	32.27	5.17	30
WCT1-7	20.44	2.29	40
WCT1-9	22.01	3.09	40
WCT1-10	25.75	3.11	35
mean	27.05	3.98	31.67
sd	5.37	1.30	8.07

Bars and Swales	SDI	CO3 Prof.Mass (g/cm2)	Depth to CO3 (cm)
WCT1-1	33.78	5.36	21
WCT1-2	36.42	8.16	19
WCT1-3	28.07	4.83	24
WCT1-4	32.27	5.17	30
WCT1-5	18.37	9.40	22
WCT1-6	34.08	9.72	25
WCT1-7	20.44	2.29	40
WCT1-8	30.67	7.36	21
WCT1-9	22.01	3.09	40
WCT1-10	25.75	3.11	35
WCT1-11	35.12	6.60	25
mean	23.28	5.03	22.00
s.d	6.62	2.66	8.07
mean without WCT1-5	28.29		
sd without WCT1-5	6.41		

Table 5b. Walnut Creek soil parameter data, including means and standard deviations.

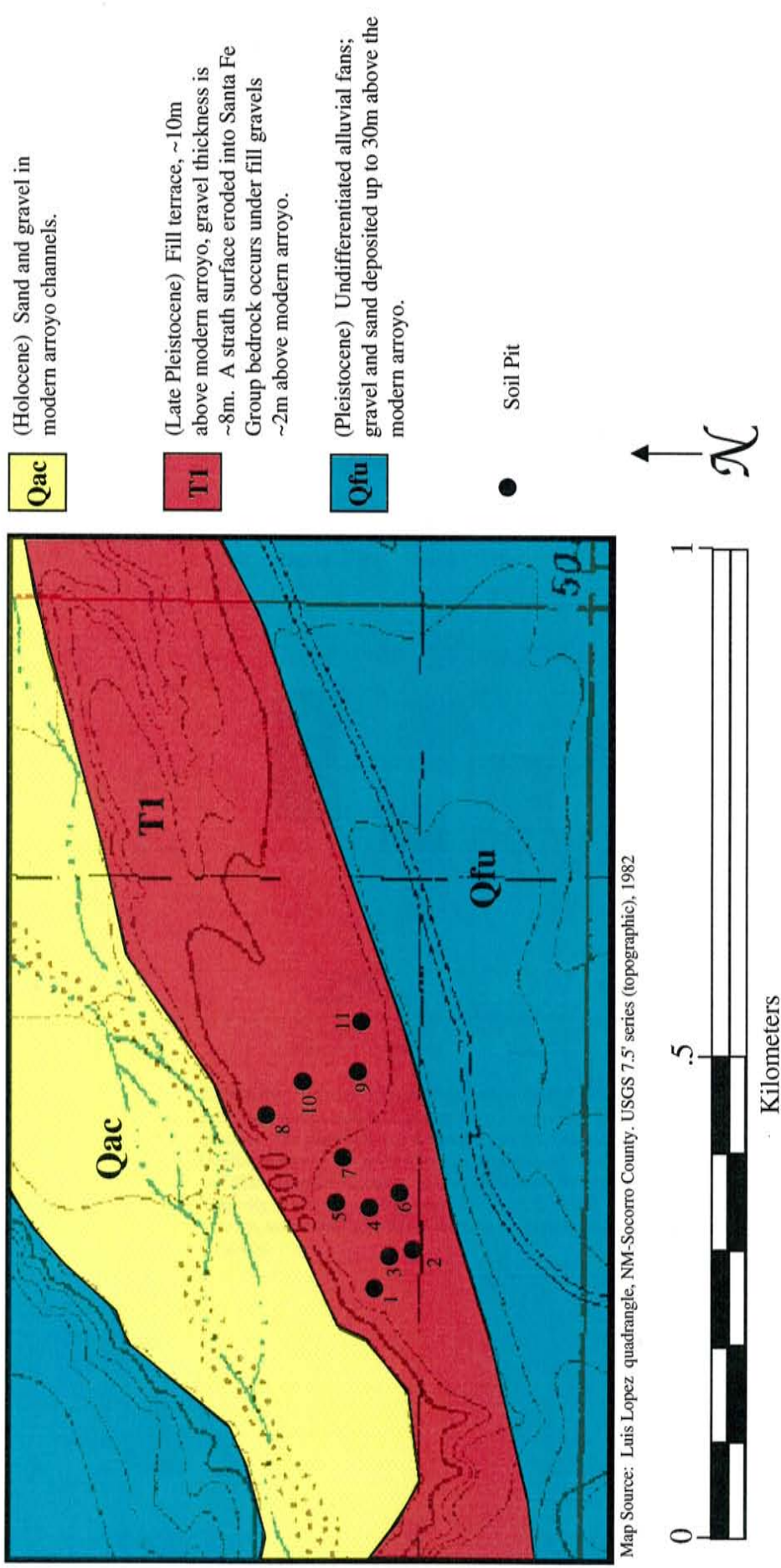


Figure 24. Soil Pit Locations on WC-T1.

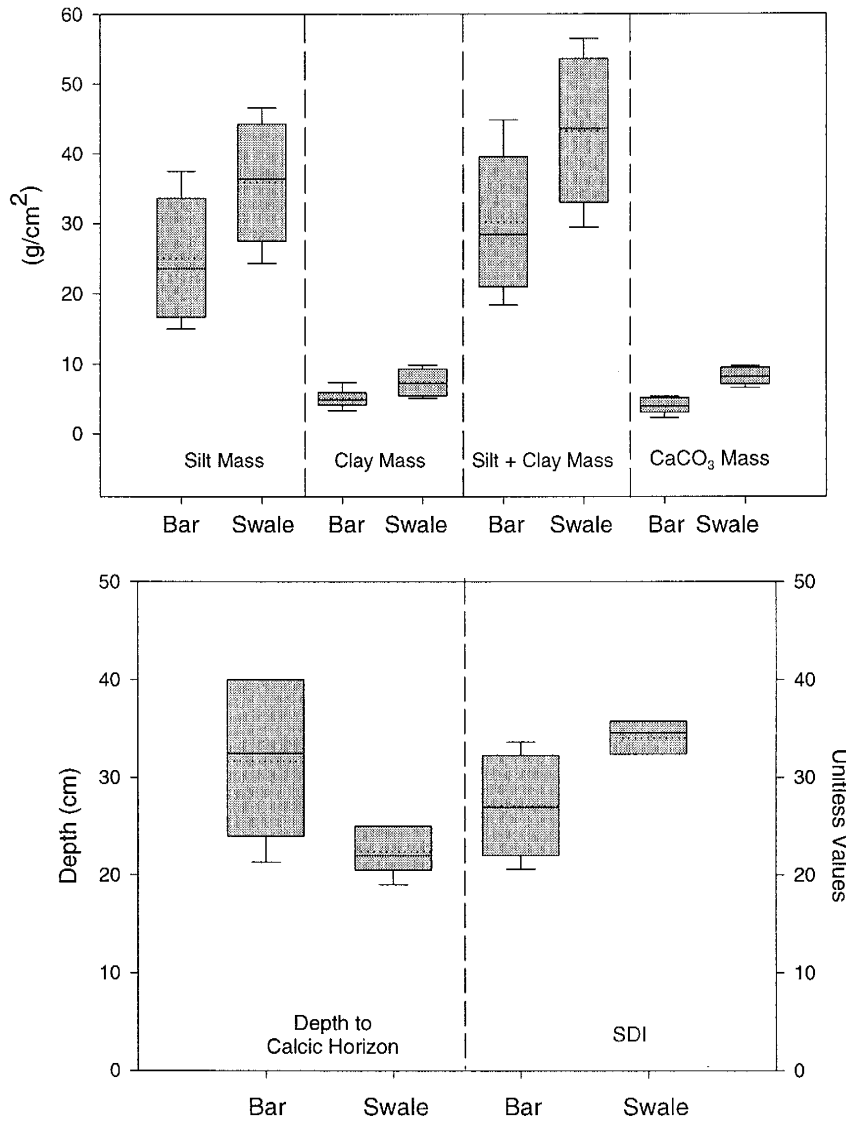


Figure 25. 25th and 75th quartile comparison of Walnut Creek bar and swale soil parameters. Shaded boxes represent 25th and 75th quartile. The dashed line is the mean and the solid line is the median. Overlap between bar and swale soil parameters (except $CaCO_3$ mass and SDI) suggests that there are not significant differences between the majority of soil parameters. However, $CaCO_3$ mass and SDI do not overlap, suggesting significant differences exist between the two soil locations.

Conversely, if the 25th or 75th quartiles of the soil parameter in one soil location overlaps the 25th or 75th quartiles of the same parameter in the other soil location, then it is assumed that there is no significant difference in this parameter between the different soil locations (Helsel and Hirsch, 1992). The overlap of the 25th and 75th quartiles for the depth to the calcic horizon, silt mass, clay mass, and silt + clay mass, suggest that there is no significant difference between the two soil locations (Fig. 25). However, the CaCO₃ mass, and SDI parameters suggest that there may be statistically significant differences between bar and swale soils. That is, the 25th and 75th quartiles do not overlap.

5.4.1.2.b. Mann-Whitney Test

The Mann-Whitney test (also called the Wilcoxon rank-sum test) is a non-parametric, distribution-independent statistical test that can be used to evaluate differences in small sample sizes. It was developed mainly to determine whether two groups belong to the same population by comparing differences between the two medians (Helsel and Hirsch, 1992). Thus, a hypothesis that the two medians *are* equal is tested against an alternative hypothesis that they *are not* equal.

If the value of the Mann-Whitney test is less than the .05 level of significance, then it can be concluded that there is a statistically significant difference between the two soil locations. For example, with respect to CaCO₃ mass, the value of .0081 is less than the .05 level of significance and thus it can be concluded that there is significant difference between bar and swale soils with respect to this parameter. The results of this test are similar to that of comparing the 25th and 75th quartile overlap. The depth to the calcic horizon, silt mass, clay mass, and silt + clay mass do not suggest a statistically

significant difference, whereas the CaCO_3 mass and SDI do suggest differences between bar and swale soils (Table 6).

5.4.1.2.c Statistics Summary

Of the six parameters used to evaluate differences between the two soil locations, only CaCO_3 mass and SDI can be used to distinguish between bar and swale sites. Therefore, the major soil forming factors of semi-arid, Pleistocene-aged terrace soils in the Socorro Basin exhibit large differences as to discriminate soils developed on bar and swale sites.

Although both tests suggest statistically significant differences between the two soil locations with respect to CaCO_3 mass and SDI, when evaluating these soils independently, statistical differences in soil parameters occur between them. That is, there are differences in means and medians, as well as small differences in standard deviations of the soil parameters (Table 5). Therefore, because most soil studies are limited to only one or two soil pits on one surface, the question arises as to the most representative location for the limited number of soil pits. That is, which soil location (bars or swales) is least variable and thus will best represent the degree of soil development on the surface.

5.4.1.3. Variability of Soils Developed in Bar and Swale Sites

The variability in soil development between bar and swale sites suggests that swale sites are better for characterizing the Pleistocene terraces. Mean and standard deviation values for the three soil parameters (SDI, CaCO_3 profile mass, and depth to

Soil Parameter	p-value	Statistical Difference Between Soil Locations
Silt Mass	0.1207	No
Clay Mass	0.1709	No
Silt+Clay Mass	0.1207	No
CaCO ₃ Mass	0.0081	Yes
Depth to Calcic Horizon	0.1003	No
SDI	0.0428	Yes

Table 6. Results of Mann-Whitney Test. The soil parameters are statistically different if the p-values are less than the .05 significance level.

calciic horizon) used to assess the differences in variability between bar and swale sites, are presented in Table 5b.

5.4.1.3.a. Soil Development Index

SDI mean values are initially 30 and 27 for swales and bars respectively. However, one swale soil (WCT1-5) has an unusually low SDI value (18), whereas the other swale soils range from 32 to 37. Therefore, the WCT1-5 soil was omitted from the swale SDI data because it is clearly an outlier with respect to this parameter. Upon removal of WCT1-5, the swale SDI mean value is 34.07. Furthermore, the standard deviation value for the swale soils (excluding WCT1-5) is 2.46 and is less than that of the bar soils (5.37). Because the swale soils vary least with respect to SDI values, swale SDI values are most representative of the soils on this terrace surface.

5.4.1.3.b. CaCO₃ Profile Mass

The mean value of CaCO₃ profile mass is 8.25 g/cm² in swale soils and 3.98 g/cm² in bar soils. Despite the apparently large difference between the mean values, the standard deviations are almost identical in both bar and swale soils (Fig. 5b). Because of the similar variability of CaCO₃ profile mass between the bar soils and the swale soils, neither soil characterizes the terrace surface better than the other. Therefore, the variability of the CaCO₃ profile mass is inconclusive as to which soil is most representative on the surface.

5.4.1.3.c. Depth to Calcic Horizon

The third parameter considered is depth to CaCO_3 . As expected, the depth to the calcic horizon is greater in the bar soils than in the swale soils (Fig. 5b). This is due mainly to the larger gravel sizes in the bar soils, which permit a deeper translocation of CaCO_3 . However, based on visual inspection, the gravel sizes within the bar soils vary considerably, thus, they have a large standard deviation. In contrast, swale soils have a small standard deviation, which is most likely due to a more consistent gravel size distribution between the swale soil pits. Therefore, the swale soils are least variable with respect to depth to the calcic horizon.

5.4.1.3.d. Bar and Swale Soil Variability Summary

Based on the results listed above, the swale soils best characterize the degree of soil development on this Walnut Creek terrace. Swale soils are favored because they typically show a lower amount of variation than do the bar soils. The conclusion that swale soils best characterize this terrace surface contrasts with previous work by Harrison et al., (1990). In their study, the terraces are no older than 12,400 +/- 1200 yr B.P., whereas in this study the terrace is ~122,000 years old. This age difference is possibly the source of the contrasting results between the two studies.

5.4.2. *Variability of Soils on Correlated Pleistocene Terraces*

The variability of soil development mentioned above is constrained to a relatively small area. That is, the soils were located on a single terrace surface and there was close spacing between soil pits. However, soil development is also commonly used for

regional correlations of geomorphic surfaces (Gile et al., 1981). Therefore, to test the validity of larger area correlations, soil parameters of correlated fluvial terraces were compared to the Walnut Creek soils to test whether or not the degree of soil development is similar for same-aged surfaces (Fig. 26). There are only two soil parameters where *both* the Socorro Canyon and Tiffany Canyon soils fall within the range of the Walnut Creek soils: silt + clay mass and CaCO₃ mass. These two parameters are associated with the accumulation of aeolian material, which is the dominant soil-forming factor in semi-arid environments. Therefore, the similarity in these parameters between tributaries suggests that they are consistent enough to be used to correlate Pleistocene geomorphic surfaces in the Socorro Basin.

5.4.3 Variability of Soils on Different Aged Terrace Surfaces

5.4.3.1. CaCO₃ Profile Mass

A general increase in soil development from younger to older terrace surfaces of the entire Socorro Basin tributary terrace sequence is apparent using CaCO₃ profile mass. The youngest surfaces have a CaCO₃ profile mass that is less than 1.15 g/cm² and the oldest surfaces have a CaCO₃ profile mass that is approximately 55 g/cm². The difference in the degree of soil development between the oldest and youngest surfaces reflects the difference in ages of these surfaces. However, in this study, the resolution diminishes considerably when differentiating the younger terrace surfaces.

Less developed soils are typically found on the lower surfaces of inset terrace sequences. However, when comparing soils on the younger terrace surfaces in the Socorro Basin tributaries, small differences from the expected trend in soil development

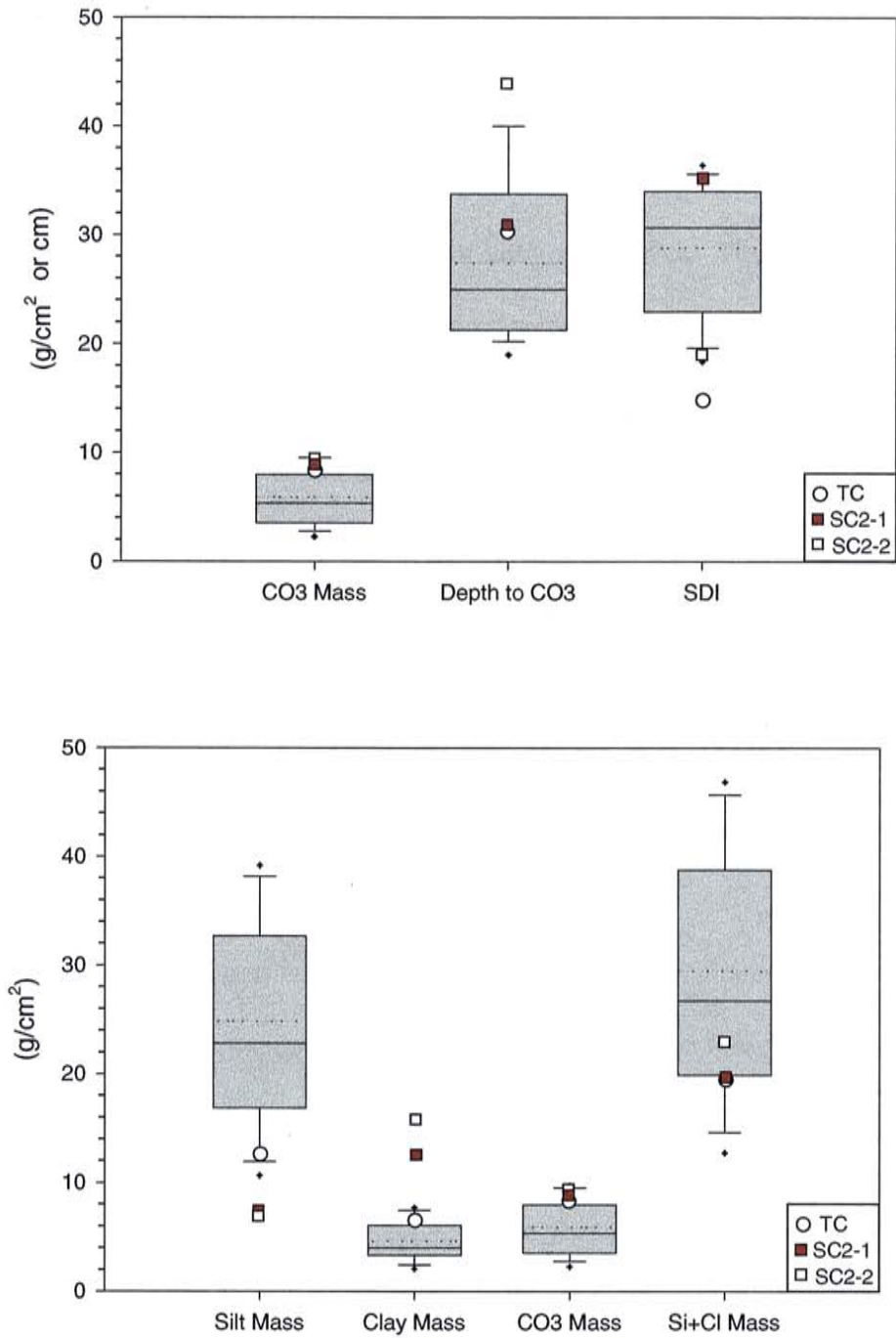


Figure 26. Comparison of soil parameters from correlated terraces to soil parameters from Walnut Creek bar and swale soils.

(CaCO₃ profile mass) are observed. For example, in Socorro Canyon and Little Nogal Arroyo, the T4 soils appear to be as developed or slightly more developed than the T3 soils (Table 2). The discrepancy of soil development between these surfaces may be explained by the geomorphic history of these younger terraces. There are small elevational differences between the flights of younger terraces. Therefore, it is likely that younger terrace deposits have overtopped older terrace surfaces. For example, in Socorro Canyon, a trench exposure across a terrace riser shows that the terrace had been under cut by a younger event after a substantial amount of time (Figure 27). That is, there is a well-developed calcic soil parallel to the slope of the terrace riser that is truncated by this undercutting, suggesting that the lower terrace level had been overtopped. Except for this discrepancy between the T3 and T4 surfaces, soil development increases with height and thus age, as is expected.

5.4.3.2. Soil Development Index

Each terrace at a particular elevation above the stream channel is assumed to be a regional surface. Therefore, the degree of soil development on these landforms should be similar. However, textural differences, as well as the geomorphic history (i.e. older surfaces being overtopped by younger deposits), influence the degree of soil development of different-aged surfaces between tributaries.

The SDI is most useful when comparing the soils on terraces within the same tributary because of the similarity of soil forming factors, such as lithology and climate, within the tributary. However, when comparing soils on tributary terraces of similar height, the SDI does not prove to be very useful. The SDI of soils on similar elevation



Figure 27. Trench exposure along SC-T2 terrace riser. Dashed line separates the terrace riser slope (with a well developed calcic soil) from a younger terrace deposit that has truncated the original terrace riser. 60 cm grubber for scale.

terraces typically has a wide range of values (Table 7b). This is a likely consequence of variable grain size distributions between the different tributaries.

Within each tributary, there is a general increase in the SDI value with age (Table 7a). One exception to this general increase in age is with the Socorro Canyon SDI values. In this tributary, SCT-3 and SCT-4 have higher SDI values than the SCT-2 surface. Because the SDI is heavily weighted towards CaCO_3 , this discrepancy, like that related to CaCO_3 mass, may also be explained by the overtopping of older surfaces by younger terrace deposits.

5.4.3.3. Depth to Calcic Horizon

The depth of calcic horizons is largely dependent on the amount of effective precipitation (Mc Donald, 1994). However, textural differences between coarser and finer grained deposits also have some control (Gile et al., 1981) as does evapotranspiration and pCO_2 . Figure 28 compares the depth to the calcic horizon for all terrace soils. The variability in depth to the calcic horizon for all Walnut Creek soils is large, however closer inspection reveals that for the most part, bar soils and swale soils can be split into two more homogeneous groups, although not necessarily two different populations.

Figure 28 also includes older and younger terrace soils as a means for comparison between very different aged soils. The oldest soil in Socorro Canyon is developed within in a swale and shows carbonate morphology of an early stage IV. Because carbonate coated clasts were found on the surface and at a shallow depth in the soil profile, this surface has likely been stripped. The amount of material that has been stripped from this surface as well as the amount of calcium carbonate that is missing is unknown.

Terrace	SDI	nSDI
LNAT-1	24.54	0.18
LNAT-2	20.34	0.15
LNAT-3	8.20	0.06
SCT-1	35.65	0.26
SCT-2	19.53	0.14
SCT-3	28.43	0.21
SCT-4	30.63	0.26
WCT-1	31.78	0.31
WCT-4	17.68	0.13
TCT-1	15.32	0.11
TCT-2	0.27	0.002

A

Elevation	SDI	nSDI
T1	35.65	0.26
T2	15 to 42	.11 to .31
T3	24 to 28	.18 to .21
T4	20 to 30	.15 to .26
T5	.2 to 17	.002 to .13

B

Table 7. Soil Development Index is a semi-quantitative measure of the degree of soil development. SDI values are based on the actual total depth of the soil whereas nSDI values are based on a common depth of 135 cm. A) SDI values for all tributary terraces. B) Range of SDI values for correlated terrace surfaces.

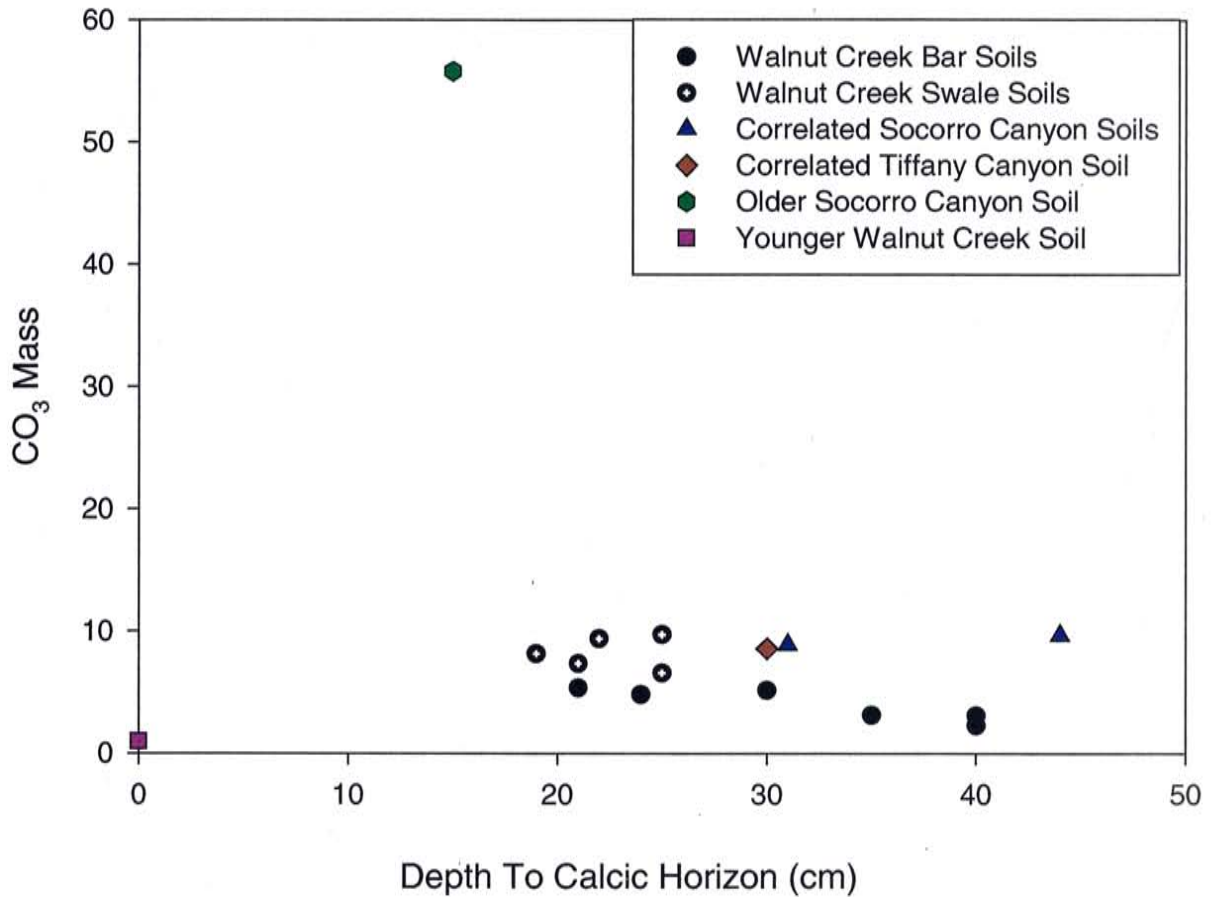


Figure 28. Comparison of soil carbonate parameters between Walnut Creek bar and swale soils and correlated tributary terrace soils. One younger Walnut Creek soil and one older Socorro Canyon soil are included to demonstrate the total range of these parameters with age.

The youngest Walnut Creek soil shown on Fig. 28 is a very young bar soil containing very little calcium carbonate and lacking carbonate morphology. This soil contains minimal amounts of calcium carbonate all of which are located near the top of the profile. Similar accumulation of CaCO_3 is also present in the uppermost horizons of older soils, which does not appear to be associated with burrowing animals. The occurrence of CaCO_3 in the upper portion of the soil profiles suggests that the effective precipitation since this recent accumulation has not been sufficient to translocate calcium carbonate into the soil profile. Historical precipitation data (Fig. 4) shows that the majority of rainfall within the study area falls during the summer monsoon season. These types of high intensity storms are not capable of translocating calcium carbonate to depth (Mc Donald, 1994).

The depth to the calcic horizon provides insight into some of the controls on the distribution of calcium carbonate. For a single-aged surface there appears to be a textural control on the distribution of calcium carbonate. That is, the depth to the calcic horizon is deeper in coarser grained deposit and shallower in finer grained deposits regardless of total profile mass of calcium carbonate. The depth to the calcic horizon is similar for soils developed on bar and swale sites on terraces in different tributaries (Figure 26).

5.5. Spatial Variation in Calcium Carbonate Accumulation Rates

CaCO_3 profile mass is a measure of the degree of soil development. CaCO_3 accumulation rates have been estimated for areas within the southwestern United States by Machette (1985), and many studies that involve calcic soils use these rates to calculate ages and correlate geomorphic surfaces (Narwold, 1999). However, few estimates of the

spatial variability of CaCO_3 accumulation rates have been made to validate regional correlation.

A terrace in Socorro Canyon (SC-T2) has a Cl-36 age of 122 kyr (Ayarbe, 2000) and a CaCO_3 profile mass of approximately 9 g/cm^2 . The Cl-36 terrace age and the soils CaCO_3 profile mass has been used to calculate a Socorro Canyon CaCO_3 accumulation rate of $.073 \text{ g/cm}^2/\text{kyr}$. This rate is similar to the rates calculated for the correlated terraces in Walnut Creek ($0.067 \text{ g/cm}^2/\text{kyr}$) and Tiffany Canyon ($0.070 \text{ g/cm}^2/\text{kyr}$) (Table 8).

Calcium-carbonate accumulation rates calculated in this study vary from those previously presented by Machette, 1985; Mc Calpin et al., (in press); and Gile, 1981 in other parts of New Mexico. The range of CaCO_3 accumulation rates calculated in this study (0.067 to $0.073 \text{ g/cm}^2/\text{kyr}$) is more than two times less than that presented by Machette (1985) for the Albuquerque area, approximately 75 miles north of present study area. However, recent work suggests that the age estimate that Machette (1985) used to calculate rates may be off by a factor of 2 or 3 (Connell et al., in press). Mc Calpin et al., (in press) calculated CaCO_3 accumulation rates for the Albuquerque area and these rates agree well with those presented by Machette (1985). Mc Calpin et al., (in press), calculated rates of $0.26 \text{ g/cm}^2/\text{kyr}$ and $0.54 \text{ g/cm}^2/\text{kyr}$ from the time periods of 4 – 82 ka and 82 – 293 ka, respectively, for soils formed in sand on the West Mesa. Near Las Cruces in southern New Mexico, Gile et al., 1981, estimated calcium carbonate accumulation rates for Early Pleistocene through Holocene surfaces. The average accumulation rate for the variously aged surfaces ranges from 0.1 to $1.0 \text{ g/cm}^2/\text{kyr}$. In addition, Gile et al., 1981, used dust trap data to calculate a present day calcium

Location	Tributary	CaCO ₃ Accumulation Rate (g.cm ³ /kyr)
North	Socorro Canyon	0.073
↓	Walnut Creek	0.067
South	Tiffany Canyon	0.07

Table 8. Range of calcium carbonate accumulation rates in the Socorro Basin.

carbonate accumulation rate of $0.02 \text{ g/cm}^2/\text{kyr}$, which is within the range of their estimated rates. The large spatial variability in accumulation rates between Albuquerque, Socorro, and Las Cruces, requires that caution be employed when using CaCO_3 profile mass and accumulation rates to correlate and assign ages to geomorphic surfaces in the desert southwest.

5.6. Formation of Correlated Tributary Terraces in the Socorro Basin

Tributary terrace sequences in the Socorro Basin record five elevations that are related to aggradation and degradation of the Rio Grande (Table 2). Two major fill terraces that are 9-10 meters (T2) and 6-7 meters (T3) are recorded in almost all tributaries. T2 is 122,000 years old (Ayarbe, 2000), and the T3 surface is estimated to be Late Pleistocene based on soil development. Three strath terraces are recorded at 29 meters (T1), 4-5 meters (T4), and <1 meter (T5). T1 is the highest and thus oldest surface and is estimated to be early-middle Pleistocene based on soil development. T4 and T5 are Late Pleistocene to Holocene surfaces estimated based on an assumed temporally consistent CaCO_3 accumulation rate as 14,000 – 15,000 years old and 9,000-12,000 years old respectively. It should be noted that although the ages for these terraces are based on soil data and one absolute date, the Late Pleistocene and Holocene age estimates are coarse and may be younger than estimated. For example, archaeological evidence in Palo Duro wash in the southern Albuquerque basin suggests that lower terrace surfaces are historical in age (Treadwell, 1996).

5.6.1. *Fill Terraces*

The base of the T2 fill terrace is exposed in Walnut Creek and Tiffany Canyon. This is represented by an erosional contact (strath surface) overlain by gravel deposits up to 8 meters thick (Fig. 19). The formation of the 122,000-year-old T2 terrace surface is possibly a consequence of climate change (marine isotope stage 6) from wetter to drier conditions. The T3 terrace is also likely to have formed as a consequence of climate change, and based on the approximate soil age, possibly during marine isotope stage 2.

The strath surface may have formed in response to Rio Grande incision during a glacial maximum when precipitation was higher than present. Higher precipitation leads to larger runoff and thus higher stream power. During this time of higher stream power, incision of the Rio Grande occurs and the tributary strath surface forms in response to the change in base level until the climate moves towards an interglacial regime. As the climate becomes more arid, stream power diminishes, vegetation ecotones shift exposing more erodable slopes, and sediment begins to accumulate in the streams. Aggradation of the arroyo continues until stream power increases or sediment supply decreases. A change in climate, which increases stream power, then initiates downcutting into the accumulated sediment and a terrace tread is left as a remnant of the former stream level.

The gravel thickness of the T2 fill terraces range from 4 to 8 meters. However, the 4-meter gravel thickness, which occurs in Socorro Canyon, is not a complete exposure of the gravels. Therefore, this is a minimum gravel thickness of this terrace surface and the true gravel thickness is likely comparable to the other terraces to which it is correlated. In addition to the similar elevations above the modern arroyo, the fact that the gravel

thickness on these correlated surfaces are fairly consistent between tributaries suggests that they were formed during the same event (Bull, 1990). Furthermore, the gravel thickness of the T3 fill terrace is thinner and does not overtop the older T2 fill terrace, which may represent a climate change of lesser magnitude (Bull, 1990).

The evidence of a climate change being responsible for the formation of the T3 terrace is supported in part by paleo-lake data in New Mexico as well as the presence of rock glaciers in the Magdalena Mountains (Blagbrough and Brown, 1983). Paleo-climate interpretations from paleo-lakes in New Mexico suggest that the last glacial maximum (~18-20Kya) generally consisted of higher precipitation and lower temperatures than the present climate. The climate record from the Estancia basin in central New Mexico suggests that the lake highstand was established approximately 23 k.y. B.P and the highstand was maintained between 20 and 15 k.y. B.P. Paleo-climate records from the Animas valley in southern New Mexico suggest a 55% to 70% increase in precipitation and an 8° to 11° C increase in summer temperatures (Kridler, 1998). In addition, paleoclimate records from the San Juan Basin in northern New Mexico, show that the last glacial maximum consisted of increased winter precipitation and a 5.5° C decrease in annual temperatures (Stute et al., 1995). Furthermore, paleoclimate records from the San Agustin Plains in central New Mexico suggest that from 21,800 to 20,600 years ago, there was a relatively stable climate with colder temperatures and about four times the moisture flux than present (Phillips et al., 1992). Further support of these climatic conditions is the presence of late Pleistocene rock glaciers in the Magdalena Mountains (Blagbrough and Brown, 1983). Rock glaciers typically represent climates indicative of lower temperatures and minimal precipitation (Blagbrough, 1994). As a whole, the

paleoclimate interpretations mentioned above are the likely climatic scenarios that occurred during the early stages of the T3 terrace formation (prior to aggradation), particularly strath formation.

The age of the T3 surface is approximately 14,000 years old and this age represents the time at which the terrace tread became abandoned. Deposition of the T3 terrace gravel corresponds with the climatic transition out of glacial maximum and towards an interglacial, where temperatures begin to increase and precipitation begins to decrease. Allen and Anderson, (2000) have identified at least nine wet/dry fluctuations between ca. 24 and 12 k.y. B.P for Lake Estancia. Specifically, they note that the climate at 13.9 k.y. B.P. (the estimated age of the T3 terrace) was as wet as the last glacial maximum.

Similar paleoclimatic conditions likely occurred during the formation of the 122,000-year-old T2 terrace. Evidence from early Lake Estancia, which is equivalent to marine oxygen isotope stage 6 (~140 kyr), suggests a cooler and wetter climate than the present (Bachhuber, 1992). In addition, the transition from stage 6 glacial maximum towards stage 5 interglacial likely had similar effects as the Pleistocene-Holocene transition discussed above.

5.6.2. *Strath Terraces*

A total of three minor strath terraces are recorded in tributaries throughout the Socorro Basin. Because they are preserved in most tributaries in the Socorro Basin, they are considered regional surfaces. The oldest and highest strath terrace (T1) is only preserved in Socorro Canyon. Lake sediments of older Rio Grande rift-fill is exposed a

few meters below the SC-T1 surface, suggesting that this terrace is probably a strath, with a thin (<2 meters) veneer of gravels at the surface. The two youngest and lowest terraces (T4 and T5) are also straths and are preserved in Little Nogal Arroyo, Socorro Canyon, and Walnut Creek. T4 and T5 are inset into the T3 fill terrace and have a gravel thickness of less than 2 meters and 30-65 cm, respectively.

The minor strath terraces represent a time at which the tributaries are either adjusting to a drop in base level or are in equilibrium with the base level. These types of terraces are not well preserved, as they are not very extensive throughout the tributaries. Furthermore, the T1 minor strath terrace is preserved as a consequence of its fortuitous location away from the avulsion direction of the Socorro Canyon stream. Therefore, it is likely that minor strath terraces had also formed inset into the T2 fill terrace, but has subsequently been eroded by more recent fluvial activity.

If high discharge events have occurred within the study area during Holocene climate fluctuations, then it is likely that these higher discharge events caused internal adjustments in the tributaries independent of the effects from the behavior of the Rio Grande. That is, because the Rio Grande base level is largely controlled by large climate changes as well as paleo lakes, smaller Holocene climate changes likely had little effect on the Rio Grande other than increasing the supply and transport of sediment. However, when considering the tributary systems, which have smaller drainage areas, internal adjustments to smaller climatic perturbations have likely occurred, thereby forming the minor strath surfaces.

Two scales of terrace development occur in the Socorro Basin tributaries; those formed by major climatic episodes, and those formed by minor climatic fluctuations. The

latter can be considered as 'noise' (representing repeated cutting and filling) at the larger scale of terraces formed by major climatic episodes, and is evidenced by the overtopping of minor terrace surfaces.

CHAPTER 6. SUMMARY

6.1. Soil Variability

Tributary terraces in the Socorro Basin were correlated based on elevation (a method independent of soil development), and are assumed to represent regional geomorphic surfaces. Correlation based on a parameter independent of soil development provides a means to assess the degree of soil spatial variability. To validate correlations and age estimates made in this study, soil variability was determined for 1) a single terrace surface, and 2) correlated terraces throughout the Socorro Basin.

Eleven soils developed in bar and swale locations on a single Pleistocene terrace surface in Walnut Creek were analyzed statistically. Statistical analysis of these soils shows that 1) swale soils are least variable overall and, 2) the soil parameters that can be used to distinguish between the bar and swale soil sites are CaCO_3 mass and SDI.

Correlated Pleistocene terrace soils throughout the Socorro Basin were compared to the Pleistocene terrace soils in Walnut Creek to determine whether or not soil development and thus soil properties are similar. There are two soil parameters where the correlated terraces fall within the range of the Walnut Creek soils; CaCO_3 mass and silt + clay mass.

6.2. *CaCO₃ Accumulation Rates*

Aridisols in the desert southwest are characterized by aeolian addition of secondary calcium carbonate, and are used as a correlative tool for geomorphic surfaces. Calcium-carbonate-accumulation rates have been estimated for areas within the southwestern United States, and these estimates are the basis for many correlations and age estimates made in geomorphic studies. However, few estimates of the variability of calcium-carbonate-accumulation rates have been made to support regional correlations. The calcium-carbonate-accumulation rates calculated in this study are based on Pleistocene soils, and are consistent throughout the Socorro Basin (0.067 g/cm²/kyr to 0.073 g/cm²/kyr). Previous estimates that have been made for the Albuquerque, NM area, are more than two times as large as the rates in the Socorro Basin. Therefore, correlation and age estimates based on calcic soil development and calcium carbonate accumulation rates without any analysis of the spatial variability must be employed cautiously. In addition, the work by Mc Calpin et al. (in press) suggests temporal variability on CaCO₃ accumulation rates. Therefore, like the spatial variability, temporal variability should also be considered when using accumulation rates to estimate ages and correlate surfaces.

6.3. *Terrace Ages and Controls on Terrace Formation*

Five tributary terrace surfaces in the Socorro Basin represent regional geomorphic surfaces assumed to be related to the Rio Grande. Two major fill terraces overlie an erosional surface and are Late Pleistocene (oxygen isotope stage 6) and Early Holocene (oxygen isotope stage 2) in age, based on calibrated soil ages. These major terrace

surfaces are the most preserved and widespread terraces in the Socorro Basin, further suggesting that they formed basin-wide as a consequence of a major controlling factor, probably climate change. Three minor strath terraces are less widespread and preserved than the major fill terraces, and except for the highest terrace preserved (early middle Pleistocene), these terraces are Holocene based on calibrated soil ages, or possibly younger. These terraces are the likely consequence of smaller climatic perturbations (than those that formed the major terraces) that resulted in internal adjustments of the tributaries.

REFERENCES CITED

- Arkley, R.J., 1963. Calculation of carbonate and water movement in soil from climatic data, *Soil Science*, v. 96, p.239-248.
- Ayarbe, J.P., 2000. Coupling a fault scarp fusion model with cosmogenic ³⁶Cl: rupture chronology of the Socorro Canyon Fault, New Mexico, Independent Study, New Mexico Institute of Mining and Technology, pp.72.
- Allen, B.D., and Anderson, R.Y., 2000. A continuous high-resolution record of late Pleistocene climate variability from the Estancia basin, New Mexico, *Geological Society of America Bulletin*, v. 112, no., 9, p. 1444-1458.
- Bachhuber, F.W., 1992. A pre-late Wisconsin paleolimnologic record from the Estancia Valley, central New Mexico, in: Clark, P.U., and Lea, P.D., eds., *The last interglacial-glacial transition in North America: Boulder, Colorado*, Geological Society of America Special Paper 270.
- Birkeland, P.W., 1999. *Soils and Geomorphology*, 3rd Ed., Oxford University Press, New York, 430pp.
- Blagbrough, J.W., 1994. Late Wisconsin climatic inferences from rock glaciers in south-central and west-central New Mexico and east-central Arizona, *New Mexico Geology*, v.16, no. 4, p. 65-71.
- Blagbrough, J.W., and Gassaway Brown III, H., 1983. Rock glaciers on the West slope of South Baldy, Magdalena Mountains, Socorro County, New Mexico, in: Charles E. Chapin (Ed.), *New Mexico Geological Society Thirty-Fourth Annual Field Conference, Socorro Region II*, p.299 –302.
- Bruning, J.E., 1973. Origin of the Popotosa Formation, north-central Socorro County, New Mexico, PhD Dissertation, New Mexico Institute of Mining and Technology, pp. 142.
- Bull, W.B., 1990. Stream-terrace genesis: implications for soil development. In: P.L.K. Knuepfer and L.D. McFadden (Eds.), *Soils and Landscape Evolution. Geomorphology*, v. 3, p.351-367.

- Bull, W.B., 1991a. *Geomorphic Response to Climate Change*, Oxford University Press, New York, 326 pp.
- Bull, W.B., 1991b. Threshold of critical power in streams, *Geological Society of America Bulletin*, part I, v.90, p. 453-464.
- Cather, S.M., Chamberlin, R.M., Chapin, C.E., and McIntosh, W.C., 1994. Stratigraphic consequences of episodic extension in the Lemitar Mountains, central Rio Grande rift, *Geological Society of America, Special Paper 291*, p.157-169.
- Chamberlin, R.M., 1983. Cenozoic domino-style crustal extension in Lemitar Mountains, New Mexico: A Summary, *New Mexico Geological Society, Guidebook 34*, p.111-118.
- Chapin, C.E., Cather, S.M., 1994. Tectonic setting of the axial basins of the Northern and Central Rio Grande Rift, in: *Basins of the Rio Grande Rift: Structure, Stratigraphy, and Tectonic Setting*, eds. G. Randy Keller and Steven M. Cather, *Geological Society of America Special Paper 291*, p. 5-25.
- Connell, S.D., Love, D.W., 2000. Stratigraphy of Rio Grande terrace deposits between San Felipe Pueblo and Los Lunas, Albuquerque Basin, New Mexico, *New Mexico Geological Society Annual Spring Meeting Abstracts*, p. 52.
- Dan, J., Yaalon, D.H., 1982. Automorphic saline soil in Israel, *Catena*, Suppl. 1, p. 103-115.
- Dethier, D.P., Harrington, C.D., Aldrich, M.J., 1988, Late Cenozoic rates of erosion in the western Espanola Basin, New Mexico: Evidence from geologic dating of erosion surfaces: *Geological Society of America Bulletin*, v. 100, p.928-937.
- Drever, J.I., 1997. *The geochemistry of natural waters: surface and groundwater environments*, 3rd Ed., Prentice Hall Publishers, New Jersey, pp. 436.
- Eaton, G.P., 1979. A plate-tectonic model for Late Cenozoic crustal spreading in the western United States, in: *Rio Grande Rift: Tectonic and Magmatism*, Robert E.Riecker, ed., p. 7-32.
- Eppes, M.C., 1998. A spatial variability and chronosequence study of soils developing on Basalt flows in the Potrillo Volcanic Field, southern New Mexico. M.S. Thesis, New Mexico Institute of Mining and Technology, pp. 95.

- Gile, L., McCall, C., Monger, C., 1996. Evolution of the Rio Grande Valley, Video, T. Coberty, Ed., New Mexico State University Board of Regents.
- Gile, L., Hawley, J., Grossman, R., 1981. Soils and geomorphology in the Basin and Range area of southwestern New Mexico-Guidebook to the Desert Project. New Mexico Bureau of Mines and Mineral Resources Memoir 39.
- Harden, J.W., 1982. A quantitative index of soil development from field descriptions: Examples from a chronosequence in central California. *Geoderma*, v. 28, p. 1-28.
- Harden, J.W., Taylor, E.M., 1983. A quantitative comparison of soil development in four climatic regimes, *Quaternary research*, v. 20, p. 342 – 359.
- Harrison, J.B.J., McFadden, L.D., Weldon III, R.J., 1990. Spatial soil variability in The Cajon Pass chronosequence: implications for the use of soils as a geochronological tool, *Geomorphology*, V. 3, p. 399-416.
- Hawley, J.W., 1998. Hydrogeologic framework of the middle Rio Grande Basin – conceptual model development in the 20th century, *New Mexico Geology*, P. 57.
- Hawley, J.W., Kottowski, F.E., 1969. Quaternary geology of the south-central New Mexico border region; *in* Kottowski, F.E., and LeMone, D.V. (eds.), *Border stratigraphy symposium*: New Mexico Bureau of Mines and Mineral Resources Circular 187, 40 pp.
- Helsel, D.R. and Hirsch, R.M., 1992. *Studies in Environmental Science 49: Statistical Methods in Water Resources*, Elsevier Science Publishing Co., New York, New York, 552 pp.
- Jenny, H., 1994. *Factors of Soil Formation: A System of Quantitative Pedology*, Dover Publishing, Inc., New York, pp.281.
- Krider, P.R., 1998. Paleoclimate significance of Late Quaternary lacustrine and alluvial stratigraphy, Animus Valley, New Mexico. *Quaternary Research*, v. 50, p. 283-289.
- Leopold, L.B., Wolman, M.G., and Miller, J.P., 1964. *Fluvial processes in geomorphology*: San Francisco, W.H. Freeman, pp.522.
- Lozinsky, R.P., 1985. *Geology and late Cenozoic history of the Elephant Butte area, Sierra County, New Mexico*, New Mexico Bureau of Mines and Mineral Resources Circular 187, 40 pp.

- Machette, M.N., 1978. Late Cenozoic geology of the San-Acacia-Bernardo area, New Mexico Bureau of Mines and Mineral Resources, Circular 163, p. 135-137.
- Machette, M., 1985. Calcic soils of the southwestern United States, in Weide, D., ed., Soils and Quaternary Geomorphology of the Southwestern United States: Geological Society of America Special Paper 203: p. 1-21.
- Machette, M.N., Long, T., Bachman, G.O., and Timbel, N.R., 1997. Laboratory data for calcic soils in central New Mexico: Background information for mapping Quaternary deposits in the Albuquerque Basin, New Mexico Bureau of Mines and Mineral Resources Circular 205, 63 pp.
- Mack, G.H., Love, D.W., Seager, W.R., 1997. Spillover models for axial rivers in regions of continental extension; the Rio Mimbres and Rio Grande in the southern Rio Grande Rift, USA, *Sedimentology*, v.44, n.4, p. 637-652.
- McDonald, E., 1994. The relative influences of climate change, desert dust, and lithologic control on soil-geomorphic processes and hydrology of calcic soils formed on Quaternary alluvial-fan deposits in the Mojave Desert, California. Ph.D. Dissertation, University of New Mexico, 383 pp.
- McGrath, D.B., Hawley, J.W., 1987. Geomorphic evolution and soil-geomorphic relationships in the Socorro area, central New Mexico, in: *Guidebook to the Socorro Area, New Mexico*, p. 55-67.
- Morgan, P., Golombek, M.P., 1984. Factors controlling the phases and styles of extension in the northern Rio Grande Rift, in: *New Mexico Geological Society Guidebook, 35th Field Conference*, p. 13-19.
- Narwold, C., 1999. Late Quaternary faulting along the Quinn River fault zone (QRfz); a soils investigation, Quaternary Geology of the Northern Quinn River and Alvord Valleys, Southeastern Oregon, 1999 Friends of the Pleistocene Field Trip Guide – Pacific Cell, p. A1-1 – A1-18.
- Phillips, F.M., Campbell, A.R., Kruger, C., Johnson, P., Roberts, R. and Keyes, E., 1992. A reconstruction of the response of the water balance in Western United States lake Basins to climatic change. New Mexico Water Resources Research Institute Report No. 269.
- Reheis, M.C., and Kihl, R., 1995, Dust Deposition in Southern Nevada and California, 1984-1989: Relations to Climate, Source Area, and Lithology, *Journal of Geophysical Research*, v. 100D5, p. 8893-8918.
- Ritter, D.F., 1986. *Process Geomorphology*, 2nd Ed., W.C. Brown Publishers, Dubuque, IA, pp. 579.

- Ruhe, R.V., 1956. Geomorphic surfaces and the nature of soils, *Soil Science*, v. 82, p. 441-455.
- Ruhe, R.V., 1974. Holocene environments and soil geomorphology in Midwestern United States, *Quaternary Research*, v. 4, n. 4, p. 487-495.
- Sanford, A.R., 1968. Gravity survey in central Socorro County, New Mexico, New Mexico Bureau of Mines and Mineral Resources Circular 91, 14 pp.
- Singer, M., Janitzky, P., (Eds.) 1986. Field and laboratory procedures used in a soil chronosequence study. Bulletin 1648. U.S. Geological Survey, Denver, CO.
- Soil Survey Staff, 1951. Soil survey manual: Washington, D.C., U.S. Department of Agriculture and U.S. Government Printing Office, Agricultural Handbook 18.
- Soil Survey Staff, 1975. Soil survey manual: Washington, D.C., U.S. Department of Agriculture and U.S. Government Printing Office, Agricultural Handbook 36.
- Strahler, A. N., 1952. Hypsometric (Area-Altitude) Analysis of Erosional Topography, *Bulletin of the Geological Society of America*, v. 63, p. 117-1142.
- Stute, M., Clark, J.F., Schlosser, P. Broecker, W.S., and Bonani, G., 1995. A 30,000 yr continental paleotemperature record derived from noble gases dissolved in groundwater from the San Juan Basin, New Mexico. *Quaternary Research*, v. 43, p.209-220.
- Tonkin, P.J., Harrison, J.B.J., Whitehouse, I.E., Campbell, A.S., 1981. Methods for Assessing lake Pleistocene and Holocene erosion history in glaciated mountain drainage basins, in: *Erosion and Sediment Transport in Pacific Rim Steeplands*, I.A.H.S. publication no. 132, Christchurch, New Zealand, p.527 - 543.
- Treadwell, C., 1996. Late Cenozoic landscape evolution, and soil geomorphic and geochemical factors influencing the storage and loss of carbon within a semi-arid, extensional landscape: Palo Duro Wash, Rio Grande Rift, Central New Mexico, Thesis (Ph.D.), University of New Mexico, pp. 261.
- Vreeken, W.J., 1975. Principal kinds of chronosequences and their significance in soil history, *Journal of Soil Science*, v. 26, p378-394.
- Washburn, A.L., 1973. *Periglacial processes and environments*: New York, St. Martin's Press, 320 pp.

Wilkins, D.W., 1986. Geohydrology of the southwest alluvial basins regional aquifer- systems analysis, parts of Colorado, New Mexico, and Texas, U.S. Geological Survey Water-Resources Investigations Report 84-4224, 61 pp.

Appendix 1 - Soil Descriptions

LNAT-1 95 cm deep creosote, mixed grasses, mesquite flat surface

Horizon	Depth (cm)	Color (m)	Color (d)	Structure	Gravel (%)	Consist. (m)	Consist. (d)	Texture (Lab)	Texture (Lab)	CO3 Stage	CO3 %	Boundary	Clay films	Roots
Ak	0-8	10YR 3.5/3	10YR 5/3	2msbk	30	ss/ps	so	SCL	SCL	0	1.0	c/w	-	1f
Btk	8-20	7.5YR 4/3	7.5YR 4/4	1fsbk	55	s/p	so	SCL	SCL	0	1.0	g/w	2m pf/br	1f/v1m
Bkt1	20-35	7.5YR 4.5/3	7.5YR 4/3	1fsbk	60	s/p	so	SCL	SCL	I	1.5	g/w	2m pf/br	v1f
Bkt2	35-65	7.5YR 4/4	7.5YR 5/3.5	1fsbk	65	so/po	sh	SL	SL	I	1.5	g/w	1f pf/br	v1f
Ck	65-95	10YR 4/3	10YR 5/4	sg	50	so/po	lo	LS	S	I	1.0	-	-	v1f

LNAT-2 85 cm deep creosote, mixed grasses, mesquite flat surface

Horizon	Depth (cm)	Color (m)	Color (d)	Structure	Gravel (%)	Consist. (m)	Consist. (d)	Texture (Lab)	Texture (Lab)	CO3 Stage	CO3 %	Boundary	Clay films	Roots
Ak	0-6	7.5YR 4/2.5	10YR 5/3	2msbk	20	so/po	sh	L	SL	0	1.0	c/w	-	2f
Btk1	6-30	7.5YR 4/3	7.5YR 4/4	1fsbk	65	s/p	sh	CL	SCL	0	1.0	i/w	2m pf/br	v1f/v1f
Btk2	30-65	7.5YR 4/3	7.5YR 5/3	1fsbk	65	ss/po	sh	SL	SL	I	1.0	g/w	1f pf/br	v1f/v1f/v1m
Ck	65-85	7.5YR 4/3	7.5YR 5/3	sg	60	so/po	lo	LS	SL	I	1.0	-	-	-

LNAT-3 60 cm deep creosote, mixed grasses, mesquite flat surface

Horizon	Depth (cm)	Color (m)	Color (d)	Structure	Gravel (%)	Consist. (m)	Consist. (d)	Texture (Lab)	Texture (Lab)	CO3 Stage	CO3 %	Boundary	Clay films	Roots
Ak	0-7	10YR 4/2.5	10YR 5/3	1msbk	40	so/po	so	SIL	SL	I	1.0	g/w	-	v1f
Bk	7-50	10YR 4/3	10YR 5/3	sg	80	ss/po	lo	CL	SL	I	1.5	c/w	-	2f/1m
Ck	50-60	10YR 4/3	10YR 5/4	sg	90	ss/po	lo	L	SL	I	1.0	-	-	v1f

LNA-pm arroyo bottom

Horizon	Depth (cm)	Color (m)	Color (d)	Structure	Gravel (%)	Consist. (m)	Consist. (d)	Texture (Lab)	Texture (Lab)	CO3 Stage	CO3 %	Boundary	Clay films	Roots
LNA-pm		10YR 4/2	10YR 6/2	sg	70	so/po	lo	S	S	-	-	-	-	-

Appendix 1 - Continued

SCT-1

Horizon	Depth (cm)	Color (m)	Color (d)	Structure	Gravel (%)	Consistence (m)	Consistence (d)	Texture			CO3	
								Texture (Lab)	Texture (d)	Texture (Lab)		Caly Films
Ak	0-6	10YR 3/3	10YR 5/3	2msbk	20	so/po	sh	SL	SCL	N/A	g/w	0.5
Bkt	6-15	10YR 3/3	10YR 5/3	2fsbk	15	ss/ps	sh	CL	SL	N/A	a/w	I
Bkt	15-35	10YR 4/3	10YR 5/3	3msbk	5	ss/ps	h	CL	L	N/A	g/w	II
K1	35-60	10YR 6/4	10YR 6/3	m	5	so/po	vh	LS	L	N/A	g/w	IV-
K2	60-95	7.5YR 7/4	7.5YR 8/3	m	5	ss/po	h	SIL	CL	N/A	N/A	III+

SCT-2

Southern wall profile

5.4m from west end of trench

Horizon	Depth (cm)	Color (m)	Color (d)	Structure	Gravel (%)	Consistence (m)	Consistence (d)	Texture			CO3	
								Texture (Lab)	Texture (d)	Texture (Lab)		Caly Films
A	0-11	7.5YR 4/4	7.5YR 5/4	1fsbk	30	so/po	so	SL	CL	N/A	g/w	0
Ak	11-17	5YR 4/3	5YR 4/6	1vfsbk	60	ss/ps	so	SCL	L	N/A	s/w	I
Bkt	17-31	5YR 4/4	5YR 4/6	1fsbk	70	s/ps	h	SC	C	1pf	s/w	I
Bk1	31-48	5YR 4/4	5YR 5/6	sg	50	s/ps	lo	SC	SCL	N/A	g/w	II
Bk2	48-65	7.5YR 4/6	7.5YR 6/6	sg	60	so/po	lo	LS	SL	N/A	s/w	I
Ck	65-100	10YR 5/3	10YR 6/2	sg	60	so/po	lo	S	S	N/A	s/w	I
Ck2	100-108	7.5YR 4/2	7.5YR 6/4	sg	50	so/po	lo	S	S	N/A	N/A	I

SCT-3

Southern wall profile

5.6m from west side of trench

Horizon	Depth (cm)	Color (m)	Color (d)	Structure	Gravel (%)	Consistence (m)	Consistence (d)	Texture			CO3	Roots	
								Texture (Lab)	Texture (d)	Texture (Lab)			Caly Films
A	0-8	7.5YR 3/4	10YR 4/6	1fsbk	50	so/po	so	L	SL	N/A	a/w	0	3f/m
Bt1	8-45	5YR 4/3	5YR 4/4	2msbk	60	s/ps	sh	SCL	SCL	2dptf	g/w	0	2f
Bt2	45-67	5YR 3/4	7.5YR 4/6	2msbk	75	ss/po	sh	LS	SL	1dptf	a/w	0	v1vf
Bk	67-110	5YR3/3	7.5YR 4/6	1fsbk	55	so/po	sh	LS	LS	N/A	N/A	I+	v1vf

SCT-4

Arroyo exposure

Horizon	Depth (cm)	Color (m)	Color (d)	Structure	Gravel (%)	Consistence (m)	Consistence (d)	Texture			CO3	Roots	
								Texture (Lab)	Texture (d)	Texture (Lab)			Caly Films
A	0-5	5YR 3/4	7.5YR 4/6	1fsbk	30	ss/ps	so	CL	CL	N/A	a/w	0	2f
Bt	5-45	5YR 3/4	7.5YR 4/4	2msbk	20	s/ps	h	SCL	CL	1fptf	a/w	0	1f
Ck	45-70	5YR 3/4	5YR 4/6	1fsbk	70	s/ps	sh	SCL	SCL	N/A	a/w	I	1f
2Ck	70-90	5YR 3/4	7.5YR 6/4	2msbk	0	ss/ps	h	L	L	N/A	N/A	I+	v1m

WCT1-1 Bar												
Horizon	Thickness (cm)	Color (m)	Color (d)	Structure	Gravel (%)	Consistence (m)	Consistence (d)	Texture	Caly Films	Boundary	CO3	roots
A	11	10YR 4/2	10YR 4/4	1msbk	5	so/po	so	L	-	gw	0	2f/1m
Bk	10	10YR 4/3	10YR 4/4	1msbk	50	s/ps	so	SiCL	1pf	gw	I	1f
Bk1	19	10YR 4/3	10YR 5/4	1fsbk	60	ss/ps	sh	SCL	-	gw	I+	1f
Bk2	13	10YR 5/3	10YR 6/3	1msbk	50	s/ps	h	CL	-	gw	II	v1f
2Bk3	39	10YR 5/3	10YR 6/4	2msbk	40	s/ps	sh	SL	-	gw	II	v1f
2K	29	10YR 5/3	10YR 7/2	m	50	so/po	eh	LS	-	gw	III	-
2Ck	14	7.5YR 3/3	7.5YR 5/3	sg	30	so/po	lo	S	-	-	I	-

WCT1-2 Swale												
Horizon	Thickness (cm)	Color (m)	Color (d)	Structure	Gravel (%)	Consistence (m)	Consistence (d)	Texture	Caly Films	Boundary	CO3	roots
A	8	10YR 3/2	10YR 4/3	2msbk	10	ss/po	so	L	-	gw	0	2f
Bk	11	7.5YR 4/3	7.5YR 4/4	2msbk	10	s/ps	sh	CL	v1pf	gw	I	v1f/v1m/v1c
Bk1	10	7.5YR 4/3	7.5YR 5/4	2msbk	10	ss/ps	sh	SCL	-	gw	I+	v1f/v1m
Bk2	51	10YR 5/3	10YR 6/3	3msbk	20	s/ps	sh	CL	-	gw	II	1f
Bk3	20	10YR 4/3	10YR 6/4	2msbk	40	so/po	h	LS	-	gw	II	-
Ck	35	7.5YR 4/3	7.5YR 5/4	1fsbk	30	ss/po	so	LS	-	-	I	-

WCT1-3 Bar												
Horizon	Thickness (cm)	Color (m)	Color (d)	Structure	Gravel (%)	Consistence (m)	Consistence (d)	Texture	Caly Films	Boundary	CO3	roots
A	9	10YR 4/2	10YR 5/3	2msbk	20	so/po	so	SCL	-	gw	0	1f
Bt	15	7.5YR 4/3	7.5YR 5/3	2msbk	50	s/p	sh	SCL	2mpf	gw	0	v1f
Bk1	16	10YR 4/4	10YR 6/4	1msbk	60	ss/po	sh	LS	1pf	gw	II	v1f
Bk1	60	10YR 5/3	10YR 6/2	1fsbk	60	ss/po	sh	LS	-	gw	II+	-
Ck	35	10YR 3/2	10YR 6/2	sg	40	so/po	lo	S	-	-	I	-

WCT1-4 Bar												
Horizon	Thickness (cm)	Color (m)	Color (d)	Structure	Gravel (%)	Consistence (m)	Consistence (d)	Texture	Caly Films	Boundary	CO3	roots
A	11	10YR 4/2	10YR 5/3	2msbk	10	so/po	so	SiCL	-	gw	0	1f/1m
Bt	19	7.5YR 4/3	7.5YR 4/4	2fsbk	40	s/ps	sh	SiCL	1pf	gw	0	1f
Bk1	30	10YR 5/3	10YR 6/3	1fsbk	50	ss/po	sh	SCL	-	gw	II	v1m
Bk1	15	10YR 5/3	10YR 7/3	1fsbk	50	ss/po	sh	SCL	-	gw	II	-
K	15	10YR 5/2	10YR 7/2	m	50	so/po	h	LS	-	gw	III	-
Ck	45	10YR 4/3	10YR 6/3	sg	60	so/po	lo	S	-	-	I	-

WCT1-5		Swale										
Horizon	Thickness (cm)	Color (m)	Color (d)	Structure	Gravel (%)	Consistence (m)	Consistence (d)	Texture	Caly Films	Boundary	CO3	roots
A	8	10YR 4/2	10YR 5/4	1msbk	10	ss/ps	so	SCL	-	gw	0	1f/1m
Bt	14	7.5YR 3/4	7.5YR 4/4	2msbk	10	s/ps	sh	SCL	1fpf	gw	0	1v1f
Bk1	23	10YR 4/4	10YR 5/4	3msbk	10	s/p	h	CL	-	gw	I+	1v1f
Bk1	25	10YR 5/3	10YR 6/3	2msbk	50	s/ps	h	SCL	-	gw	II	-
K	23	10YR 6/4	10YR 6/3	m	50	so/ps	h	SL	-	gw	III	-
Ck	52	7.5YR 4/3	7.5YR 6/3	sg	80	so/ps	lo	S	-	-	I	-

WCT1-6		Swale										
Horizon	Thickness (cm)	Color (m)	Color (d)	Structure	Gravel (%)	Consistence (m)	Consistence (d)	Texture	Caly Films	Boundary	CO3	roots
A	6	10YR 4/3	10YR 4/4	2msbk	10	ss/ps	so	CL	-	gw	0	1f/1m
Bt	19	10YR 3/4	10YR 4/4	3msbk	10	s/ps	sh	CL	1fpf	gw	0	1f
Bk1	25	10YR 4/4	10YR 5/4	3msbk	30	s/ps	h	SCL	-	gw	II	1v1f
Bk1	25	10YR 5/4	10YR 6/4	3msbk	30	s/ps	h	SCL	-	gw	II	1v1f
Bk2	15	10YR 5/4	10YR 6/4	3msbk	30	s/ps	h	SCL	-	gw	II	1v1f
2K	30	10YR 5/3	10YR 7/3	m	40	ss/ps	h	LS	-	gw	III	-
2Ck	15	10YR 4/4	10YR 5/4	sg	80	so/ps	lo	S	-	-	I	-

WCT1-7		Bar										
Horizon	Thickness (cm)	Color (m)	Color (d)	Structure	Gravel (%)	Consistence (m)	Consistence (d)	Texture	Caly Films	Boundary	CO3	roots
A	10	10YR 4/2	10YR 5/3	1fsbk	10	ss/ps	so	SL	-	gw	0	1f
Bt	15	7.5YR 4/3	7.5YR 4/4	1fsbk	50	s/p	sh	SCL	2fpf	gw	0	1f
Bk1	15	10YR 3/4	10YR 4/4	1fsbk	70	s/p	sh	SCL	1fpf	gw	I	1v1f
Bk	35	10YR 5/3	10YR 6/4	2msbk	70	ss/ps	lo	SL	-	gw	II	-
Ck	60	10YR 4/2	10YR 6/3	sg	50	so/ps	lo	S	-	-	I	-

WCT1-8		Swale										
Horizon	Thickness (cm)	Color (m)	Color (d)	Structure	Gravel (%)	Consistence (m)	Consistence (d)	Texture	Caly Films	Boundary	CO3	roots
A	8	10YR 4/3	10YR 4/4	1fsbk	10	ss/ps	so	CL	-	gw	0	2f/1m
Bk1	13	10YR 4/3	10YR 4/4	2msbk	20	s/ps	sh	SCL	1fpf	gw	I	1v1f
Bk1	14	10YR 4/4	10YR 5/4	2msbk	50	s/ps	sh	CL	-	gw	II	-
Bk	25	10YR 4/4	10YR 5/4	2msbk	50	ss/ps	sh	SL	-	gw	II	-
K	45	7.5YR 6/2	7.5YR 7/2	m	40	ss/ps	h	SL	-	gw	III	-
Ck	30	10YR 4/3	10YR 6/3	sg	40	so/ps	lo	S	-	-	I	-

WCT1-9		Bar												
Horizon	Thickness (cm)	Color (m)	Color (d)	Structure	Gravel (%)	Consistence (m)	Consistence (d)	Texture	Caly Films	Boundary	CO3	roots		
A	9	10YR 3/3	10YR 4/4	1msbk	10	so/po	so	SL	-	gw	0	1f/v1m		
Bt	21	7.5YR 4/3	7.5YR 4/4	1msbk	60	s/p	sh	CL	2pfp	cw	0	v1f/v1m/v1vc		
Bkt	20	10YR 4/4	10YR 5/3	1fsbk	60	ss/po	sh	SCL	-	cw	I	-		
Bk	22	10YR 5/4	10YR 6/3	2fsbk	60	ss/ps	sh	SCL	-	cw	II	v1f/v1c		
Ck	12	10YR 4/3	10YR 5/4	sg	50	ss/po	lo	SCL	-	-	I	-		

WCT1-10		Bar												
Horizon	Thickness (cm)	Color (m)	Color (d)	Structure	Gravel (%)	Consistence (m)	Consistence (d)	Texture	Caly Films	Boundary	CO3	roots		
A	10	10YR 4/2	10YR 4/3	2fsbk	20	ss/p	so	SiCL	-	gw	0	v1m		
Bt	15	10YR 4/3	10YR 4/4	2msbk	10	s/p	sh	SiCL	1pfp	gw	0	v1m		
Bkt	20	10YR 4/3	10YR 5/4	3msbk	10	s/p	sh	SCL	-	cw	I	v1f/v1m		
Bk	30	7.5YR 5/3	7.5YR 6/4	1fsbk	60	so/po	sh	LS	-	cw	II	1v1		
Ck	60	10YR 4/2	10YR 6/2	sg	50	so/po	lo	S	-	-	I	-		

WCT1-11		Swale												
Horizon	Thickness (cm)	Color (m)	Color (d)	Structure	Gravel (%)	Consistence (m)	Consistence (d)	Texture	Caly Films	Boundary	CO3	roots		
A	11	10YR 4/2	10YR 4/3	1fsbk	30	ss/ps	so	SiCL	-	gw	0	1f		
Bkt	24	7.5YR 4/3	7.5YR 4/4	1msbk	60	s/p	sh	CL	2mpf	cw	I	1m		
Bk	15	10YR 5/4	10YR 6/3	1msbk	50	s/ps	sh	SCL	-	gw	II	v1f		
K	20	10YR 6/3	10YR 7/3	m	60	ss/po	h	SCL	-	cw	III	-		
K	25	10YR 6/3	10YR 7/3	m	60	ss/po	h	SCL	-	cw	III	-		
Ck	40	10YR 4/3	10YR 6/3	sg	60	ss/po	lo	LS	-	-	I	-		

WCT3		Bar												
Horizon	Thickness (cm)	Color (m)	Color (d)	Structure	Gravel (%)	Consistence (m)	Consistence (d)	Texture	Caly Films	Boundary	CO3	roots		
AC	6	10YR 3/3	10YR 5/3	1msbk	5	so/po	so	SL	-	gw	0	2f/2m		
2Ajk	42	8.75YR 3/3	8.75YR 5/3	1msbk	5	so/po	so	SL	-	cw	0	1f/v1m		
3Bk	32	10YR 3/3	10YR 4/3	2msbk	15	ss/po	sh	SL	-	gw	I	1f		
Ck	55	10YR 3/3	10YR 5/3	sg	60	so/po	sh	S	-	-	I	1f		

WCT-PM		arroyo bottom												
Horizon	Thickness (cm)	Color (m)	Color (d)	Structure	Gravel (%)	Consistence (m)	Consistence (d)	Texture	Caly Films	Boundary	CO3	roots		
PM	-	10YR 4/2	10YR 5/3	sg	60	so/po	lo	S	-	-	-	roots		

Appendix 1 - Continued

TCT-1

Horizon	Depth (cm)	Color (m)	Color (d)	Structure	Gravel (%)	Consistence (m)	Consistence (d)	Texture	Texture (Lab)	Caly Films	Boundary	CO3	Roots
Avk	0-5	7.5YR 4/3	10YR 5/3	3msbk	10	so/po	sh	Sil	SL	N/A	c/w	I-	1f
Bk1	5-30	7.5YR 4/3	7.5YR 5/3	2msbk	20	ss/po	sh	SCL	SCL	N/A	a/w	I-	1f,1m,1c
Bk2	30-60	7.5YR 5/3	7.5YR 6/2	m/sg	50	ss/ps	eh/lo	S	SL	N/A	g/w	II+	v1f,v1m
Ck	60-95	7.5YR 4/3	8.25YR 5/2	sg	70	so/po	lo	S	S	N/A	N/A	I-	v1vf

TCT-2

Horizon	Depth (cm)	Color (m)	Color (d)	Structure	Gravel (%)	Consistence (m)	Consistence (d)	Texture	Texture (Lab)	Caly Films	Boundary	CO3	Roots
Ak	0-22	10YR 3/3	10YR 5/3	sg	40	so/po	lo	S	S	N/A	s/w	I-	1f,v1c,v1m
Ck	22-85	7.5YR 3/3	7.5YR 5/3	sg	40	so/po	lo	S	S	N/A	N/A	I-	v1m

Appendix 2 - Soil Development Index

LNAT-1

Horizon	Thickness (cm)	Structure	Texture (Lab)	Carbonate	Subtotal	Index	Weighted	Normalized to 135 cm
Ak	8	0.50	0.44	0.03	0.98	0.33	2.61	
Btk	12	0.33	0.78	0.05	1.16	0.39	4.63	
Bkt1	15	0.33	0.78	0.03	1.15	0.38	5.73	
Bkt2	30	0.33	0.22	0.04	0.60	0.20	5.96	
Ck	30	0.33	0.22	0.01	0.56	0.19	5.61	
							24.54	0.18

LNAT-2

Horizon	Thickness (cm)	Structure	Texture (Lab)	Carbonate	Subtotal	Index	Weighted	Normalized to 135 cm
Ak	6	0.50	0.22	0.03	0.75	0.25	1.51	
Btk1	24	0.33	0.78	0.04	1.15	0.38	9.17	
Btk2	35	0.33	0.33	0.02	0.69	0.23	8.03	
Ck	20	0.00	0.22	0.02	0.24	0.08	1.63	
							20.34	0.15

LNAT-3

Horizon	Thickness (cm)	Structure	Texture (Lab)	Carbonate	Subtotal	Index	Weighted	Normalized to 135 cm
Ak	7	0.33	0.22	0.04	0.60	0.20	1.39	
Bk	43	0.00	0.33	0.06	0.40	0.13	5.66	
Ck	10	0.00	0.33	0.01	0.34	0.11	1.14	
							8.20	0.06

Appendix 2 - Continued

SCT-1

Horizon	Thickness (cm)	Structure	Texture (Lab)	Carbonate	Subtotal	Index	Weighted	Normalized to 135 cm
Ak	6	0.50	0.33	0.09	0.92	0.31	1.85	
Bkt	9	0.50	0.44	0.13	1.07	0.36	3.21	
Bkt	20	0.67	0.56	0.22	1.45	0.48	9.64	
K1	25	0.00	0.33	0.60	0.93	0.31	7.79	
K2	35	0.00	0.56	0.57	1.13	0.38	13.16	
							35.65	0.26

SCT-2

Horizon	Thickness (cm)	Structure	Texture (Lab)	Carbonate	Subtotal	Index	Weighted	Normalized to 135 cm
A	11	0.33	0.44	0.01	0.78	0.26	2.87	
Ak	6	0.33	0.56	0.01	0.89	0.30	1.79	
Bkt	14	0.33	0.89	0.00	1.23	0.41	5.72	
Bk1	17	0.00	0.67	0.12	0.79	0.26	4.46	
Bk2	17	0.00	0.22	0.15	0.37	0.12	2.11	
Ck	35	0.00	0.00	0.00	0.00	0.00	0.01	
tube	10			0.26	0.26	0.26	2.56	
							19.53	0.14

SCT-3

Horizon	Thickness (cm)	Structure	Texture (Lab)	Carbonate	Subtotal	Index	Weighted	Normalized to 135 cm
A	8	0.33	0.22	0.00	0.56	0.19	1.49	
Bt1	37	0.50	0.67	0.00	1.17	0.39	14.42	
Bt2	22	0.50	0.33	0.00	0.84	0.28	6.13	
Bk	43	0.33	0.11	0.00	0.45	0.15	6.40	
							28.43	0.21

SCT-4

Horizon	Thickness (cm)	Structure	Texture (Lab)	Carbonate	Subtotal	Index	Weighted	Normalized to 135 cm
A	5	0.33	0.67	0.00	1.00	0.33	1.67	
Bt	40	0.50	0.78	0.00	1.28	0.43	17.08	
Ck	35	0.33	0.67	0.02	1.02	0.34	11.88	
							30.63	0.26

Appendix 2 - Continued

WCT-1

Horizon	Thickness (cm)	Structure	Texture (Lab)	Carbonate	Subtotal	Index	Weighted	Normalized to 135 cm
A	8	0.50	0.33	0.01	0.84	0.28	2.24	
Btk	11	0.50	0.56	0.01	1.07	0.36	3.92	
Bk1	10	0.50	0.44	0.04	0.99	0.33	3.29	
Bk2	51	0.67	0.56	0.08	1.30	0.43	22.15	
Bk3	20	0.50	0.22	0.04	0.76	0.25	5.09	
Ck	25	0.33	0.33	0.03	0.69	0.23	5.77	
							42.45	0.31

WCT-4

Horizon	Thickness (cm)	Structure	Texture (Lab)	Carbonate	Subtotal	Index	Weighted	Normalized to 135 cm
AC	6	0.33	0.11	0.02	0.46	0.15	0.92	
2Ajk	42	0.33	0.22	0.00	0.56	0.19	7.82	
3Bk	32	0.50	0.22	0.00	0.73	0.24	7.75	
Ck	30	0.00	0.11	0.01	0.12	0.04	1.19	
							17.68	0.13

Appendix 2 - Continued

TCT-1								
Horizon	Thickness (cm)	Structure	Texture (Lab)	Carbonate	Subtotal	Index	Weighted	Normalized to 135 cm
Avk	5	0.67	0.22	0.03	0.92	0.31	1.54	
Bk1	25	0.50	0.44	0.03	0.98	0.33	8.14	
Bk2	30	0.00	0.44	0.10	0.54	0.18	5.44	
Ck	35	0.00	0.00	0.02	0.02	0.01	0.21	
							15.32	0.11

TCT-2								
Horizon	Thickness (cm)	Structure	Texture (Lab)	Carbonate	Subtotal	Index	Weighted	Normalized to 135 cm
Ak	22	0.00	0.00	0.03	0.03	0.01	0.20	
Ck	63	0.00	0.00	0.00	0.00	0.00	0.08	
							0.27	0.002